

EUROPEAN ORGANISATION FOR NUCLEAR RESEARCH (CERN)



Submitted to: JHEP



CERN-PH-EP-2015-208
10th December 2015

Measurement of the $t\bar{t}W$ and $t\bar{t}Z$ production cross sections in pp collisions at $\sqrt{s} = 8$ TeV with the ATLAS detector

The ATLAS Collaboration

Abstract

The production cross sections of top-quark pairs in association with massive vector bosons have been measured using data from pp collisions at $\sqrt{s} = 8$ TeV. The dataset corresponds to an integrated luminosity of 20.3 fb^{-1} collected by the ATLAS detector in 2012 at the LHC. Final states with two, three or four leptons are considered. A fit to the data considering the $t\bar{t}W$ and $t\bar{t}Z$ processes simultaneously yields a significance of 5.0σ (4.2σ) over the background-only hypothesis for $t\bar{t}W$ ($t\bar{t}Z$) production. The measured cross sections are $\sigma_{t\bar{t}W} = 369^{+100}_{-91} \text{ fb}$ and $\sigma_{t\bar{t}Z} = 176^{+58}_{-52} \text{ fb}$. The background-only hypothesis with neither $t\bar{t}W$ nor $t\bar{t}Z$ production is excluded at 7.1σ . All measurements are consistent with next-to-leading-order calculations for the $t\bar{t}W$ and $t\bar{t}Z$ processes.

© 2015 CERN for the benefit of the ATLAS Collaboration.

Reproduction of this article or parts of it is allowed as specified in the CC-BY-3.0 license.

Contents

1	Introduction	2
2	The ATLAS detector	3
3	Simulated event samples	4
4	Object reconstruction	6
5	Event selection and background estimation	7
5.1	Opposite-sign dilepton channel	8
5.2	Same-sign dilepton channel	9
5.3	Trilepton channel	14
5.4	Tetralepton channel	15
6	Systematic uncertainties	20
6.1	Uncertainties on reconstructed objects	20
6.2	Uncertainties on signal modelling	20
6.3	Uncertainties on background modelling	21
7	Results	23
8	Conclusion	25

1 Introduction

The top quark is the heaviest known elementary particle, and its large coupling to the Higgs boson suggests that it might be closely connected to electroweak (EW) symmetry breaking. Despite the fact that the top quark was discovered two decades ago [1, 2] some of its properties, in particular, its coupling to the Z boson, have never been directly measured. Several extensions of the Standard Model, such as technicolour [3–7] or other scenarios with a strongly coupled Higgs sector [8] modify the top quark couplings.

With the centre-of-mass energy and integrated luminosity of the collected data samples at the Large Hadron Collider (LHC), the processes in which the electroweak Standard Model bosons (γ , Z , W and H) are produced in association with top quarks become experimentally accessible. Measurements of the $t\bar{t}Z$, $t\bar{t}\gamma$ and $t\bar{t}H$ processes provide a means of directly determining top quark couplings to bosons [9–11], while the $t\bar{t}W$ process is a Standard Model (SM) source of same-sign dilepton events, which are a signature of many models of physics beyond the SM. Example leading-order Feynman diagrams for $t\bar{t}W$ and $t\bar{t}Z$ production at the LHC are shown in Figure 1. Previous searches for $t\bar{t}W$ and $t\bar{t}Z$ production at the LHC have been carried out by the CMS collaboration at $\sqrt{s} = 7$ TeV and $\sqrt{s} = 8$ TeV [12, 13].

This paper presents measurements of the $t\bar{t}W$ and $t\bar{t}Z$ cross sections based on an analysis of 20.3 fb^{-1} of proton–proton (pp) collision data at $\sqrt{s} = 8$ TeV collected by the ATLAS detector. Depending on the decays of the top quarks, W and Z bosons, between zero and four prompt, isolated leptons¹ may be

¹ In this note, lepton is used to denote electron or muon, including those coming from leptonic tau decays.

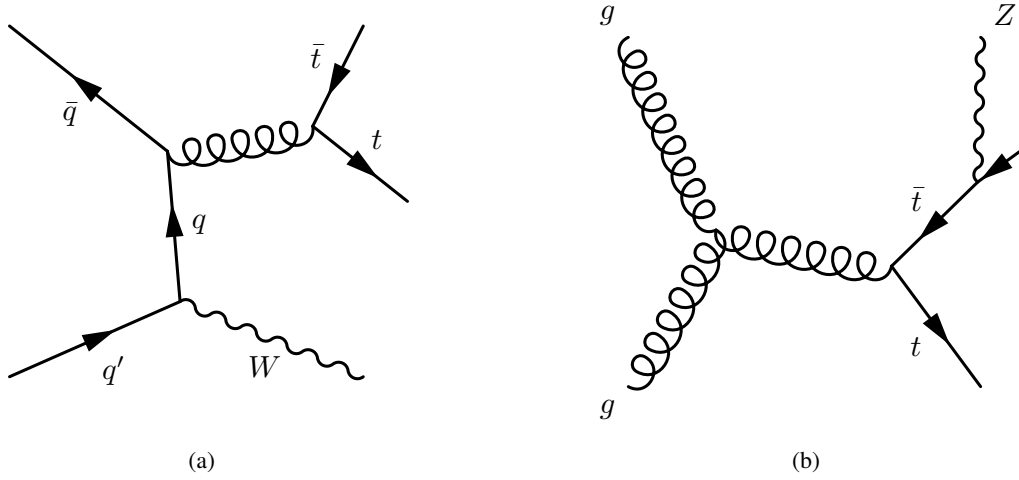


Figure 1: Example leading-order Feynman diagrams for (a) $t\bar{t}W$ and (b) $t\bar{t}Z$ production.

produced. Channels with two (both with same-sign and opposite-sign charge), three, and four leptons are considered in this analysis. The opposite-sign (OS) dilepton, trilepton and tetralepton channels are mostly sensitive to $t\bar{t}Z$ production, while the same-sign (SS) dilepton channel targets $t\bar{t}W$ production. Table 1 lists the analysis channels and the targeted decay modes of the $t\bar{t}W$ and $t\bar{t}Z$ processes. Each channel is divided into multiple analysis regions in order to enhance the sensitivity to the signal. A simultaneous fit is performed to all signal regions and selected control regions in the four channels to extract cross sections for $t\bar{t}W$ and $t\bar{t}Z$ production.

Process	$t\bar{t}$ decay	Boson decay	Channel	$Z \rightarrow \ell^+ \ell^-$
$t\bar{t}W^\pm$	$(\ell^\pm \nu b)(q\bar{q}b)$	$\ell^\mp \nu$	OS dilepton	no
	$(\ell^\pm \nu b)(\ell^\mp \nu b)$	$q\bar{q}$	OS dilepton	no
	$(\ell^\pm \nu b)(q\bar{q}b)$	$\ell^\pm \nu$	SS dilepton	no
	$(\ell^\pm \nu b)(\ell^\mp \nu b)$	$\ell^\pm \nu$	Trilepton	no
$t\bar{t}Z$	$(\ell^\pm \nu b)(\ell^\mp \nu b)$	$q\bar{q}$	OS dilepton	no
	$(q\bar{q}b)(q\bar{q}b)$	$\ell^+ \ell^-$	OS dilepton	yes
	$(\ell^\pm \nu b)(q\bar{q}b)$	$\ell^+ \ell^-$	Trilepton	yes
	$(\ell^\pm \nu b)(\ell^\mp \nu b)$	$\ell^+ \ell^-$	Tetralepton	yes

Table 1: List of $t\bar{t}W$ and $t\bar{t}Z$ decay modes and analysis channels targeting them. The last column indicates whether a final state lepton pair is expected from a Z boson decay.

2 The ATLAS detector

The ATLAS detector [14] consists of four main subsystems: an inner tracking system, electromagnetic (EM) and hadronic calorimeters, and a muon spectrometer. The inner detector provides tracking in-

formation from pixel and silicon microstrip detectors in the pseudorapidity² range $|\eta| < 2.5$ and from a transition radiation tracker (TRT) covering $|\eta| < 2.0$, all immersed in a 2 T magnetic field provided by a superconducting solenoid. The EM sampling calorimeter uses lead and liquid argon (LAr) and is divided into barrel ($|\eta| < 1.475$) and endcap ($1.375 < |\eta| < 3.2$) regions. Hadron calorimetry is provided by a steel/scintillator-tile calorimeter, segmented into three barrel structures in the range $|\eta| < 1.7$, and two copper/LAr hadronic endcap calorimeters that cover the region $1.5 < |\eta| < 3.2$. The solid angle coverage is completed with forward copper/LAr and tungsten/LAr calorimeter modules, optimised for EM and hadronic measurements respectively, and covering the region $3.1 < |\eta| < 4.9$. The muon spectrometer measures the deflection of muon tracks in the range $|\eta| < 2.7$ using multiple layers of high-precision tracking chambers located in toroidal magnetic fields of approximately 0.5 T and 1 T in the central and endcap regions of ATLAS, respectively. The muon spectrometer is also instrumented with separate trigger chambers covering $|\eta| < 2.4$.

3 Simulated event samples

Monte Carlo (MC) samples are used to optimise the event selection and the choice of signal regions, and to model all signal and certain background processes. In the following, the simulation of signal and background events is described in detail. For all MC samples, the top quark mass is taken to be $m_t = 172.5$ GeV, and the Higgs boson mass is set to 125 GeV.

The $t\bar{t}V$ ($V = W, Z$) process is simulated using the MADGRAPH5 leading-order (LO) generator [15] with up to one additional parton, using the CTEQ6L1 [16] parton distribution function (PDF) set. PYTHIA 6.425 [17] with the AUET2B underlying-event set of tunable parameters (tune) [18] is used to simulate showering and hadronisation. The $t\bar{t}V$ samples are normalised to the inclusive next-to-leading-order (NLO) cross-section predictions, using MADGRAPH5_AMC@NLO [19], including the off-shell $t\bar{t}Z/\gamma^*$ contribution and interference. An invariant mass of at least 5 GeV is required for any opposite-sign, same-flavour pair of leptons appearing in the matrix element. The obtained cross sections are $\sigma_{t\bar{t}W} = 232 \pm 32$ fb and $\sigma_{t\bar{t}Z} = 215 \pm 30$ fb, compatible with other NLO QCD calculations [20, 21]. The quoted uncertainties include renormalisation and factorisation scale and PDF uncertainties, including α_S variations.

The ALPGEN v2.14 [22] LO generator and the CTEQ6L1 PDF set are used to simulate W/Z production. Parton showers and hadronisation are modelled with PYTHIA 6.425. The W/Z samples are generated with up to five additional light partons, separately for W/Z , $W/Z+b\bar{b}$, $W/Z+c\bar{c}$ and Wc , and normalised to the respective inclusive next-to-next-to-leading-order (NNLO) theoretical cross sections [23]. To avoid double-counting of partonic configurations generated by both the matrix-element calculation and the parton-shower evolution, a parton–jet matching scheme (MLM matching) [24] is employed. The overlap between $W/Z+Q\bar{Q}$ ($Q = b, c$) events generated from the matrix-element calculation and those generated from parton-shower evolution in the W/Z +light-jet samples is avoided via an algorithm based on the distance in η – ϕ space between the heavy quarks: if $\Delta R(Q, \bar{Q}) > 0.4$, the matrix-element prediction is used, otherwise the parton-shower prediction is used.

² ATLAS uses a right-handed coordinate system with its origin at the nominal interaction point (IP) in the centre of the detector and the z -axis coinciding with the axis of the beam pipe. The x -axis points from the IP to the centre of the LHC ring, and the y -axis points upward. Cylindrical coordinates (r, ϕ) are used in the transverse plane, ϕ being the azimuthal angle around the beam pipe. The pseudorapidity is defined in terms of the polar angle θ as $\eta = -\ln \tan(\theta/2)$, and the distance between two objects in η – ϕ space is measured in terms of $\Delta R \equiv \sqrt{(\Delta\eta)^2 + (\Delta\phi)^2}$.

Diboson samples are generated using the SHERPA 1.4.1 [25] generator with the CT10 PDF set [26], with massive b - and c -quarks and with up to three additional partons in the LO matrix element. Samples are normalised to their NLO QCD theoretical cross sections [27]. Alternative models for the diboson background are provided by the POWHEG-BOX 2.0 [28–30] generator, which implements the NLO matrix elements, interfaced with PYTHIA 6.425 or PYTHIA 8.1 [31].

Simulated $t\bar{t}$ and single-top-quark backgrounds corresponding to the t -channel, Wt and s -channel production mechanisms are generated using the POWHEG-BOX generator, with the CT10 PDF set. All samples are interfaced with PYTHIA 6.425 with the CTEQ6L1 PDF set and the Perugia2011C [32] underlying event tune. Overlaps between the $t\bar{t}$ and Wt final states are removed through the diagram removal scheme [33]. The $t\bar{t}$ sample is normalised to the Top++2.0 [34] theoretical calculation performed at NNLO in QCD that includes resummation of next-to-next-to-leading logarithmic soft gluon terms [35–39]. The single-top-quark samples are normalised to the approximate NNLO theoretical cross sections [40–42] calculated using the MSTW2008 NNLO PDF set [43, 44].

The production of a single top quark in association with a Z boson through the t - and s -channels, of the WtZ process, and of a top quark pair in association with a W boson pair ($t\bar{t} WW$) are simulated with MADGRAPH5 LO and the CTEQ6L1 PDF set. MADGRAPH is interfaced with PYTHIA 6.425 using the AUET2B tune and the CTEQ6L1 PDF set. The relevant samples are normalised to the NLO theoretical predictions calculated with MADGRAPH5_AMC@NLO [19]. The production of three vector bosons that decay to three or four leptons is also simulated with MADGRAPH5 and PYTHIA 6.425. The LO cross section obtained from the generator is used to normalise the samples. The production of two W bosons with the same charge is modelled using the SHERPA generator, including diagrams of order α_{EW}^4 and $\alpha_{EW}^2\alpha_S^2$. The LO cross section obtained from the generator is used to normalise the samples. The four-top-quark process ($t\bar{t}t\bar{t}$) is simulated with MADGRAPH5 interfaced with PYTHIA 8.

Associated $t\bar{t}H$ production is simulated using NLO matrix elements obtained from the HELAC-ONELOOP package [45]. The POWHEG-BOX program served as an interface for shower MC programs. Samples were produced using the CT10NLO PDF set and showered with PYTHIA 8.1 with the CTEQ6L1 PDF and the AU2 underlying-event tune [46]. The $t\bar{t}H$ cross section and Higgs boson decay branching fractions are taken from the theoretical calculations collected in Ref. [47]. The process $gg \rightarrow H \rightarrow 4\ell$ is modelled using the POWHEG-BOX interfaced with PYTHIA 8.1. WH and ZH production are modelled using PYTHIA 8.1. The samples are normalised to the NNLO QCD cross sections with NLO electroweak corrections [47].

All simulated samples produced with PYTHIA use PHOTOS 2.15 [48] to simulate photon radiation and TAUOLA 1.20 [49] to simulate τ decays. Events from minimum-bias interactions from the same bunch crossing as the hard-scattering process and in neighbouring bunch crossings, known as pile-up, are simulated with the PYTHIA 8.1 generator with the MSTW2008 LO PDF set and the AUET2 [50] tune. These are superimposed on the simulated hard-scatter events in a manner which reproduces the luminosity profile of the recorded data.

All samples are processed through a simulation of the detector geometry and response [51] either using GEANT4 [52], or GEANT4 with a fast simulation of the calorimeter response [53]. All samples are processed by the same reconstruction software as the data. Simulated events are corrected so that the object identification, reconstruction and trigger efficiencies, energy scales and energy resolutions match those determined from data control samples.

4 Object reconstruction

The final states of interest in this analysis contain electrons, muons, jets, b -jets and missing transverse momentum.

Electron candidates [54] are reconstructed from energy deposits (clusters) in the EM calorimeter that are associated with reconstructed tracks in the inner detector. The electrons are required to have $|\eta_{\text{cluster}}| < 2.47$, where η_{cluster} is the pseudorapidity of the calorimeter energy deposit associated with the electron candidate. Candidates in the EM calorimeter barrel/endcap transition region $1.37 < |\eta_{\text{cluster}}| < 1.52$ are excluded. The electron identification relies on a likelihood-based selection [55].

To reduce the background from misidentified or non-prompt (labelled as “fake” throughout this paper) electrons, i.e. from decays of hadrons (including heavy flavour), electron candidates are required to be isolated. In the opposite-sign dilepton and tetralepton channels, in which such background is small, the electron isolation is defined using only tracking information. In the opposite-sign dilepton channel, the ratio of $p_{\text{T}}^{\Delta R < 0.3}$, the sum of track transverse momenta in a cone of size $\Delta R = 0.3$ around the electron track, excluding the electron track itself, to the transverse momentum (p_{T}^e) of the electron is required to be less than 0.12. In the tetralepton channel, the requirement is loosened to $p_{\text{T}}^{\Delta R < 0.3}/p_{\text{T}}^e < 0.18$. In the trilepton and same-sign dilepton channels, in which the background with fake leptons is more prominent, additional requirements are imposed on the electron isolation. For electrons with $p_{\text{T}}^e < 50$ GeV, both the ratio of the additional calorimeter energy within a cone of $\Delta R = 0.2$ around the electron ($E_{\text{T}}^{\Delta R < 0.2}$) to the p_{T}^e of the electron, and $p_{\text{T}}^{\Delta R < 0.3}/p_{\text{T}}^e$ are required to be less than 0.12. For $p_{\text{T}}^e \geq 50$ GeV, both $E_{\text{T}}^{\Delta R < 0.2}$ and $p_{\text{T}}^{\Delta R < 0.3}$ are required to be less than 6 GeV.

Muon candidates are reconstructed from track segments in the various layers of the muon spectrometer, and matched with tracks identified in the inner detector [56]. The final muon candidates are refitted using the complete track information from both detector systems, and are required to have $|\eta| < 2.5$. Additionally, muons are required to be separated by $\Delta R > 0.4$ from any jet and to satisfy a p_{T} -dependent track-based isolation requirement [57] that has good performance under high pile-up conditions. This requires that the scalar sum of the track transverse momenta in a cone of variable size $\Delta R = (10 \text{ GeV}/p_{\text{T}}^{\mu})$ around the muon (excluding the muon track itself) must be less than $0.05 p_{\text{T}}^{\mu}$.

For both the electrons and muons, the track longitudinal impact parameter with respect to the primary vertex,³ z_0 , is required to be less than 2 mm. In the same-sign dilepton channel, in which backgrounds from fake leptons are dominant, it is also required to satisfy $|z_0 \sin \theta| < 0.4$ mm, and the significance of the transverse impact parameter d_0 is required to satisfy $|d_0/\sigma(d_0)| < 3$, where $\sigma(d_0)$ is the uncertainty on d_0 .

Jets are reconstructed with the anti- k_t algorithm [58–60] with radius parameter $R = 0.4$ from calibrated topological clusters [14] built from energy deposits in the calorimeters. Prior to jet finding, a local cluster calibration scheme [61, 62] is applied to correct the topological cluster energies for the effects of non-compensating calorimeter response, dead material and out-of-cluster leakage. The jets are calibrated to restore the jet energy scale to that of jets reconstructed from stable simulated particles, using energy- and η -dependent calibration factors derived from simulations. Additional corrections to account for residual differences between simulation and data are applied [63]. After calibration, jets are required to have $p_{\text{T}} > 25$ GeV and $|\eta| < 2.5$. To avoid selecting jets from pile-up interactions, an additional requirement,

³ A primary vertex candidate is defined as a vertex with at least five associated tracks, consistent with the beam collision region. If more than one such vertex is found, the vertex candidate with the largest sum of squared transverse momenta of its associated tracks is taken as the primary vertex.

referred to as the jet vertex fraction criterion (JVF), is imposed on jets with $p_T < 50$ GeV and $|\eta| < 2.4$. It requires that at least 50% of the scalar sum of the transverse momenta of tracks with $p_T > 1$ GeV, associated with a jet, comes from tracks compatible with originating from the primary vertex. During jet reconstruction, no distinction is made between identified electrons and jet energy deposits. Therefore, if any of the jets lie $\Delta R < 0.2$ from an electron, the closest jet is discarded in order to avoid double counting of electrons as jets. After this overlap removal, electrons and muons which lie $\Delta R < 0.4$ from any remaining jet are removed.

Jets containing b -hadrons are tagged by an algorithm (MV1) [64] that uses multivariate techniques to compute weights by combining information from the impact parameters of displaced tracks as well as topological properties of secondary and tertiary decay vertices reconstructed within the jet. Larger weights indicate that a jet is more likely to contain b -hadrons. The working point used for this measurement corresponds to 70% efficiency to tag a b -quark jet, as determined for b -jets with $p_T > 20$ GeV and $|\eta| < 2.5$ in simulated $t\bar{t}$ events. The rejection factors for light-jets and c -quark jets are approximately 130 and 5, respectively. The efficiency of b -tagging in simulation is corrected to that in data using a $t\bar{t}$ based calibration [65].

The missing transverse momentum $\mathbf{p}_T^{\text{miss}}$, with magnitude E_T^{miss} , is reconstructed [66] as the negative sum of transverse momenta of all electrons, muons, jets and calibrated calorimeter energy clusters not associated with any of these objects.

5 Event selection and background estimation

The measurements presented here are based on data collected by the ATLAS experiment in pp collisions at $\sqrt{s} = 8$ TeV in 2012. The corresponding integrated luminosity is 20.3 fb^{-1} . Only events collected using a single-electron or single-muon trigger under stable beam conditions, that satisfy the standard data quality criteria, are accepted. The trigger p_T thresholds are 24 or 60 GeV for electrons and 24 or 36 GeV for muons: the triggers with the lower p_T thresholds include isolation requirements on the candidate lepton, resulting in inefficiencies at high p_T that are recovered by the triggers with higher p_T thresholds. Events are required to have at least one reconstructed primary vertex. In all selections considered, at least one lepton with $p_T > 25$ GeV is required to match ($\Delta R < 0.15$) a lepton with the same flavour, reconstructed by the trigger algorithm.

Four channels are defined based on the number and charges of the reconstructed leptons, which are sorted according to their transverse momentum in decreasing order. For the opposite-sign dilepton channel, two leptons with opposite charge and $p_T > 15$ GeV are required. In the same-sign dilepton channel, events are required to contain two same-sign leptons with $p_T > 25$ GeV. In both dilepton channels, events containing additional leptons with $p_T > 15$ GeV are rejected. For the trilepton channel, events are required to contain three leptons with $p_T > 15$ GeV. For the tetralepton channel, exactly four leptons with $p_T > 7$ GeV are required. Events satisfying both the trilepton and tetralepton channel selections are attributed to the trilepton channel and removed from the tetralepton channel. The dilepton channels are not explicitly required to be orthogonal with the tetralepton channel, but the overlap is found to be negligibly small in simulated samples and non-existent in data.

Background events containing well-identified prompt leptons are modelled by simulation. The normalisations used for the backgrounds in this category are taken from data control regions if the resulting normalisation uncertainty is lower than that from the theoretical prediction. The yields in the data control

regions are extrapolated to the signal regions using the simulation. Background sources involving one or more incorrectly identified lepton, e.g. instrumental backgrounds, are modelled using data events from control regions, except in the opposite-sign dilepton channel, where this background is very small.

The following sections describe additional selection requirements and the background evaluation in each of the four channels.

5.1 Opposite-sign dilepton channel

In the opposite-sign dilepton channel, events are required to have at least three jets, one or two of which are b -tagged. Two orthogonal selections are defined to separate $t\bar{t}W$ and $t\bar{t}Z$ final states. The first (2ℓ -noZ) selects different-flavour lepton (DF) events with the scalar sum of the p_T of leptons and jets, H_T , above 130 GeV, and same-flavour lepton (SF) events that are not compatible with Z boson or low-mass resonance production, by requiring $|m_{\ell\ell} - m_Z| > 10$ GeV, $m_{\ell\ell} > 15$ GeV and $E_T^{\text{miss}} > 40$ GeV. The 2ℓ -Z selection contains SF events within the mass window $|m_{\ell\ell} - m_Z| < 10$ GeV. In both selections an additional requirement on the average distance between two jets, calculated using all possible jet pairs in the event, $\Delta R_{\text{ave}}^{jj} > 0.75$, is applied to remove the low-dijet-mass region where the ALPGEN+PYTHIA simulation does not provide a good description of the Z boson background [67].

For 2ℓ -noZ events, the $t\bar{t}V$ signal contribution originates mainly from the $t\bar{t}$ dilepton final state accompanied by a hadronic W/Z boson decay and from the $t\bar{t}$ single-lepton final state with a leptonic W boson decay. For 2ℓ -Z events, the contribution of $t\bar{t}W$ production is negligible while the $t\bar{t}Z$ contribution comes from the fully hadronic $t\bar{t}$ final state with a leptonic Z boson decay.

After event selection the dominant backgrounds are $t\bar{t}$ and Z production in 2ℓ -noZ and 2ℓ -Z respectively, and the extraction of the signal relies on discriminating it from these backgrounds, based on well-modelled event kinematics. To improve the modelling of the $t\bar{t}$ background, the simulated $t\bar{t}$ events are reweighted to account for the observed differences in the top quark p_T and the $t\bar{t}$ system p_T between data and POWHEG+PYTHIA simulation in measurements of differential cross sections at $\sqrt{s} = 7$ TeV [68]. To improve Z background modelling, the simulation is reweighted to account for the difference in the Z p_T spectrum between data and simulation [67], and the $ZQ\bar{Q}$ ($Q = b, c$) component of the Z background is adjusted to match data in a $ZQ\bar{Q}$ -dominated control region with at least one b -tagged jet. Small background contributions arise from single-top-quark Wt channel production, diboson (WW , WZ , ZZ) processes, the associated production of a Higgs boson and a $t\bar{t}$ pair, the associated production of a WW and a $t\bar{t}$ pair, and the associated production of a single top quark and a Z boson. All of these backgrounds are determined from simulation.

In the 2ℓ -noZ region, W boson, $t\bar{t}$ (with a single lepton in the final state) and t - and s -channel single-top-quark production processes can satisfy the selection requirements due to fake leptons. These backgrounds are a small fraction of the total estimated background, and their yields are estimated using simulation and cross-checked with a data-driven technique based on the selection of a same-sign lepton pair.

Events are categorised according to the number of jets and the number of b -tagged jets. In the 2ℓ -noZ selection, events with one or two b -tagged jets are separated into three exclusive regions according to the jet multiplicity, with three (2ℓ -noZ-3j), four (2ℓ -noZ-4j), and five or more (2ℓ -noZ-5j) jets. In the 2ℓ -Z selection, events with exactly two b -tagged jets are separated into three regions according to the same scheme: 2ℓ -Z-3j, 2ℓ -Z-4j and 2ℓ -Z-5j.

A neural network (NN) discriminant built using the NeuroBayes [69] package is used to separate the combined $t\bar{t}W$ and $t\bar{t}Z$ signal from the background in the signal-rich regions $2\ell\text{-noZ-4j}$, $2\ell\text{-noZ-5j}$ and $2\ell\text{-Z-5j}$. The other regions considered in the opposite-sign dilepton channel have lower sensitivity and are used as control regions; event counting is used in the $2\ell\text{-noZ-3j}$ region, while the scalar sum of the jet transverse momenta (H_T^{had}) is used as a discriminant in the $2\ell\text{-Z-3j}$ and $2\ell\text{-Z-4j}$ regions. The inclusion of these highly populated control regions, enriched in $t\bar{t}$ or Z backgrounds, in the fit used to extract the $t\bar{t}V$ signals, strongly constrains the normalisation uncertainties of these backgrounds. This in turn improves the background predictions in the signal-rich regions. The signal and control regions are summarised in Table 2.

Region	Targeting	Sample fraction [%]
$2\ell\text{-noZ-4j}$	$t\bar{t}W$ and $t\bar{t}Z$	0.68
$2\ell\text{-noZ-5j}$		1.2
$2\ell\text{-Z-5j}$	$t\bar{t}Z$	3.3
$2\ell\text{-noZ-3j}$	$t\bar{t}$	92
$2\ell\text{-Z-3j}$	Z	70
$2\ell\text{-Z-4j}$		66

Table 2: Signal and control regions of the opposite-sign dilepton channel, together with the processes targeted and the expected fraction of the sample represented by the targeted process.

The set of variables used as input to the NN discriminant is chosen separately for each signal region, based on the ranking procedure implemented in the NeuroBayes package which takes into account the statistical separation power of the variables and the correlations between them. All variables used for the NN training are required to show good agreement between data and background expectation in the control regions. Seven variables are selected in each signal region. The list of selected variables and their ranking is shown in Table 3.

Figure 2 illustrates the discrimination between the $t\bar{t}V$ signal and background provided by the NN discriminants. Since in the $2\ell\text{-noZ}$ region the contributions from both $t\bar{t}W$ and $t\bar{t}Z$ production are comparable in size and have similar kinematics, they result in a similar NN discriminant shape and are thus fitted together. In the $2\ell\text{-Z}$ region, the $t\bar{t}W$ contribution is negligible, and thus the NN discriminant shape is driven by the $t\bar{t}Z$ signal.

The expected sample compositions in each of the three signal and three control regions are summarised in Table 4 along with the number of events observed in data. The distributions of discriminants in the control regions are shown in Figure 3. The data and simulation agree within the expected uncertainties.

5.2 Same-sign dilepton channel

The same-sign dilepton channel targets the $t\bar{t}W$ process. Events are required to have $E_T^{\text{miss}} > 40$ GeV, $H_T > 240$ GeV and to contain at least two b -tagged jets. The same-sign dilepton channel is divided into three orthogonal regions based on the flavour combination of the lepton pair: $2e\text{-SS}$, $e\mu\text{-SS}$, and $2\mu\text{-SS}$. In the $2e\text{-SS}$ region, an additional requirement on the dilepton mass removing events with $75 \text{ GeV} < m_{ee} < 105 \text{ GeV}$ is imposed to reduce the contamination by $Z \rightarrow ee$ events where the charge of one electron is misidentified. A similar requirement is not imposed on the $e\mu\text{-SS}$ or $2\mu\text{-SS}$ regions, since the probability

Variable	Definition	NN rank		
		2 ℓ -noZ-4j	2 ℓ -noZ-5j	2 ℓ -Z-5j
$m_{uu}^{p_T, \text{ord}}$	Invariant mass of the two highest p_T untagged jets in events with exactly two b -tags, or of the two highest p_T untagged jets, excluding the jet with the second highest b -tag weight, in events with exactly one b -tag	1st	7th	-
Centrality _{jet}	Sum of p_T divided by sum of E for all jets	2nd	1st	6th
H_1	2nd Fox-Wolfram moment [70]	3rd	2nd	-
$m_{jj}^{\min \Delta R}$	Invariant mass of the combination of the two jets with the smallest ΔR	4th	6th	-
$\max m_{\ell b}^{\min \Delta R}$	Larger of the invariant masses of the two (lepton, b -tagged jet) pairs, which are built based on the minimum $\Delta R(\ell, b)$ for each lepton	5th	5th	-
p_T^{jet3}	Third-jet p_T	6th	-	-
p_T^{jet4}	Fourth-jet p_T	-	3rd	-
$\Delta R_{\text{ave}}^{jj}$	Average ΔR for all jet pairs	7th	-	-
$N_{\text{jet}}^{ m_{jj}-m_V <30}$	Number of jet pairs with mass within a 30 GeV window around 85 GeV	-	4th	2nd
N_{40}^{jet}	Number of jets with $p_T > 40$ GeV	-	-	1st
$m_{bb}^{\max p_T}$	Invariant mass of the combination of two b -tagged jets with the largest vector sum p_T	-	-	3rd
$\Delta R_{\ell_1 \ell_2}$	ΔR between the two leptons	-	-	4th
$m_{bj}^{\max p_T}$	Invariant mass of the combination of the two jets with the largest vector sum p_T ; one jet must be b -tagged	-	-	5th
H_1^{jet}	2nd Fox-Wolfram moment built from only jets	-	-	7th

Table 3: Definitions and rankings of the variables considered in each of the regions where a NN is used in the opposite-sign dilepton channel.

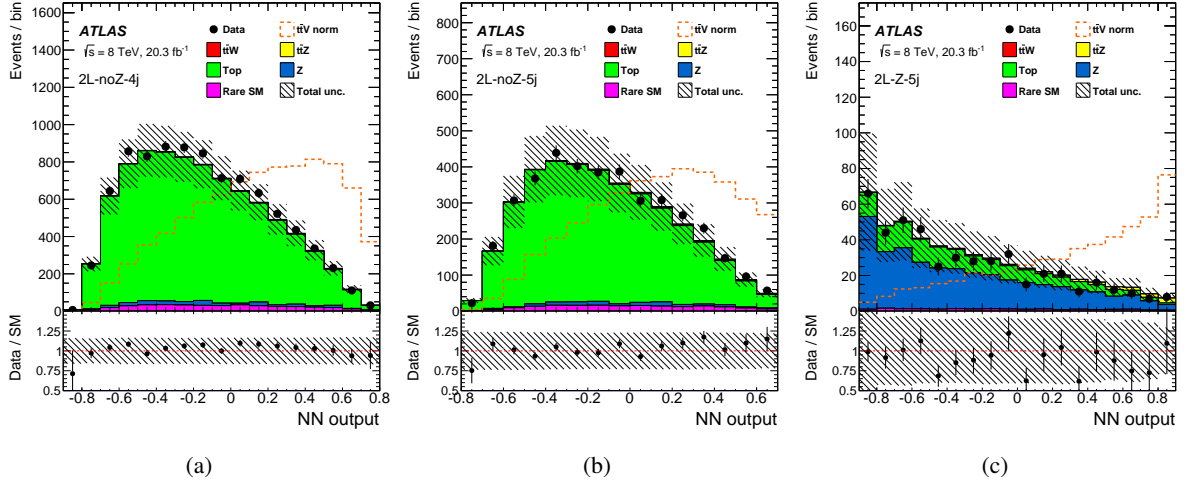


Figure 2: The NN output distributions for the three signal regions in the opposite-sign dilepton channel, before the fit to data. The distributions are shown in the (a) $2\ell\text{-noZ-}4j$, (b) $2\ell\text{-noZ-}5j$ and (c) $2\ell\text{-Z-}5j$ regions. The orange dashed lines show the $t\bar{t}V$ signal normalised to the background yield. “Rare SM” comprises the diboson, single-top, tZ , WtZ , $t\bar{t}H$ processes and the fake lepton background. The hatched area corresponds to the total uncertainty on the predicted yields. The “Data/SM” plots show the ratio of the data to the total Standard Model expectation.

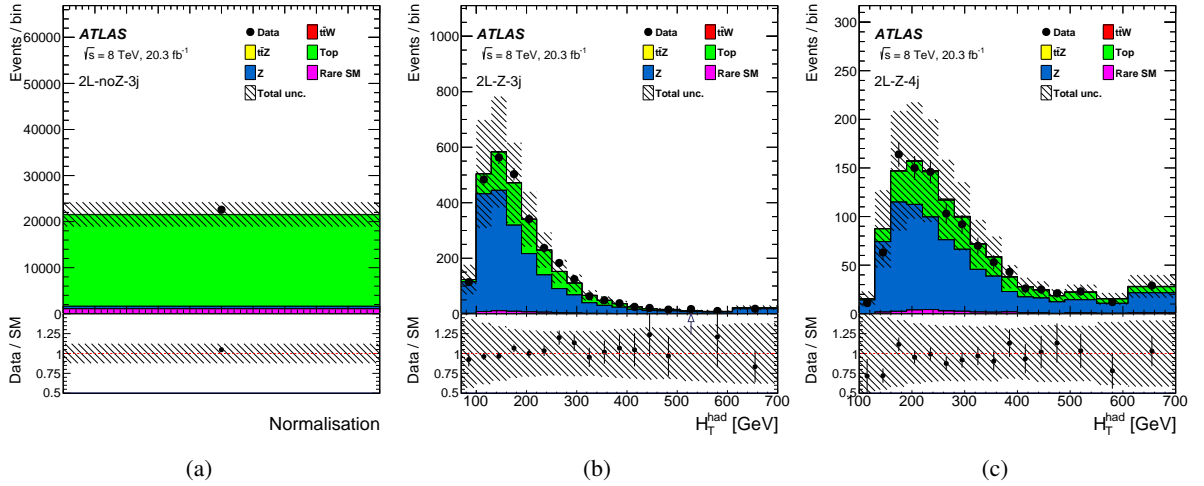


Figure 3: Control region distributions in the opposite-sign dilepton channel, before the fit to data. The distributions are shown in the (a) $2\ell\text{-noZ-}3j$, (b) $2\ell\text{-Z-}3j$ and (c) $2\ell\text{-Z-}4j$ regions. For the $2\ell\text{-noZ-}3j$ region only the event count is used in the fit. The hatched area corresponds to the total uncertainty on the predicted yields. “Rare SM” comprises the diboson, single-top, tZ , WtZ , $t\bar{t}H$ processes and the fake lepton background. The “Data/SM” plots show the ratio of the data to the total expected Standard Model expectation.

Region	$t + X$	Bosons	Fake leptons charge misID	Total expected background	$t\bar{t}W$	$t\bar{t}Z$	Data
2ℓ -noZ-3j*	20800 ± 2600	600 ± 200	160 ± 80	21600 ± 2700	42.0 ± 2.8	23.2 ± 1.5	22585
2ℓ -noZ-4j	8200 ± 1400	240 ± 90	80 ± 40	8600 ± 1400	36.6 ± 1.8	22.4 ± 1.1	8909
2ℓ -noZ-5j	3700 ± 850	100 ± 40	47 ± 23	3810 ± 870	24.9 ± 2.2	22.4 ± 2.0	3901
2ℓ -Z-3j*	800 ± 140	1960 ± 880	4.1 ± 2.1	2760 ± 890	1.24 ± 0.13	3.71 ± 0.38	2806
2ℓ -Z-4j*	330 ± 70	740 ± 390	2.2 ± 1.1	1100 ± 400	1.31 ± 0.11	7.21 ± 0.58	1031
2ℓ -Z-5j	170 ± 40	340 ± 200	1.4 ± 0.7	510 ± 210	0.89 ± 0.07	17.7 ± 1.4	471
$2e$ -SS	0.66 ± 0.13	0.17 ± 0.10	8.9 ± 2.4	9.8 ± 2.6	2.97 ± 0.30	0.93 ± 0.23	16
$e\mu$ -SS	1.9 ± 0.35	0.39 ± 0.28	14.1 ± 4.5	16.4 ± 5.1	8.67 ± 0.76	2.16 ± 0.51	34
2μ -SS	0.94 ± 0.17	0.25 ± 0.14	0.93 ± 0.55	2.12 ± 0.86	4.79 ± 0.40	1.12 ± 0.27	13
3ℓ -Z-0b3j*	1.11 ± 0.32	67 ± 16	15.2 ± 6.0	83 ± 15	0.05 ± 0.03	1.86 ± 0.47	86
3ℓ -Z-1b4j	1.58 ± 0.42	3.8 ± 1.3	2.4 ± 1.1	7.8 ± 1.6	0.14 ± 0.05	7.1 ± 1.6	8
3ℓ -Z-2b3j	1.29 ± 0.34	0.68 ± 0.33	0.19 ± 0.13	2.16 ± 0.42	0.21 ± 0.07	2.76 ± 0.69	3
3ℓ -Z-2b4j	1.00 ± 0.29	0.48 ± 0.24	0.42 ± 0.37	1.93 ± 0.49	0.14 ± 0.07	6.6 ± 1.6	11
3ℓ -noZ-2b	1.06 ± 0.25	0.27 ± 0.17	1.31 ± 0.90	2.7 ± 0.9	3.7 ± 0.9	1.23 ± 0.32	6
4ℓ -DF-0b	0.06 ± 0.01	0.11 ± 0.04	0.03 ± 0.17	0.21 ± 0.22	-	0.28 ± 0.01	2
4ℓ -DF-1b	0.22 ± 0.03	0.05 ± 0.03	0.13 ± 0.22	0.39 ± 0.27	-	1.05 ± 0.03	1
4ℓ -DF-2b	0.11 ± 0.02	<0.01	0.11 ± 0.19	0.22 ± 0.21	-	0.64 ± 0.02	1
4ℓ -ZZ*	0.01 ± 0.00	134.2 ± 1.2	0.27 ± 0.18	134.5 ± 1.3	-	0.07 ± 0.01	158
4ℓ -SF-1b	0.16 ± 0.02	0.29 ± 0.06	0.14 ± 0.19	0.61 ± 0.27	-	0.91 ± 0.02	2
4ℓ -SF-2b	0.08 ± 0.01	0.09 ± 0.03	0.04 ± 0.18	0.21 ± 0.23	-	0.64 ± 0.02	1

Table 4: Expected event yields for signal and backgrounds, and the observed data in all signal and control regions (marked with an asterisk) used in the fit to extract the $t\bar{t}W$ and $t\bar{t}Z$ cross sections. The quoted uncertainties on expected event yields represent systematic uncertainties including MC statistical uncertainties. The $t\bar{t}$, single-top, tZ , WtZ , $t\bar{t}H$ and $t\bar{t}t$ processes are denoted $t + X$. The Z , WW , WZ , ZZ , $t\bar{t}WW$ and $W^\pm W^\pm$ processes are denoted ‘Bosons’.

for the muon charge to be misidentified is found to be negligible, and Z +jets is not a dominant background in the $e\mu$ region.

Signal events from the $t\bar{t}W$ process are produced when the associated W boson decays leptonically and the $t\bar{t}$ system decays in the ℓ +jets channel.

A smaller contribution from $t\bar{t}Z$ comes from a leptonic decay of the Z boson where one lepton is not reconstructed, together with a leptonic decay of one of the two W bosons coming from the top quark decays.

The main backgrounds vary depending on the lepton flavour: events containing a lepton with misidentified charge are dominant in the $2e$ -SS region and prevalent in the $e\mu$ -SS region, whereas events with a fake lepton contribute significantly in all regions, but are dominant in the 2μ -SS region. Backgrounds from the production of prompt leptons with correctly identified charge come primarily from WZ production, but these are small compared to the instrumental backgrounds.

Processes featuring an opposite-sign lepton pair, like $t\bar{t}$ and Z boson production, can enter this channel through the misidentification of the electron charge. Charge misidentification rates, parameterised in

p_T and $|\eta|$ of the electrons, are measured in a control region containing events with two electrons with $75 < m_{ee} < 105$ GeV, which is divided into same-sign and opposite-sign subregions with non- $Z \rightarrow ee$ backgrounds subtracted. A likelihood function is constructed relating the number of observed events in the two subregions with the probability for an electron falling in a given $(p_T, |\eta|)$ bin to be reconstructed with the wrong charge, and maximised to obtain the charge misidentification rates.

A template is then constructed using opposite-sign data with event selection identical to that used in the signal region except for the requirement on the charge of the leptons. A weight given by

$$w = \frac{\varepsilon_1 + \varepsilon_2 - 2\varepsilon_1\varepsilon_2}{1 - (\varepsilon_1 + \varepsilon_2 - 2\varepsilon_1\varepsilon_2)} \quad (1)$$

is applied to each event and used to construct the template, where the charge misidentification rates for the two leptons are $\varepsilon_{1,2}$. These are set to zero in the case of muons.

To estimate the background from fake leptons in the same-sign dilepton channel a set of scale factors are measured. The scale factors are defined as $f = N_T/N_L$, the ratio of the number of observed tight leptons, i.e. leptons satisfying all selection criteria, to the number of loose leptons. Loose leptons differ from tight leptons in that they are required to fail isolation requirements; loose muons additionally have relaxed selection criteria, requiring $|z_0| < 2$ mm with no requirement on d_0 . The scale factors are measured in a control region (2ℓ -SS-CR) containing two same-sign leptons (vetoing events with a third lepton, as is done in the signal region), at least one b -tagged jet, and $H_T < 240$ GeV. The missing transverse momentum distributions in this control region are shown in Figure 4. A template for fake lepton backgrounds is

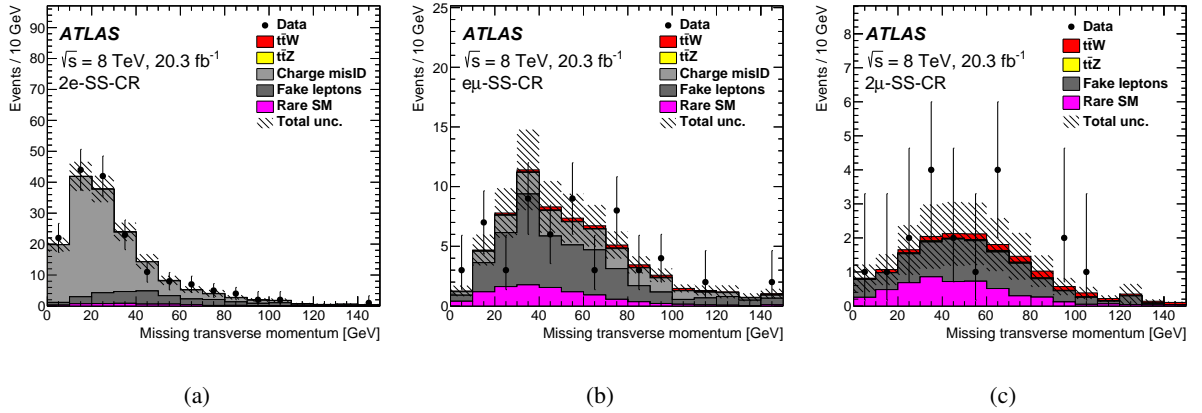


Figure 4: Distributions of E_T^{miss} for events in a same-sign dilepton control region with $H_T < 240$ GeV and at least one b -tagged jet for the different lepton flavour combinations, (a) ee , (b) $e\mu$ and (c) $\mu\mu$. “Rare SM” contains small background contributions mainly consisting of the WW and WZ processes. The predictions are shown before fitting to data in the control region. The instrumental backgrounds, including fake leptons and leptons with misidentified charge are predicted using data-driven methods. The hatched area corresponds to the total uncertainty on the predicted yields. The last bin in each histogram includes the overflow.

constructed in the control region from the loose lepton sample, using the expression

$$N_{\text{fake}} = \left[\sum_{N_{LT}} f_1 + \sum_{N_{TL}} f_2 - \sum_{N_{LL}} f_1 f_2 \right]_{\text{data}} - \left[\sum_{N_{LT}} f_1 + \sum_{N_{TL}} f_2 - \sum_{N_{LL}} f_1 f_2 \right]_{\text{MC,prompt}}, \quad (2)$$

where N_{TL} is the number of events in which the first lepton is a tight lepton and the second is loose, and N_{LT} , N_{LL} are defined in a similar fashion. The $f_{1,2}$ are the scale factors for the first and second leptons. A subtracted term, shown in the brackets labelled “MC, prompt” is included to remove contamination from prompt lepton production in the loose lepton sample. This subtraction accounts for about 2–3% of the total estimate. The background template for fake leptons is fitted to data in the control region in bins of lepton p_T to obtain the scale factors f_i , which are measured separately for electrons and muons and also binned in lepton p_T . With the measured scale factors, the background templates are produced in the signal region according to Eq. (2).

Potential overlap between the estimates of charge misidentification and fake leptons is taken into account with an additional subtraction step. A background template for fake leptons is produced for opposite-sign events (using a selection and binning otherwise the same as the signal region), and the charge misidentification rates are applied to this template to obtain a representation of the overlap of these two backgrounds. This new template is then subtracted from the total estimate of the fake lepton background. This subtraction represents about 2%–5% of the total yield.

To improve the separation of the $t\bar{t}W$ signal from backgrounds, events in the $e\mu$ -SS and 2μ -SS regions are further divided into four bins based on jet multiplicity and missing transverse momentum. Events are classified as low- N_{jets} ($N_{\text{jets}} = 2$ or 3) or high- N_{jets} ($N_{\text{jets}} \geq 4$) and low- E_T^{miss} ($40 < E_T^{\text{miss}} < 80$ GeV) or high- E_T^{miss} ($E_T^{\text{miss}} \geq 80$ GeV). No further event classification is used in the $2e$ -SS region. The expected and observed contributions in each of the three dilepton flavour regions are summarised in Table 4 and plotted in Figure 5.

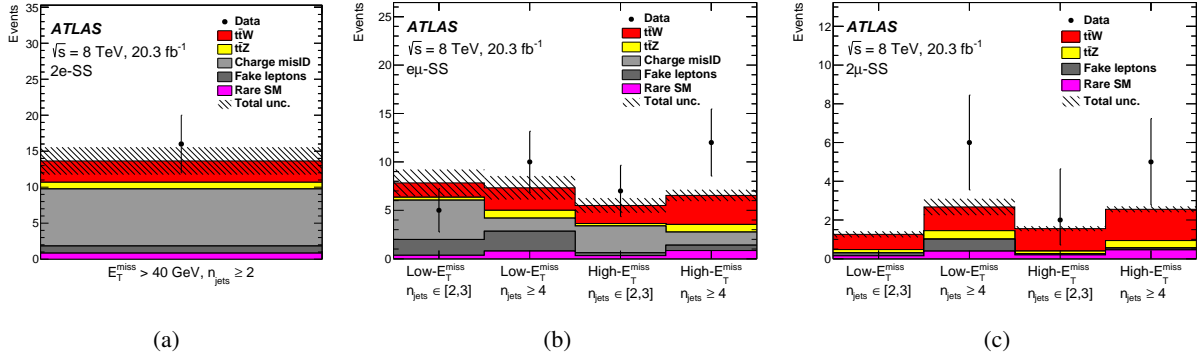


Figure 5: Event yields in the same-sign dilepton signal regions according to the binning used in the final likelihood fit in the (a) $2e$ -SS (b) $e\mu$ -SS and (c) 2μ -SS regions. The distributions are shown before the fit. The bins labelled “Low- E_T^{miss} ” correspond to $E_T^{\text{miss}} \in (40, 80)$ GeV, and those labelled “High- E_T^{miss} ” correspond to $E_T^{\text{miss}} \geq 80$ GeV. “Rare SM” contains small background contributions mainly consisting of the $t\bar{t}H$ and WZ processes. Instrumental backgrounds, including fake leptons and leptons with misidentified charge are predicted using data-driven methods. The hatched area corresponds to the total uncertainty on the predicted yields.

5.3 Trilepton channel

In the trilepton channel two preselections are considered, referred to as 3ℓ -Z and 3ℓ -noZ. The 3ℓ -Z region targets the $t\bar{t}Z$ process, while 3ℓ -noZ aims at measuring the $t\bar{t}W$ process. In the region 3ℓ -Z, at least one pair of leptons is required to have the opposite sign and same flavour (OSSF) and have an invariant

mass within 10 GeV of the Z boson mass. Region 3ℓ -noZ contains the remaining trilepton events with a requirement that the leptons must not all have the same sign.

The trilepton channel signal regions are determined as follows. First, the preselected samples are split into categories according to the jet multiplicity and the number of b -tagged jets. The categories with similar predicted signal-to-background ratio (S/B) and systematic uncertainties are grouped together. The final selection in each group is optimised for maximal expected significance, including both the statistical and systematic uncertainties, using requirements on $E_{\text{T}}^{\text{miss}}$ and lepton p_{T} . It is found that optimal significance is obtained without a requirement on $E_{\text{T}}^{\text{miss}}$.

Four signal regions are defined as a result of the grouping and optimisation: 3ℓ -Z-1b4j, 3ℓ -Z-2b3j, 3ℓ -Z-2b4j and 3ℓ -noZ-2b. In the 3ℓ -Z-1b4j region, at least four jets are required, exactly one of which is b -tagged. In the 3ℓ -Z-2b3j region, exactly three jets with at least two b -tagged jets are required. In the 3ℓ -Z-2b4j region at least four jets are required, of which at least two jets are b -tagged. In the 3ℓ -noZ-2b region at least two and at most three jets are required, of which at least two jets are b -tagged. For events in which the third leading lepton is an electron, the minimum p_{T} requirement on the third lepton is raised to 20 GeV in the 3ℓ -Z-1b4j, 3ℓ -Z-2b3j and 3ℓ -Z-2b4j regions, and to 25 GeV in the 3ℓ -noZ-2b region.

The 3ℓ -Z preselection is dominated by WZ events, with a significant contribution from events with fake leptons. To constrain the WZ background, a control region called 3ℓ -Z-0b3j is defined and included in the fit. In this region, the presence of exactly three jets, with exactly zero b -tags, is required in addition to the requirements of the 3ℓ -Z preselection. The normalisation correction for the WZ background with respect to the Standard Model expectations is obtained from the fit and found to be 0.98 ± 0.20 . The quoted uncertainty includes both the statistical and systematic components. The modelling of WZ production in association with heavy-flavour jets is further validated in a control region 3ℓ -Z-1b-CR, defined by requiring the presence of one to three jets, exactly one of which is b -tagged.

The fake lepton background is estimated by using the so-called matrix method [71], which makes use of an orthogonal control region in which lepton isolation and electron identification criteria are relaxed. The efficiencies for real and fake leptons used in the matrix method are measured in events containing two leptons and one b -tagged jet. To validate the estimate of the background containing fake leptons, a control region 3ℓ -noZ-1b-CR is defined by requiring exactly one jet to be b -tagged in addition to the requirements of the 3ℓ -noZ region. Figure 6 shows distributions of $E_{\text{T}}^{\text{miss}}$ and third-lepton p_{T} in the 3ℓ -noZ-1b-CR and 3ℓ -Z-1b-CR regions, respectively. The level of agreement between data and expectation is good.

The signal and control regions of the trilepton channel used in the fit are summarised in Table 5. The expected and observed yields in the signal and control regions are shown in Table 4. Event yields summarising the signal regions with different lepton flavour combinations (3ℓ -Z-SR) and the distribution of the minimum invariant mass of jet triplets (minimum m_{jjj}) for events in the 3ℓ -Z-2b4j region are shown in Figure 7. Considering the four leading jets, the momentum vector sum of the minimum invariant jet triplet mass is found to give a powerful estimate of the hadronically decaying top direction. Good agreement between data and expectation is observed.

5.4 Tetralepton channel

The tetralepton channel targets the $t\bar{t}Z$ process for the case where both W bosons resulting from top quark decays and the Z boson decay leptonically, and uses an event counting approach in five signal regions. Events with two pairs of opposite-sign leptons are selected, among which at least one pair is same flavour.

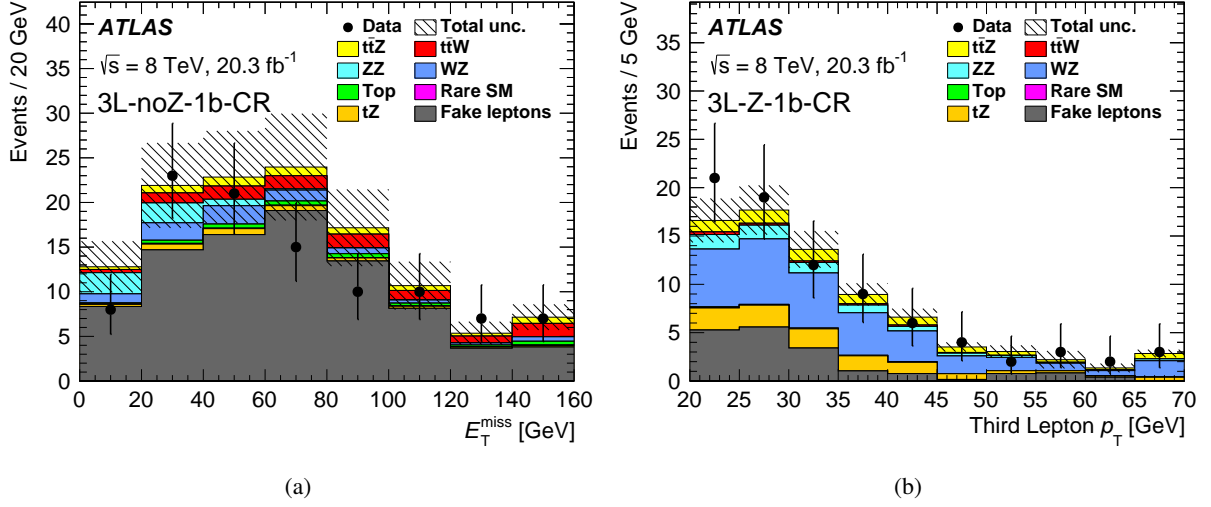


Figure 6: Distributions of (a) E_T^{miss} in the $3\ell\text{-noZ-1b}$ region and (b) third-lepton p_T in the $3\ell\text{-Z-1b}$ region. “Rare SM” contains small background contributions consisting of the WWW , WWZ , $H \rightarrow ZZ$ and $t\bar{t}WW$ processes. The hatched area corresponds to the total uncertainty on the predicted yields. The distributions are shown before the fit. The last bin in each histogram includes the overflow.

Region	Targeting	Sample fraction [%]
$3\ell\text{-Z-1b4j}$		47
$3\ell\text{-Z-2b3j}$	$t\bar{t}Z$	54
$3\ell\text{-Z-2b4j}$		76
$3\ell\text{-noZ-2b}$	$t\bar{t}W$	48
$3\ell\text{-Z-0b3j}$	WZ	68

Table 5: Signal and control regions of the trilepton channel used in the fit, together with the processes targeted and the expected fraction of the sample represented by the targeted process.

The OSSF lepton pair with reconstructed invariant mass closest to m_Z is attributed to the Z boson decay and denoted in the following as Z_1 . The two remaining leptons are used to define Z_2 . The signal regions are defined according to the relative flavour of the two remaining leptons, different or same flavour, and the number of b -tagged jets: zero, one, or at least two ($0b$, $1b$, $2b$). The signal regions are thus $4\ell\text{-DF-0b}$, $4\ell\text{-DF-1b}$, $4\ell\text{-DF-2b}$, $4\ell\text{-SF-1b}$ and $4\ell\text{-SF-2b}$. The ZZ background mostly affects the SF regions and therefore events with a Z_2 SF lepton pair and no b -tagged jets are discarded.

Further requirements are applied in each signal region such that the expected statistical uncertainty on the measured $t\bar{t}Z$ signal cross section is minimised. Events in the $4\ell\text{-SF-1b}$ region are rejected if they are compatible with a ZZ event, i.e. if $E_T^{\text{miss}} < 80$ (40) GeV for m_{Z_2} inside (outside) a 10 GeV region centred at the Z boson mass. This requirement on E_T^{miss} is relaxed by 40 GeV for the $4\ell\text{-SF-2b}$ region. The impact of events with fake leptons decreases with the number of reconstructed b -tagged jets. To suppress these backgrounds, additional requirements on the scalar sum of the transverse momenta of the third and fourth leptons (p_{T34}) are imposed in the lower b -tag multiplicity regions. In the $4\ell\text{-SF-1b}$, $4\ell\text{-DF-1b}$ and $4\ell\text{-DF-0b}$ regions events are required to satisfy $p_{T34} > 25$ GeV, $p_{T34} > 35$ GeV and $p_{T34} > 45$ GeV,

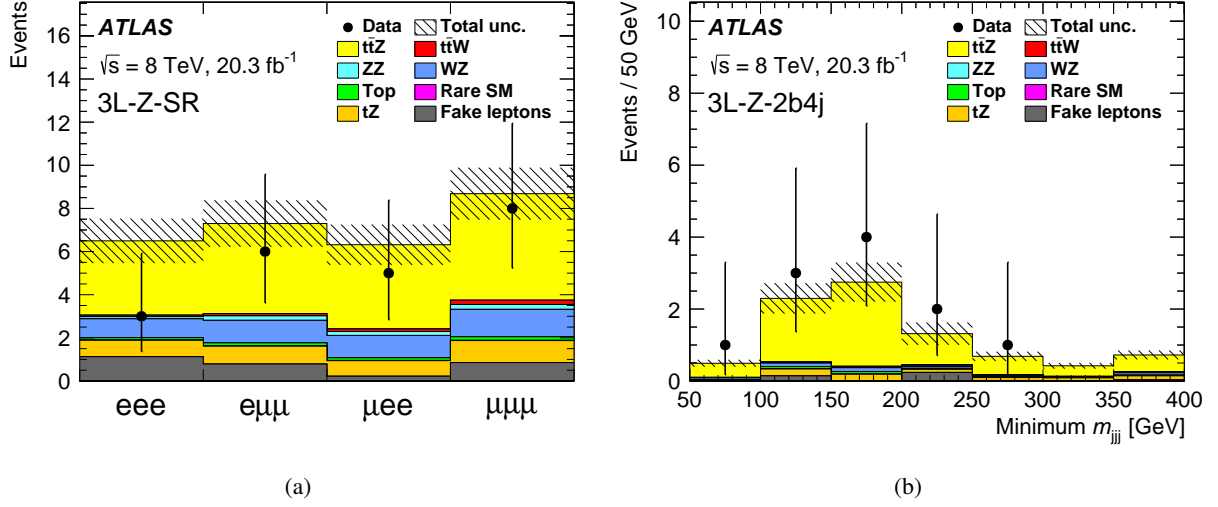


Figure 7: (a) Event yields in the trilepton channel summarising the signal regions with different lepton flavour combinations and (b) the minimum three-jet invariant mass for events in the 3ℓ -Z-2b4j signal region. “Rare SM” contains small background contributions consisting of the WWW , WWZ , $H \rightarrow ZZ$ and $t\bar{t}WW$ processes. The distributions are shown before the fit. The hatched area corresponds to the total uncertainty on the predicted yields. The last bin in (b) includes the overflow.

respectively. In the 4ℓ -DF-0b region the requirement on the fourth lepton is raised to $p_T > 10$ GeV and at least two jets must be reconstructed in the event. In all regions, the invariant mass of any two reconstructed OS leptons is required to be larger than 10 GeV. The definitions of the signal regions are summarised in Table 6.

Region	Z_2 leptons	p_{T4}	p_{T34}	$ m_{\ell\ell} - m_{Z_2} $	E_T^{miss}	N_{jets}	$N_{b\text{-jets}}$
4ℓ -DF-0b	$e^\pm\mu^\mp$	> 10 GeV	> 45 GeV	-	-	≥ 2	0
4ℓ -DF-1b	$e^\pm\mu^\mp$	> 7 GeV	> 35 GeV	-	-	-	1
4ℓ -DF-2b	$e^\pm\mu^\mp$	> 7 GeV	-	-	-	-	≥ 2
4ℓ -SF-1b	$e^\pm e^\mp, \mu^\pm\mu^\mp$	> 7 GeV	> 25 GeV	$\left\{ \begin{array}{l} > 10 \text{ GeV} \\ < 10 \text{ GeV} \end{array} \right\}$	$\left\{ \begin{array}{l} > 40 \text{ GeV} \\ > 80 \text{ GeV} \end{array} \right\}$	-	1
4ℓ -SF-2b	$e^\pm e^\mp, \mu^\pm\mu^\mp$	> 7 GeV	-	$\left\{ \begin{array}{l} > 10 \text{ GeV} \\ < 10 \text{ GeV} \end{array} \right\}$	$\left\{ \begin{array}{l} - \\ > 40 \text{ GeV} \end{array} \right\}$	-	≥ 2

Table 6: Definitions of the five signal regions in the tetralepton channel.

The ZZ background is large in the tetralepton channel, and therefore a control region, 4ℓ -ZZ, is defined to constrain the ZZ normalisation in the SF region, and is included in the fit. Both lepton pairs are required to satisfy $|m_{Z_{1,2}} - m_Z| < 10$ GeV, and events are retained if $E_T^{\text{miss}} < 50$ GeV. The fitted normalisation correction with respect to the Standard Model expectation is 1.16 ± 0.12 . The quoted uncertainties include both the statistical and systematic components. The number of jets and b -tagged jets in the 4ℓ -ZZ region are shown in Figure 8. Data distributions agree with expectations from simulation.

The tetralepton channel backgrounds with at least one fake lepton are estimated using simulation, where

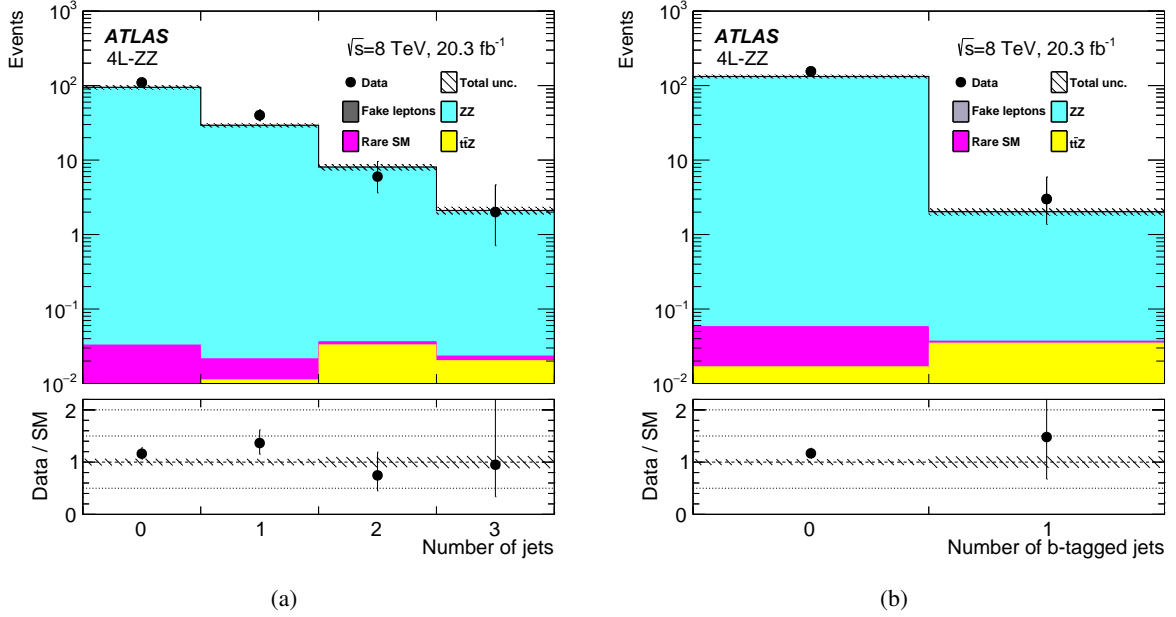


Figure 8: Distributions of (a) the number of jets and (b) the number of b -tagged jets in the ZZ control region of the tetralepton channel 4ℓ - ZZ . The hatched area corresponds to the total uncertainty on the predicted yields. The distributions are shown before the fit. “Rare SM” contains small background contributions mainly consisting of the WtZ and $t\bar{t}H$ processes. The “Data/SM” plots show the ratio of the data events to the total Standard Model expectation.

the prediction is corrected with a constant factor to improve agreement in control regions with enhanced fraction of single fake leptons. By probing the fake muon and electron background in a Z +fake-lepton-candidate control region and in a $t\bar{t}$ +fake-lepton-candidate region, two equations per lepton flavour f can be constructed and the correction factors c_f^{CR} for these two processes can be determined: $c_e^{t\bar{t}} = 1.23 \pm 0.13$, $c_\mu^{t\bar{t}} = 1.25 \pm 0.09$, $c_e^Z = 1.35 \pm 0.05$, and $c_\mu^Z = 1.61 \pm 0.05$. The quoted uncertainties include systematic effects. The control regions are required to contain three leptons and are either Z - or $t\bar{t}$ -like. In the first case an OSSF lepton pair is required together with $E_T^{\text{miss}} < 30$ GeV. In addition, the transverse mass of the non- Z_1 lepton ℓ is required to satisfy $m_T < 35$ GeV, where m_T is defined as

$$m_T = \sqrt{2p_T^\ell E_T^{\text{miss}} - 2\mathbf{p}_T^\ell \cdot \mathbf{p}_T^{\text{miss}}}. \quad (3)$$

The non- Z_1 lepton is then used as the fake lepton candidate. In the second case an OS lepton pair is required together with at least one jet with $p_T > 30$ GeV, and events with an OSSF lepton pair are rejected. The lowest- p_T same-sign lepton is then used as the candidate. The background from events with two fake leptons is evaluated from simulation with relaxed requirements and extrapolated in several steps into the signal region. The total background yield and its uncertainty are dominated by the estimate extracted from simulation of trilepton events with only one additional fake lepton.

The expected sample composition of the six tetralepton regions is summarised in Table 4 along with the number of events observed in data. Seven events are observed in the five signal regions (4L-SR). Figure 9 shows good agreement between data and expectation for the distributions of the number of jets, number of b -tagged jets, as well as the invariant masses of the two pairs of leptons.

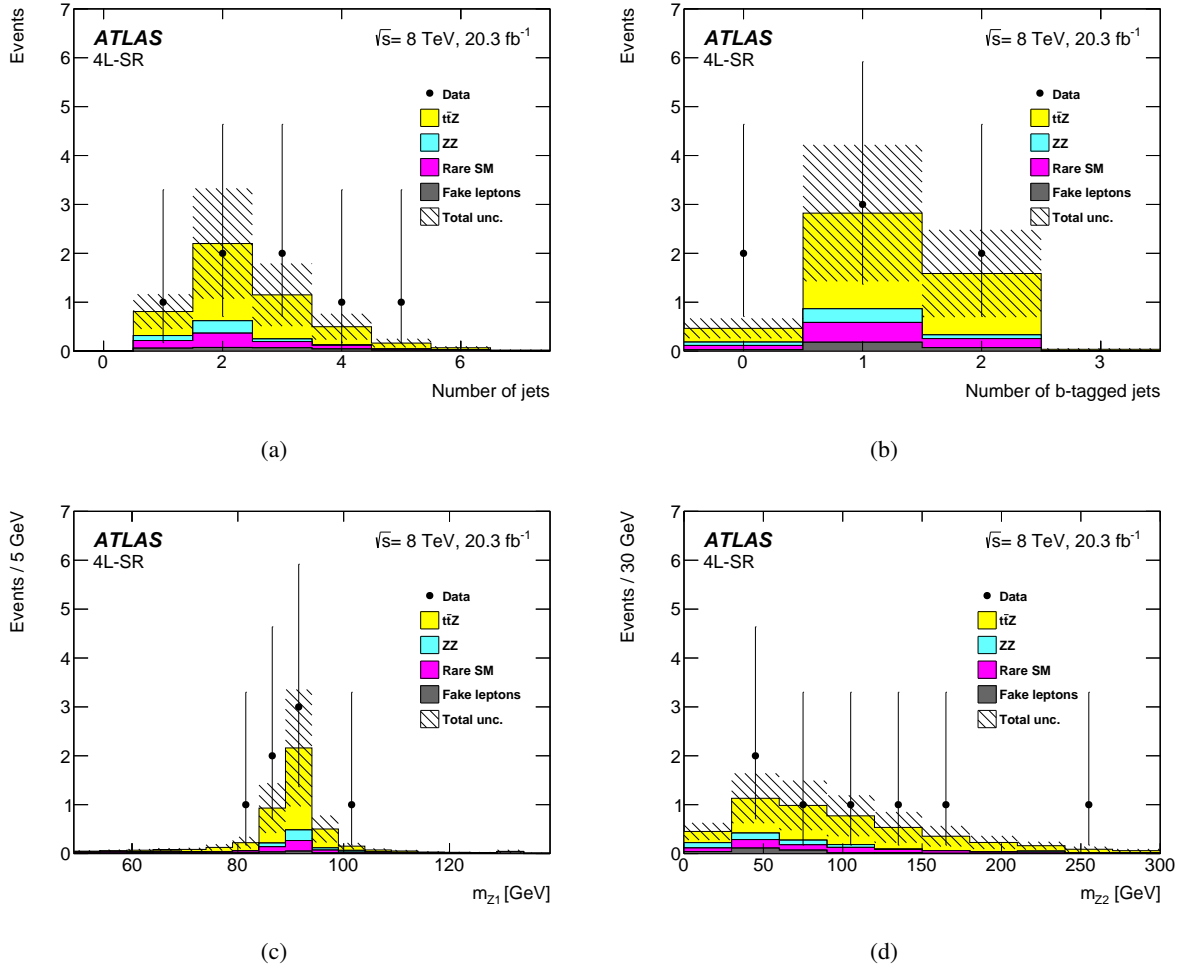


Figure 9: Distributions of (a) number of jets, (b) number of b -tagged jets, invariant mass of the (c) Z_1 and (d) Z_2 dilepton pair for the tetralepton signal region selection. The distributions are shown before the fit. The distributions of the seven observed events are compared to expectation. The hatched area corresponds to the total uncertainty on the predicted yields. “Rare SM” contains small background contributions mainly consisting of the WtZ and $t\bar{t}H$ processes.

6 Systematic uncertainties

Several sources of systematic uncertainty are considered that can affect the normalisation of signal and background in each channel and/or the shape of the discriminant distributions in the opposite-sign dilepton channel.

The luminosity estimate has an uncertainty of 2.8%, determined using beam-separation scans [72]. This systematic uncertainty is assigned to all background contributions obtained from MC simulation.

6.1 Uncertainties on reconstructed objects

Uncertainties associated with the lepton selection arise from the imperfect knowledge of the trigger, reconstruction, identification and isolation efficiencies, and lepton momentum scale and resolution. The uncertainty on the electron identification efficiency is the largest systematic uncertainty in the trilepton channel and among the most important ones in the tetralepton channel.

Uncertainties associated with the jet selection arise from the jet energy scale (JES), JVF requirement, jet energy resolution (JER) and jet reconstruction efficiency. The JES and its uncertainty are derived combining information from test-beam data, collision data and simulation [63]. JES uncertainty components arising from the in-situ calibration and the jet flavour composition are among the dominant uncertainties in the opposite-sign dilepton, same-sign dilepton and trilepton channels. The uncertainties in the JER and JVF have a significant effect at low jet p_T . The JER uncertainty is the second largest uncertainty in the trilepton channel while the JVF uncertainty is not negligible in the opposite-sign dilepton, trilepton and tetralepton channels.

The efficiency of the flavour tagging algorithm is measured for each jet flavour using control samples in data and in simulation. From these measurements, correction factors are defined to correct the tagging rates in the simulation. In the case of b -jets, correction factors and their uncertainties are estimated based on observed and simulated b -tagging rates in $t\bar{t}$ dilepton events [65]. In the case of c -jets, they are derived based on jets with identified D^* mesons [73]. In both cases the correction factors are parameterised as a function of jet p_T . In the case of light-flavour jets, correction factors are derived using dijet events, and are parameterised as a function of jet p_T and η [73]. Sources of uncertainty affecting the b - and c -tagging efficiencies are considered as a function of jet p_T , including bin-to-bin correlations [65]. An additional uncertainty is assigned to account for the extrapolation of the b -tagging efficiency measurement from the p_T region used to determine the scale factors to regions with higher p_T . For the light-jet tagging efficiency the dependence of the uncertainty on the jet p_T and η is considered. These systematic uncertainties are taken as uncorrelated between b -jets, c -jets, and light-flavour jets.

The treatment of the uncertainties on reconstructed objects is common to all four channels, and thus these are considered as correlated among different regions.

6.2 Uncertainties on signal modelling

To assess the factorisation and renormalisation scale uncertainties on $t\bar{t}V$ modelling, the scales are varied up and down by a factor of two in a correlated manner. Radiation uncertainties are assessed by simultaneously varying the scale of the momentum transfer Q in the running strong coupling $\alpha_S(Q^2)$ in the matrix-element calculation and in the PYTHIA parton shower, up or down by a factor of two [74].

In addition, the jet p_T matching threshold and the amount of radiation in the parton shower are independently varied up and down by a factor of two. The dominant systematic uncertainty comes from the variation of Q in $\alpha_S(Q^2)$ in the matrix element calculation and in the PYTHIA parton shower. This variation has a significant effect on the distribution of the number of jets in $t\bar{t}V$ events.

Systematic uncertainties due to the choice of PDF are evaluated using the uncertainty sets of the CT10 NLO, MSTW2008 68% confidence level (CL) NLO and NNPDF 2.3 NLO [75] PDFs following the PDF4LHC recommendations [76].

The uncertainties on the $t\bar{t}V$ modelling are among the dominant ones in the tetralepton channel but they have a negligible impact in all other channels. Signal modelling and PDF uncertainties are treated as correlated among channels.

6.3 Uncertainties on background modelling

Uncertainties on the background modelling differ significantly among the channels due to large differences in the background composition.

Z boson background: This dominates in the 2ℓ -Z regions of the opposite-sign dilepton channel. Four sources of uncertainty are considered: those associated with the cross section, the Z boson p_T correction, the scale choice for parton emission, and the choice of generator, evaluated by comparing the nominal ALPGEN sample to a SHERPA sample generated using SHERPA 1.4.1 with up to three additional partons in the LO matrix element and the CT10 PDF set.

$t\bar{t}$ background: This dominates in the 2ℓ -noZ regions of the opposite-sign dilepton channel. A number of systematic uncertainties affecting the modelling of the $t\bar{t}$ process are considered in this channel: those due to the uncertainty on the cross section which amount to $+5\%/ -6\%$, due to the choice of parton shower and hadronisation model (evaluated by comparing events produced by POWHEG interfaced with PYTHIA or HERWIG [77]), due to the choice of generator (evaluated by comparing a sample generated using MADGRAPH interfaced with PYTHIA to the default $t\bar{t}$ sample), and due to the reweighting procedure applied to correct the $t\bar{t}$ MC modelling. An additional 50% normalisation uncertainty is assigned to $t\bar{t}$ +heavy-flavour (HF) jets production to account for limited knowledge of this process.

Single-top background: This is small and affects only the opposite-sign dilepton channel. An uncertainty of 6.8% is assigned to the cross section for single-top production [42], corresponding to the theoretical uncertainty on Wt production, the only process contributing to this final state. An additional contribution arises from the comparison of predictions using different schemes to account for interference between Wt and $t\bar{t}$.

Diboson background: In the trilepton and same-sign dilepton channels the diboson background is dominated by WZ production, while in the tetralepton channel ZZ production is dominant. In the opposite-sign dilepton channel the diboson background includes WW , WZ and ZZ production and the uncertainties are assigned to the sum of these processes.

In the trilepton and same-sign dilepton channels, the normalisation of the WZ background is treated as a floating parameter in the fit used to extract the $t\bar{t}V$ signal. The uncertainty on the extrapolation of the WZ background estimate from the control region to signal regions with specific jet and b -tag multiplicities is evaluated by comparing the nominal SHERPA sample to the prediction of POWHEG, as well as by using variations of the simulation parameters. The uncertainty amounts to 20%–35%.

In the tetralepton, trilepton and same-sign dilepton channels the normalisation of the ZZ background is treated as a floating parameter in the fit used to extract the $t\bar{t}V$ signal. In the tetralepton channel, several uncertainties on the ZZ background estimate are considered. They arise from the extrapolation from the 4ℓ - ZZ control region (corresponding to on-shell ZZ production) to the signal region (with off-shell ZZ background) and from the extrapolation from the control region without jets to the signal region with at least one jet. Using data-driven techniques, these uncertainties are found to be 30% and 20%, respectively. An additional uncertainty of 10%–30% is assigned to the normalisation of the heavy-flavour content of the ZZ background based on a data-to-simulation comparison of events with one Z boson and additional jets, and cross-checked with a comparison between different ZZ simulations.

In the opposite-sign dilepton channel, in which the diboson background is small, a 20% uncertainty is assigned to the WZ and ZZ background normalisation. This is estimated from the level of agreement between data and prediction in the 3ℓ - Z -0 b 3 j control region.

$t\bar{t}H$ background: An uncertainty of 12% is assigned to the $t\bar{t}H$ production cross section [47] in all channels. Additional uncertainties that affect $t\bar{t}H$ kinematics are assigned in the opposite-sign dilepton channel and are negligible for the other channels. These uncertainties come from the choice of factorisation and renormalisation scales, and the functional form of the scale in $t\bar{t}H$ samples.

tZ and WtZ background: In the opposite-sign dilepton and trilepton channels, tZ and WtZ backgrounds are summed and an uncertainty of 20% is assigned to their cross section. An additional uncertainty on the shape of this background is considered in the trilepton channel for which this background is important. The shape uncertainty is evaluated by varying the factorisation and renormalisation scales and α_S in simulation up and down by a factor of two with respect to the nominal value, in a correlated manner. The α_S variation has the largest effect, ranging from 10% to 20% depending on the number of jets and b -jets.

The WtZ background is important in the tetralepton channel. An uncertainty of 10% is assigned to the cross section, coming from the variation of renormalisation and factorisation scales. An additional uncertainty arises from the modelling of the additional jet in WtZ events. It is evaluated by varying parameters in simulation as described above.

Other prompt lepton backgrounds: Uncertainties of 20% are assigned to the normalisations of the WH and ZH processes, based on calculations from Ref. [78]. An uncertainty of 100% is considered for triboson and same-sign WW processes.

Misidentified lepton charge background: This affects mainly the $2e$ -SS and $e\mu$ -SS regions. Uncertainties on it arise from a variety of statistical and systematic effects. The main uncertainty comes from the limited statistical precision in the measurement of charge misidentification rates. These are treated as correlated among all p_T and $|\eta|$ bins, but uncorrelated between the $2e$ -SS and $e\mu$ -SS regions. This approach is comparable to treating each binned rate measurement as uncorrelated. Additional systematic uncertainties arise from the background subtraction in the $Z \rightarrow ee$ sample used to measure charge misidentification rates and from the difference in charge misidentification rates between $Z \rightarrow ee$ and $t\bar{t}$ events. The latter are evaluated by measuring charge misidentification rates in $Z \rightarrow ee$ MC events, assigning them to $t\bar{t}$ simulated events and comparing the prediction to the number of true charge-misidentified events in the $t\bar{t}$ sample. This uncertainty is found to be 10%.

Fake lepton background: This is important in the same-sign dilepton, trilepton, and tetralepton channels. The uncertainty on this background is estimated by propagating the statistical uncertainty on the measurement of the fake lepton efficiencies. Additionally, the normalisation of backgrounds in the control regions (from prompt leptons or charge-misidentified electrons) is varied to estimate a systematic uncertainty on these efficiencies. The variation assigned (20–25%) depends on the composition of each control region, and is chosen to conservatively cover the largest uncertainty on the backgrounds. In the trilepton channel an additional uncertainty is considered by measuring the rates of real and fake leptons in two orthogonal regions, one with three or more jets and the other with one or two jets. In the same-sign dilepton channel, statistical uncertainties are dominant and no further systematic uncertainties are considered. All uncertainties associated with fake leptons are considered to be uncorrelated among analysis channels and regions.

In the opposite-sign dilepton channel the fake lepton background is small compared to the other background contributions. An uncertainty of 50% is assigned to the fake lepton yield across all regions in this channel to cover the maximum difference between yields obtained from the simulation and from same-sign dilepton events in data. An additional uncertainty is assigned to cover the difference in shape of the distribution of the scalar sum of the transverse momenta of all reconstructed jets and charged leptons in the simulated and same-sign data events.

7 Results

The observed yields in the 15 signal and 5 control regions are shown together with the expected numbers of events in Table 4.

The production cross sections $\sigma_{t\bar{t}W}$ and $\sigma_{t\bar{t}Z}$ are determined simultaneously using a binned maximum-likelihood fit over all regions and discriminant bins considered in the analysis. The fit is based on the profile likelihood technique, in which the systematic uncertainties are treated as nuisance parameters with prior uncertainties that can be constrained by the fit. The calculation of confidence intervals and hypothesis testing is performed using a modified frequentist method as implemented in RooStats [79, 80]. Significance is calculated using the asymptotic formula of Ref. [81].

A summary of the fit to all four channels with their corresponding fit regions used to measure the $t\bar{t}W$ and $t\bar{t}Z$ production cross sections is shown in Figure 10. The normalisations of the WZ and ZZ processes are determined as well, as described in Sections 5.3 and 5.4.

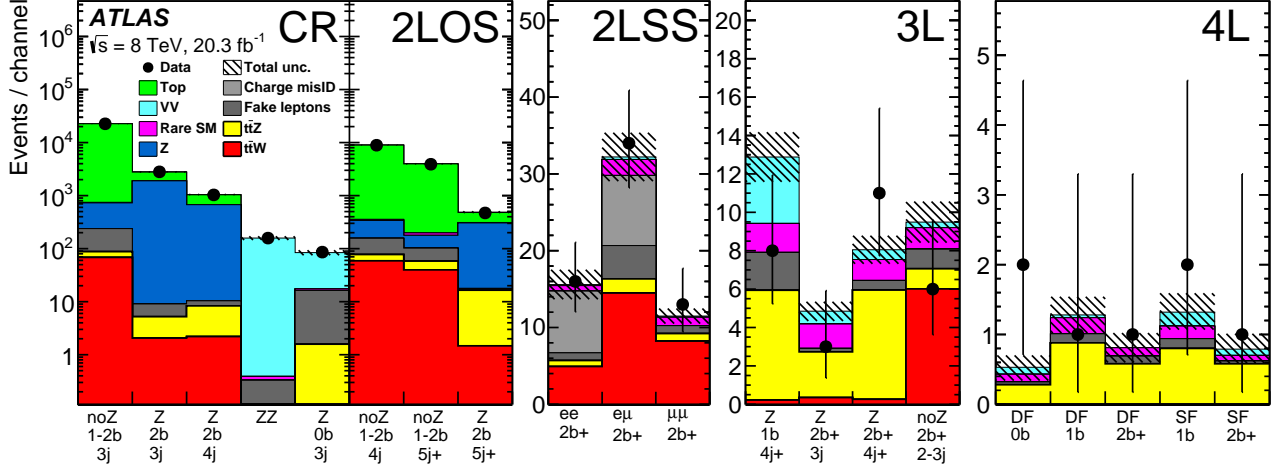


Figure 10: Expected yields after the fit compared to data in the five control regions (CR), used to constrain the $t\bar{t}$, Z , ZZ and WZ backgrounds, the three signal regions in the opposite-sign dilepton channel (2LOS), the three signal regions in the same-sign dilepton channel (2LSS), the four signal regions in the trilepton channel (3L) and the five signal regions in the tetralepton channel (4L). In the two dilepton channels the fit also includes shape information. The “Rare SM” background summarises all other backgrounds described in Section 3 and mainly consists of the $t\bar{t}H$, $t\bar{t}Z$ and WtZ processes, which are the largest contributions to this background category in the dilepton, trilepton and tetralepton channels, respectively. The hatched area corresponds to the total uncertainty on the predicted yields.

Table 7 provides a breakdown of the total uncertainties on the measured $t\bar{t}W$ and $t\bar{t}Z$ cross sections, determined by fitting each signal individually with the other fixed to its expected SM value. For both processes, the precision of the measurement is dominated by statistical uncertainties. For the $t\bar{t}W$ fit, the dominant systematic uncertainty source is the modelling of fake leptons and background processes with misidentified charge. For the $t\bar{t}Z$ fit, the dominant systematic uncertainty source is the modelling of backgrounds from simulation.

Uncertainty	$\sigma_{t\bar{t}W}$	$\sigma_{t\bar{t}Z}$
Luminosity	3.2%	4.6%
Reconstructed objects	3.7%	7.4%
Backgrounds from simulation	5.8%	8.0%
Fake leptons and charge misID	7.5%	3.0%
Signal modelling	1.8%	4.5%
Total systematic	12%	13%
Statistical	+24% / -21%	+30% / -27%
Total	+27% / -24%	+33% / -29%

Table 7: Breakdown of uncertainties on the measured cross sections of the $t\bar{t}W$ and $t\bar{t}Z$ processes from individual fits. Systematic uncertainties are symmetrised.

The sensitivity to the $t\bar{t}W$ process is dominated by the same-sign dilepton channel, while the $t\bar{t}Z$ process is mainly measured in the trilepton and tetralepton channels. The result of the simultaneous fit of the $t\bar{t}W$

Channel	$t\bar{t}W$ significance		$t\bar{t}Z$ significance	
	Expected	Observed	Expected	Observed
$2\ell OS$	0.4	0.1	1.4	1.1
$2\ell SS$	2.8	5.0	-	-
3ℓ	1.4	1.0	3.7	3.3
4ℓ	-	-	2.0	2.4
Combined	3.2	5.0	4.5	4.2

Table 8: Expected and observed signal significances for the $t\bar{t}W$ and $t\bar{t}Z$ processes determined from the fit to the separate channels and from the combined fit to all channels. The significance for each signal process is calculated assuming the null hypothesis for the process in question and treating the other as a free parameter in the fit.

and $t\bar{t}Z$ processes using all four channels is summarised in Table 8. The observed (expected) significance of the measurements are 5.0σ (3.2σ) for the $t\bar{t}W$ process and 4.2σ (4.5σ) for the $t\bar{t}Z$ process. The background-only hypothesis with neither $t\bar{t}Z$ nor $t\bar{t}W$ production is excluded at 7.1σ (5.9σ).

The result of the combined simultaneous fit to the two parameters of interest is

$$\sigma_{t\bar{t}W} = 369^{+86}_{-79} \text{ (stat.)} \pm 44 \text{ (syst.) fb} = 369^{+100}_{-91} \text{ fb} \quad (4)$$

and

$$\sigma_{t\bar{t}Z} = 176^{+52}_{-48} \text{ (stat.)} \pm 24 \text{ (syst.) fb} = 176^{+58}_{-52} \text{ fb.} \quad (5)$$

Figure 11 provides a comparison of these measurements with NLO QCD theoretical calculations using MADGRAPH5_AMC@NLO.

8 Conclusion

Measurements of the production cross sections of a top quark pair in association with a W or Z boson using 20.3 fb^{-1} of data collected by the ATLAS detector in $\sqrt{s} = 8 \text{ TeV}$ pp collisions at the LHC have been presented. Final states with two, three or four charged leptons are analysed. From a simultaneous fit to 15 signal regions and 5 control regions, the $t\bar{t}W$ and $t\bar{t}Z$ production cross sections are measured to be $\sigma_{t\bar{t}W} = 369^{+100}_{-91} \text{ fb}$ and $\sigma_{t\bar{t}Z} = 176^{+58}_{-52} \text{ fb}$. The fit to the data considering both signal processes simultaneously yields significances of 5.0σ and 4.2σ over the background-only hypothesis for the $t\bar{t}W$ and $t\bar{t}Z$ processes, respectively. All measurements are consistent with the NLO QCD theoretical calculations for $t\bar{t}W$ and $t\bar{t}Z$ processes.

Acknowledgements

We thank CERN for the very successful operation of the LHC, as well as the support staff from our institutions without whom ATLAS could not be operated efficiently.

We acknowledge the support of ANPCyT, Argentina; YerPhI, Armenia; ARC, Australia; BMWFW and FWF, Austria; ANAS, Azerbaijan; SSTC, Belarus; CNPq and FAPESP, Brazil; NSERC, NRC and

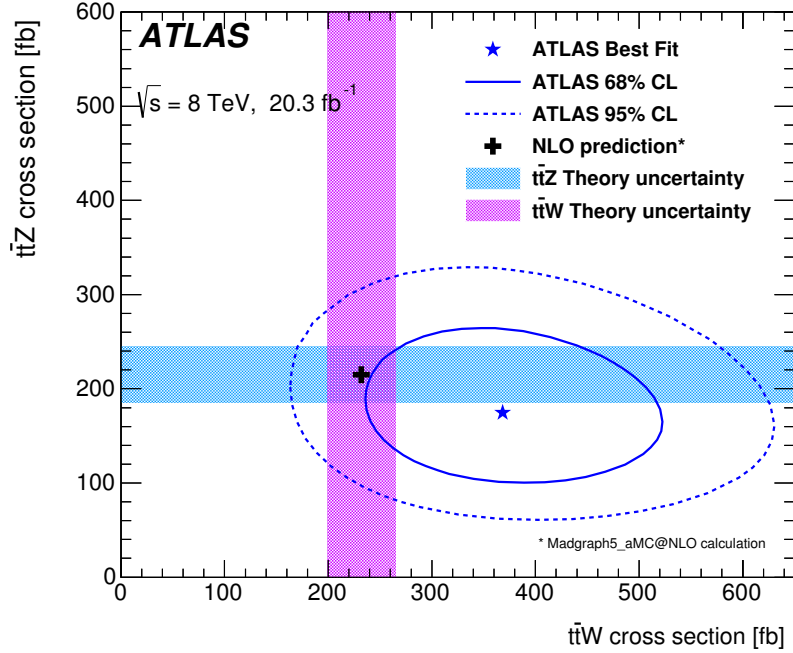


Figure 11: The result of the simultaneous fit to the $t\bar{t}W$ and $t\bar{t}Z$ cross sections along with the 68% and 95% CL uncertainty contours. The shaded areas correspond to 14% uncertainty, which includes renormalisation and factorisation scale uncertainties as well as PDF uncertainties including α_S variations.

CFI, Canada; CERN; CONICYT, Chile; CAS, MOST and NSFC, China; COLCIENCIAS, Colombia; MSMT CR, MPO CR and VSC CR, Czech Republic; DNRF, DNSRC and Lundbeck Foundation, Denmark; IN2P3-CNRS, CEA-DSM/IRFU, France; GNSF, Georgia; BMBF, HGF, and MPG, Germany; GSRT, Greece; RGC, Hong Kong SAR, China; ISF, I-CORE and Benoziyo Center, Israel; INFN, Italy; MEXT and JSPS, Japan; CNRST, Morocco; FOM and NWO, Netherlands; RCN, Norway; MNiSW and NCN, Poland; FCT, Portugal; MNE/IFA, Romania; MES of Russia and NRC KI, Russian Federation; JINR; MESTD, Serbia; MSSR, Slovakia; ARRS and MIZŠ, Slovenia; DST/NRF, South Africa; MINECO, Spain; SRC and Wallenberg Foundation, Sweden; SERI, SNSF and Cantons of Bern and Geneva, Switzerland; MOST, Taiwan; TAEK, Turkey; STFC, United Kingdom; DOE and NSF, United States of America. In addition, individual groups and members have received support from BCKDF, the Canada Council, CANARIE, CRC, Compute Canada, FQRNT, and the Ontario Innovation Trust, Canada; EPLANET, ERC, FP7, Horizon 2020 and Marie Skłodowska-Curie Actions, European Union; Investissements d’Avenir Labex and Idex, ANR, Region Auvergne and Fondation Partager le Savoir, France; DFG and AvH Foundation, Germany; Herakleitos, Thales and Aristeia programmes co-financed by EU-ESF and the Greek NSRF; BSF, GIF and Minerva, Israel; BRF, Norway; the Royal Society and Leverhulme Trust, United Kingdom.

The crucial computing support from all WLCG partners is acknowledged gratefully, in particular from CERN and the ATLAS Tier-1 facilities at TRIUMF (Canada), NDGF (Denmark, Norway, Sweden), CC-IN2P3 (France), KIT/GridKA (Germany), INFN-CNAF (Italy), NL-T1 (Netherlands), PIC (Spain), ASGC (Taiwan), RAL (UK) and BNL (USA) and in the Tier-2 facilities worldwide.

References

- [1] F. Abe et al. (CDF Collaboration), *Observation of top quark production in $p\bar{p}$ collisions*, *Phys. Rev. Lett.* **74** (1995) 2626, arXiv:[hep-ex/9503002](#).
- [2] S. Abachi et al. (D0 Collaboration), *Observation of the top quark*, *Phys. Rev. Lett.* **74** (1995) 2632, arXiv:[hep-ex/9503003](#).
- [3] R. S. Chivukula, S. B. Selipsky and E. H. Simmons, *Nonoblique effects in the $Zb\bar{b}$ vertex from ETC dynamics*, *Phys. Rev. Lett.* **69** (1992) 575, arXiv:[hep-ph/9204214](#).
- [4] R. Chivukula, E. H. Simmons and J. Terning, *A Heavy top quark and the $Zb\bar{b}$ vertex in noncommuting extended technicolor*, *Phys. Lett. B* **331** (1994) 383, arXiv:[hep-ph/9404209](#).
- [5] K. Hagiwara and N. Kitazawa, *Extended technicolor contribution to the Zbb vertex*, *Phys. Rev. D* **52** (1995) 5374, arXiv:[hep-ph/9504332](#).
- [6] U. Mahanta, *Noncommuting ETC corrections to $Zt\bar{t}$ vertex*, *Phys. Rev. D* **55** (1997) 5848, arXiv:[hep-ph/9611289](#).
- [7] U. Mahanta, *Probing noncommuting ETC effects by $e^+e^- \rightarrow t\bar{t}$ at NLC*, *Phys. Rev. D* **56** (1997) 402.
- [8] M. Perelstein, *Little Higgs models and their phenomenology*, *Prog. Part. Nucl. Phys.* **58** (2007) 247, arXiv:[hep-ph/0512128](#).
- [9] U. Baur et al., *Probing electroweak top quark couplings at hadron colliders*, *Phys. Rev. D* **71** (2005) 054013, arXiv:[hep-ph/0412021](#).
- [10] U. Baur et al., *Improved measurement of $t\bar{t}Z$ couplings at the CERN LHC*, *Phys. Rev. D* **73** (2006) 034016, arXiv:[hep-ph/0512262](#).
- [11] U. Baur et al., *Probing electroweak top quark couplings at hadron and lepton colliders*, *Nucl. Phys. Proc. Suppl.* **160** (2006) 17, arXiv:[hep-ph/0606264](#).
- [12] CMS Collaboration, *Measurement of associated production of vector bosons and top quark-antiquark pairs at $\sqrt{s} = 7$ TeV*, *Phys. Rev. Lett.* **110** (2013) 172002, arXiv:[1303.3239](#).
- [13] CMS Collaboration, *Measurement of top quark-antiquark pair production in association with a W or Z boson in pp collisions at $\sqrt{s} = 8$ TeV*, *Eur. Phys. J. C* **74** (2014) 3060, arXiv:[1406.7830](#).
- [14] ATLAS Collaboration, *The ATLAS Experiment at the CERN Large Hadron Collider*, *JINST* **3** (2008) S08003.
- [15] J. Alwall et al., *MadGraph/MadEvent v4: the new web generation*, *JHEP* **0709** (2007) 028, arXiv:[0706.2334](#).
- [16] J. Pumplin et al., *New generation of parton distributions with uncertainties from global QCD analysis*, *JHEP* **0207** (2002) 012, arXiv:[hep-ph/0201195](#).
- [17] T. Sjöstrand, S. Mrenna and P. Z. Skands, *PYTHIA 6.4 Physics and Manual*, *JHEP* **0605** (2006) 026, arXiv:[hep-ph/0603175](#).
- [18] ATLAS Collaboration, *ATLAS tunes of PYTHIA 6 and Pythia 8 for MC11*, ATL-PHYS-PUB-2011-009, 2011, URL: <http://cds.cern.ch/record/1363300>.
- [19] J. Alwall et al., *The automated computation of tree-level and next-to-leading order differential cross sections, and their matching to parton shower simulations*, *JHEP* **07** (2014) 079, arXiv:[1405.0301](#).

- [20] J. M. Campbell and R. K. Ellis, $t\bar{t}W^\pm$ production and decay at NLO, *JHEP* **07** (2012) 052, arXiv:1204.5678.
- [21] M. Garzelli et al., $t\bar{t}W^\pm$ and $t\bar{t}Z$ hadroproduction at NLO accuracy in QCD with Parton Shower and Hadronization effects, *JHEP* **11** (2012) 056, arXiv:1208.2665.
- [22] M. L. Mangano et al., *ALPGEN*, a generator for hard multiparton processes in hadronic collisions, *JHEP* **0307** (2003) 001, arXiv:hep-ph/0206293.
- [23] K. Melnikov and F. Petriello, Electroweak gauge boson production at hadron colliders through $O(\alpha_s^2)$, *Phys. Rev. D* **74** (2006) 114017, arXiv:hep-ph/0609070.
- [24] M. L. Mangano, M. Moretti and R. Pittau, Multijet matrix elements and shower evolution in hadronic collisions: $Wb\bar{b} + n$ jets as a case study, *Nucl. Phys. B* **632** (2002) 343, arXiv:hep-ph/0108069.
- [25] T. Gleisberg et al., Event generation with *SHERPA 1.1*, *JHEP* **0902** (2009) 007, arXiv:0811.4622.
- [26] H.-L. Lai et al., New parton distributions for collider physics, *Phys. Rev. D* **82** (2010) 074024, arXiv:1007.2241.
- [27] J. M. Campbell and R. K. Ellis, Update on vector boson pair production at hadron colliders, *Phys. Rev. D* **60** (1999) 113006, arXiv:hep-ph/9905386.
- [28] P. Nason, A new method for combining NLO QCD with shower Monte Carlo algorithms, *JHEP* **0411** (2004) 040, arXiv:hep-ph/0409146.
- [29] S. Frixione, P. Nason and C. Oleari, Matching NLO QCD computations with parton shower simulations: the POWHEG method, *JHEP* **0711** (2007) 070, arXiv:0709.2092.
- [30] S. Alioli et al., A general framework for implementing NLO calculations in shower Monte Carlo programs: the POWHEG BOX, *JHEP* **06** (2010) 043, arXiv:1002.2581.
- [31] T. Sjöstrand, S. Mrenna and P. Z. Skands, A brief introduction to *PYTHIA 8.1*, *Comput. Phys. Commun.* **178** (2008) 852, arXiv:0710.3820.
- [32] P. Z. Skands, Tuning Monte Carlo Generators: The Perugia Tunes, *Phys. Rev. D* **82** (2010) 074018, arXiv:1005.3457.
- [33] S. Frixione et al., Single-top production in MC@NLO, *JHEP* **0603** (2006) 092, arXiv:hep-ph/0512250.
- [34] M. Czakon and A. Mitov, *Top++*: a program for the calculation of the top-pair cross-section at hadron colliders, *Comput. Phys. Commun.* **185** (2014) 2930, arXiv:1112.5675.
- [35] M. Cacciari et al., Top-pair production at hadron colliders with next-to-next-to-leading logarithmic soft-gluon resummation, *Phys. Lett. B* **710** (2012) 612, arXiv:1111.5869.
- [36] P. Bärnreuther, M. Czakon and A. Mitov, Percent Level Precision Physics at the Tevatron: First Genuine NNLO QCD Corrections to $q\bar{q} \rightarrow t\bar{t}$, *Phys. Rev. Lett.* **109** (2012) 132001, arXiv:1204.5201.
- [37] M. Czakon and A. Mitov, NNLO corrections to top-pair production at hadron colliders: the all-fermionic scattering channels, *JHEP* **12** (2012) 054, arXiv:1207.0236.
- [38] M. Czakon and A. Mitov, NNLO corrections to top-pair production at hadron colliders: the quark-gluon reaction, *JHEP* **01** (2013) 080, arXiv:1210.6832.
- [39] M. Czakon, P. Fiedler and A. Mitov, The total top quark pair production cross-section at hadron colliders through $O(\alpha_s^4)$, *Phys. Rev. Lett.* **110** (2013) 252004, arXiv:1303.6254.

- [40] N. Kidonakis, *Next-to-next-to-leading-order collinear and soft gluon corrections for t-channel single top quark production*, *Phys. Rev. D* **83** (2011) 091503(R), arXiv:1103.2792.
- [41] N. Kidonakis, *Next-to-next-to-leading logarithm resummation for s-channel single top quark production*, *Phys. Rev. D* **81** (2010) 054028, arXiv:1001.5034.
- [42] N. Kidonakis, *Two-loop soft anomalous dimensions for single top quark associated production with a W^- or H^-* , *Phys. Rev. D* **82** (2010) 054018, arXiv:1005.4451.
- [43] A. Martin et al., *Parton distributions for the LHC*, *Eur. Phys. J. C* **63** (2009) 189, arXiv:0901.0002.
- [44] A. Martin et al., *Uncertainties on α_s in global PDF analyses and implications for predicted hadronic cross sections*, *Eur. Phys. J. C* **64** (2009) 653, arXiv:0905.3531.
- [45] G. Bevilacqua et al., *HELAC-NLO*, *Comput. Phys. Commun.* **184** (2013) 986, arXiv:1110.1499.
- [46] ATLAS Collaboration, *Summary of ATLAS Pythia 8 tunes*, ATL-PHYS-PUB-2012-003, URL: <http://cds.cern.ch/record/1474107>.
- [47] S. Dittmaier et al., *Handbook of LHC Higgs Cross Sections: 1. Inclusive Observables*, 2011, arXiv:1101.0593.
- [48] P. Golonka and Z. Was, *PHOTOS Monte Carlo: A precision tool for QED corrections in Z and W decays*, *Eur. Phys. J. C* **45** (2006) 97, arXiv:hep-ph/0506026.
- [49] S. Jadach, J. H. Kühn and Z. Was, *TAUOLA — a library of Monte Carlo programs to simulate decays of polarized τ leptons*, *Comput. Phys. Commun.* **64** (1991) 275.
- [50] ATLAS Collaboration, *ATLAS tunes of PYTHIA6 and PYTHIA8 for MC11*, ATL-PHYS-PUB-2011-008, 2011, URL: <http://cds.cern.ch/record/1363300>.
- [51] ATLAS Collaboration, *The ATLAS Simulation Infrastructure*, *Eur. Phys. J. C* **70** (2010) 823, arXiv:1005.4568.
- [52] S. Agostinelli et al., *GEANT4 — a simulation toolkit*, *Nucl. Instr. Meth. A* **506** (2003) 250.
- [53] ATLAS Collaboration, *The simulation principle and performance of the ATLAS fast calorimeter simulation FastCaloSim*, ATL-PHYS-PUB-2010-013, 2010, URL: <http://cds.cern.ch/record/1300517>.
- [54] ATLAS Collaboration, *Electron reconstruction and identification efficiency measurements with the ATLAS detector using the 2011 LHC proton–proton collision data*, *Eur. Phys. J. C* **74** (2014) 2941, arXiv:1404.2240.
- [55] ATLAS Collaboration, *Electron efficiency measurements with the ATLAS detector using the 2012 LHC proton–proton collision data*, ATLAS-CONF-2014-032, 2014, URL: <http://cdsweb.cern.ch/record/1706245>.
- [56] ATLAS Collaboration, *Measurement of the muon reconstruction performance of the ATLAS detector using 2011 and 2012 LHC proton–proton collision data*, *Eur. Phys. J. C* **74** (2014) 3130, arXiv:1407.3935.
- [57] K. Rehermann and B. Tweedie, *Efficient identification of boosted semileptonic top quarks at the LHC*, *JHEP* **03** (2011) 059, arXiv:1007.2221.
- [58] M. Cacciari, G. P. Salam and G. Soyez, *The anti- k_r jet clustering algorithm*, *JHEP* **04** (2008) 063, arXiv:0802.1189.
- [59] M. Cacciari and G. P. Salam, *Dispelling the N^3 myth for the k_r jet-finder*, *Phys. Lett. B* **641** (2006) 57–61, arXiv:hep-ph/0512210.

- [60] M. Cacciari, G. P. Salam and G. Soyez, URL: <http://fastjet.fr/>.
- [61] C. Cojocaru et al., *Hadronic calibration of the ATLAS liquid argon end-cap calorimeter in the pseudorapidity region $1.6 < |\eta| < 1.8$ in beam tests*, *Nucl. Instr. Meth. A* **531** (2004) 481, arXiv:[physics/0407009](https://arxiv.org/abs/physics/0407009).
- [62] ATLAS Collaboration, *Local hadronic calibration*, ATL-LARG-PUB-2009-001, 2009, URL: <http://cds.cern.ch/record/1112035>.
- [63] ATLAS Collaboration, *Jet energy measurement and its systematic uncertainty in proton–proton collisions at $\sqrt{s} = 7$ TeV with the ATLAS detector*, *Eur. Phys. J. C* **75** (2015) 17, arXiv:[1406.0076](https://arxiv.org/abs/1406.0076).
- [64] ATLAS Collaboration, *Commissioning of the ATLAS high performance b-tagging algorithms in the 7 TeV collision data*, ATLAS-CONF-2011-102, 2011, URL: <http://cdsweb.cern.ch/record/1369219>.
- [65] ATLAS Collaboration, *Calibration of b-tagging using dileptonic top pair events in a combinatorial likelihood approach with the ATLAS experiment*, ATLAS-CONF-2014-004, 2014, URL: <http://cdsweb.cern.ch/record/1664335>.
- [66] ATLAS Collaboration, *Performance of missing transverse momentum reconstruction in proton–proton collisions at $\sqrt{s} = 7$ TeV with ATLAS*, *Eur. Phys. J. C* **72** (2012) 1844, arXiv:[1108.5602](https://arxiv.org/abs/1108.5602).
- [67] ATLAS Collaboration, *Measurement of the production cross section of jets in association with a Z boson in pp collisions at $\sqrt{s} = 7$ TeV with the ATLAS detector*, *JHEP* **07** (2013) 032, arXiv:[1304.7098](https://arxiv.org/abs/1304.7098).
- [68] ATLAS collaboration, *Measurements of normalized differential cross sections for $t\bar{t}$ production in pp collisions at $\sqrt{s} = 7$ TeV using the ATLAS detector*, *Phys. Rev. D* **90** (2014) 072004, arXiv:[1407.0371](https://arxiv.org/abs/1407.0371).
- [69] Phi-T GmbH, *NeuroBayes package*, URL: <http://neurobayes.phi-t.de/>.
- [70] G. C. Fox and S. Wolfram, *Observables for the Analysis of Event Shapes in e^+e^- Annihilation and Other Processes*, *Phys. Rev. Lett.* **41** (1978) 1581.
- [71] ATLAS Collaboration, *Measurement of the top quark-pair production cross section with ATLAS in pp collisions at $\sqrt{s} = 7$ TeV*, *Eur. Phys. J. C* **71** (2011) 1577, arXiv:[1012.1792](https://arxiv.org/abs/1012.1792).
- [72] ATLAS Collaboration, *Improved luminosity determination in pp collisions at $\sqrt{s} = 7$ TeV using the ATLAS detector at the LHC*, *Eur. Phys. J. C* **73** (2013) 2518, arXiv:[1302.4393](https://arxiv.org/abs/1302.4393).
- [73] ATLAS Collaboration, *Calibration of the performance of b-tagging for c and light-flavour jets in the 2012 ATLAS data*, ATLAS-CONF-2014-046, 2014, URL: <http://cdsweb.cern.ch/record/1741020>.
- [74] B. Cooper et al., *Importance of a consistent choice of α_S in the matching of AlpGen and Pythia*, *Eur. Phys. J. C* **72** (2012) 2078, arXiv:[1109.5295](https://arxiv.org/abs/1109.5295).
- [75] R. D. Ball et al., *Parton distributions with LHC data*, *Nucl. Phys. B* **867** (2013) 244, arXiv:[1207.1303](https://arxiv.org/abs/1207.1303).
- [76] M. Botje et al., *The PDF4LHC Working Group Interim Recommendations*, 2011, arXiv:[1101.0538](https://arxiv.org/abs/1101.0538).
- [77] G. Corcella et al., *HERWIG 6: an event generator for hadron emission reactions with interfering gluons (including supersymmetric processes)*, *JHEP* **01** (2001) 010.

- [78] S Heinemeyer et al., *Handbook of LHC Higgs Cross Sections: 3. Higgs Properties*, arXiv:[1307.1347](#).
- [79] W. Verkerke and D. Kirkby, *The RooFit toolkit for data modeling*, arXiv:[physics/0306116](#).
- [80] W. Verkerke and D. Kirkby, *RooFit Users Manual v2.91*, URL: <http://rootfit.sourceforge.net>.
- [81] G. Cowan et al., *Asymptotic formulae for likelihood-based tests of new physics*, *Eur. Phys. J. C* **71** (2011) 1554, Erratum: *C* **73** (2013) 2501, arXiv:[1007.1727](#).

The ATLAS Collaboration

G. Aad⁸⁵, B. Abbott¹¹³, J. Abdallah¹⁵¹, O. Abdinov¹¹, R. Aben¹⁰⁷, M. Abolins⁹⁰, O.S. AbouZeid¹⁵⁸, H. Abramowicz¹⁵³, H. Abreu¹⁵², R. Abreu¹¹⁶, Y. Abulaiti^{146a,146b}, B.S. Acharya^{164a,164b,a}, L. Adamczyk^{38a}, D.L. Adams²⁵, J. Adelman¹⁰⁸, S. Adomeit¹⁰⁰, T. Adye¹³¹, A.A. Affolder⁷⁴, T. Agatonovic-Jovin¹³, J. Agricola⁵⁴, J.A. Aguilar-Saavedra^{126a,126f}, S.P. Ahlen²², F. Ahmadov^{65,b}, G. Aielli^{133a,133b}, H. Akerstedt^{146a,146b}, T.P.A. Åkesson⁸¹, A.V. Akimov⁹⁶, G.L. Alberghi^{20a,20b}, J. Albert¹⁶⁹, S. Albrand⁵⁵, M.J. Alconada Verzini⁷¹, M. Aleksa³⁰, I.N. Aleksandrov⁶⁵, C. Alexa^{26b}, G. Alexander¹⁵³, T. Alexopoulos¹⁰, M. Alhroob¹¹³, G. Alimonti^{91a}, L. Alio⁸⁵, J. Alison³¹, S.P. Alkire³⁵, B.M.M. Allbrooke¹⁴⁹, P.P. Allport¹⁸, A. Aloisio^{104a,104b}, A. Alonso³⁶, F. Alonso⁷¹, C. Alpigiani¹³⁸, A. Altheimer³⁵, B. Alvarez Gonzalez³⁰, D. Álvarez Piqueras¹⁶⁷, M.G. Alviggi^{104a,104b}, B.T. Amadio¹⁵, K. Amako⁶⁶, Y. Amaral Coutinho^{24a}, C. Amelung²³, D. Amidei⁸⁹, S.P. Amor Dos Santos^{126a,126c}, A. Amorim^{126a,126b}, S. Amoroso⁴⁸, N. Amram¹⁵³, G. Amundsen²³, C. Anastopoulos¹³⁹, L.S. Ancu⁴⁹, N. Andari¹⁰⁸, T. Andeen³⁵, C.F. Anders^{58b}, G. Anders³⁰, J.K. Anders⁷⁴, K.J. Anderson³¹, A. Andreazza^{91a,91b}, V. Andrei^{58a}, S. Angelidakis⁹, I. Angelozzi¹⁰⁷, P. Anger⁴⁴, A. Angerami³⁵, F. Anghinolfi³⁰, A.V. Anisenkov^{109,c}, N. Anjos¹², A. Annovi^{124a,124b}, M. Antonelli⁴⁷, A. Antonov⁹⁸, J. Antos^{144b}, F. Anulli^{132a}, M. Aoki⁶⁶, L. Aperio Bella¹⁸, G. Arabidze⁹⁰, Y. Arai⁶⁶, J.P. Araque^{126a}, A.T.H. Arce⁴⁵, F.A. Arduh⁷¹, J-F. Arguin⁹⁵, S. Argyropoulos⁶³, M. Arik^{19a}, A.J. Armbruster³⁰, O. Arnaez³⁰, H. Arnold⁴⁸, M. Arratia²⁸, O. Arslan²¹, A. Artamonov⁹⁷, G. Artoni²³, S. Asai¹⁵⁵, N. Asbah⁴², A. Ashkenazi¹⁵³, B. Åsman^{146a,146b}, L. Asquith¹⁴⁹, K. Assamagan²⁵, R. Astalos^{144a}, M. Atkinson¹⁶⁵, N.B. Atlay¹⁴¹, K. Augsten¹²⁸, M. Aurousseau^{145b}, G. Avolio³⁰, B. Axen¹⁵, M.K. Ayoub¹¹⁷, G. Azuelos^{95,d}, M.A. Baak³⁰, A.E. Baas^{58a}, M.J. Baca¹⁸, C. Bacci^{134a,134b}, H. Bachacou¹³⁶, K. Bachas¹⁵⁴, M. Backes³⁰, M. Backhaus³⁰, P. Bagiachi^{132a,132b}, P. Bagnaia^{132a,132b}, Y. Bai^{33a}, T. Bain³⁵, J.T. Baines¹³¹, O.K. Baker¹⁷⁶, E.M. Baldin^{109,c}, P. Balek¹²⁹, T. Balestri¹⁴⁸, F. Balli⁸⁴, W.K. Balunas¹²², E. Banas³⁹, Sw. Banerjee¹⁷³, A.A.E. Bannoura¹⁷⁵, L. Barak³⁰, E.L. Barberio⁸⁸, D. Barberis^{50a,50b}, M. Barbero⁸⁵, T. Barillari¹⁰¹, M. Barisonzi^{164a,164b}, T. Barklow¹⁴³, N. Barlow²⁸, S.L. Barnes⁸⁴, B.M. Barnett¹³¹, R.M. Barnett¹⁵, Z. Barnovska⁵, A. Baroncelli^{134a}, G. Barone²³, A.J. Barr¹²⁰, F. Barreiro⁸², J. Barreiro Guimarães da Costa⁵⁷, R. Bartoldus¹⁴³, A.E. Barton⁷², P. Bartos^{144a}, A. Basalae¹²³, A. Bassalat¹¹⁷, A. Basye¹⁶⁵, R.L. Bates⁵³, S.J. Batista¹⁵⁸, J.R. Batley²⁸, M. Battaglia¹³⁷, M. Bauce^{132a,132b}, F. Bauer¹³⁶, H.S. Bawa^{143,e}, J.B. Beacham¹¹¹, M.D. Beattie⁷², T. Beau⁸⁰, P.H. Beauchemin¹⁶¹, R. Beccherle^{124a,124b}, P. Bechtel²¹, H.P. Beck^{17,f}, K. Becker¹²⁰, M. Becker⁸³, M. Beckingham¹⁷⁰, C. Becot¹¹⁷, A.J. Beddall^{19b}, A. Beddall^{19b}, V.A. Bednyakov⁶⁵, C.P. Bee¹⁴⁸, L.J. Beemster¹⁰⁷, T.A. Beermann³⁰, M. Begel²⁵, J.K. Behr¹²⁰, C. Belanger-Champagne⁸⁷, W.H. Bell⁴⁹, G. Bella¹⁵³, L. Bellagamba^{20a}, A. Bellerive²⁹, M. Bellomo⁸⁶, K. Belotskiy⁹⁸, O. Beltramello³⁰, O. Benary¹⁵³, D. Bencheikroun^{135a}, M. Bender¹⁰⁰, K. Bendtz^{146a,146b}, N. Benekos¹⁰, Y. Benhammou¹⁵³, E. Benhar Noccioli⁴⁹, J.A. Benitez Garcia^{159b}, D.P. Benjamin⁴⁵, J.R. Bensinger²³, S. Bentvelsen¹⁰⁷, L. Beresford¹²⁰, M. Beretta⁴⁷, D. Berge¹⁰⁷, E. Bergeas Kuutmann¹⁶⁶, N. Berger⁵, F. Berghaus¹⁶⁹, J. Beringer¹⁵, C. Bernard²², N.R. Bernard⁸⁶, C. Bernius¹¹⁰, F.U. Bernlochner²¹, T. Berry⁷⁷, P. Berta¹²⁹, C. Bertella⁸³, G. Bertoli^{146a,146b}, F. Bertolucci^{124a,124b}, C. Bertsche¹¹³, D. Bertsche¹¹³, M.I. Besana^{91a}, G.J. Besjes³⁶, O. Bessidskaia Bylund^{146a,146b}, M. Bessner⁴², N. Besson¹³⁶, C. Betancourt⁴⁸, S. Bethke¹⁰¹, A.J. Bevan⁷⁶, W. Bhimji¹⁵, R.M. Bianchi¹²⁵, L. Bianchini²³, M. Bianco³⁰, O. Biebel¹⁰⁰, D. Biedermann¹⁶, S.P. Bieniek⁷⁸, M. Biglietti^{134a}, J. Bilbao De Mendizabal⁴⁹, H. Bilokon⁴⁷, M. Bindi⁵⁴, S. Binet¹¹⁷, A. Bingul^{19b}, C. Bini^{132a,132b}, S. Biondi^{20a,20b}, D.M. Bjergaard⁴⁵, C.W. Black¹⁵⁰, J.E. Black¹⁴³, K.M. Black²², D. Blackburn¹³⁸, R.E. Blair⁶, J.-B. Blanchard¹³⁶, J.E. Blanco⁷⁷, T. Blazek^{144a}, I. Bloch⁴², C. Blocker²³, W. Blum^{83,*}, U. Blumenschein⁵⁴, S. Blunier^{32a}, G.J. Bobbink¹⁰⁷,

V.S. Bobrovnikov^{109,c}, S.S. Bocchetta⁸¹, A. Bocci⁴⁵, C. Bock¹⁰⁰, M. Boehler⁴⁸, J.A. Bogaerts³⁰, D. Bogavac¹³, A.G. Bogdanchikov¹⁰⁹, C. Bohm^{146a}, V. Boisvert⁷⁷, T. Bold^{38a}, V. Boldea^{26b}, A.S. Boldyrev⁹⁹, M. Bomben⁸⁰, M. Bona⁷⁶, M. Boonekamp¹³⁶, A. Borisov¹³⁰, G. Borissov⁷², S. Borroni⁴², J. Bortfeldt¹⁰⁰, V. Bortolotto^{60a,60b,60c}, K. Bos¹⁰⁷, D. Boscherini^{20a}, M. Bosman¹², J. Boudreau¹²⁵, J. Bouffard², E.V. Bouhova-Thacker⁷², D. Boumediene³⁴, C. Bourdarios¹¹⁷, N. Bousson¹¹⁴, S.K. Boutle⁵³, A. Boveia³⁰, J. Boyd³⁰, I.R. Boyko⁶⁵, I. Bozic¹³, J. Bracnik¹⁸, A. Brandt⁸, G. Brandt⁵⁴, O. Brandt^{58a}, U. Bratzler¹⁵⁶, B. Brau⁸⁶, J.E. Brau¹¹⁶, H.M. Braun^{175,*}, W.D. Breaden Madden⁵³, K. Brendlinger¹²², A.J. Brennan⁸⁸, L. Brenner¹⁰⁷, R. Brenner¹⁶⁶, S. Bressler¹⁷², K. Bristow^{145c}, T.M. Bristow⁴⁶, D. Britton⁵³, D. Britzger⁴², F.M. Brochu²⁸, I. Brock²¹, R. Brock⁹⁰, J. Bronner¹⁰¹, G. Brooijmans³⁵, T. Brooks⁷⁷, W.K. Brooks^{32b}, J. Brosamer¹⁵, E. Brost¹¹⁶, P.A. Bruckman de Renstrom³⁹, D. Bruncko^{144b}, R. Bruneliere⁴⁸, A. Bruni^{20a}, G. Bruni^{20a}, M. Bruschi^{20a}, N. Brusino²¹, L. Bryngemark⁸¹, T. Buanes¹⁴, Q. Buat¹⁴², P. Buchholz¹⁴¹, A.G. Buckley⁵³, S.I. Buda^{26b}, I.A. Budagov⁶⁵, F. Buehrer⁴⁸, L. Bugge¹¹⁹, M.K. Bugge¹¹⁹, O. Bulekov⁹⁸, D. Bullock⁸, H. Burckhart³⁰, S. Burdin⁷⁴, C.D. Burgard⁴⁸, B. Burghgrave¹⁰⁸, S. Burke¹³¹, I. Burmeister⁴³, E. Busato³⁴, D. Büscher⁴⁸, V. Büscher⁸³, P. Bussey⁵³, J.M. Butler²², A.I. Butt³, C.M. Buttar⁵³, J.M. Butterworth⁷⁸, P. Butti¹⁰⁷, W. Buttinger²⁵, A. Buzatu⁵³, A.R. Buzykaev^{109,c}, S. Cabrera Urbán¹⁶⁷, D. Caforio¹²⁸, V.M. Cairo^{37a,37b}, O. Cakir^{4a}, N. Calace⁴⁹, P. Calafiura¹⁵, A. Calandri¹³⁶, G. Calderini⁸⁰, P. Calfayan¹⁰⁰, L.P. Caloba^{24a}, D. Calvet³⁴, S. Calvet³⁴, R. Camacho Toro³¹, S. Camarda⁴², P. Camarri^{133a,133b}, D. Cameron¹¹⁹, R. Caminal Armadans¹⁶⁵, S. Campana³⁰, M. Campanelli⁷⁸, A. Campoverde¹⁴⁸, V. Canale^{104a,104b}, A. Canepa^{159a}, M. Cano Bret^{33c}, J. Cantero⁸², R. Cantrill^{126a}, T. Cao⁴⁰, M.D.M. Capeans Garrido³⁰, I. Caprini^{26b}, M. Caprini^{26b}, M. Capua^{37a,37b}, R. Caputo⁸³, R. Cardarelli^{133a}, F. Cardillo⁴⁸, T. Carli³⁰, G. Carlino^{104a}, L. Carminati^{91a,91b}, S. Caron¹⁰⁶, E. Carquin^{32a}, G.D. Carrillo-Montoya³⁰, J.R. Carter²⁸, J. Carvalho^{126a,126c}, D. Casadei⁷⁸, M.P. Casado¹², M. Casolino¹², E. Castaneda-Miranda^{145a}, A. Castelli¹⁰⁷, V. Castillo Gimenez¹⁶⁷, N.F. Castro^{126a,g}, P. Catastini⁵⁷, A. Catinaccio³⁰, J.R. Catmore¹¹⁹, A. Cattai³⁰, J. Caudron⁸³, V. Cavaliere¹⁶⁵, D. Cavalli^{91a}, M. Cavalli-Sforza¹², V. Cavasinni^{124a,124b}, F. Ceradini^{134a,134b}, B.C. Cerio⁴⁵, K. Cerny¹²⁹, A.S. Cerqueira^{24b}, A. Cerri¹⁴⁹, L. Cerrito⁷⁶, F. Cerutti¹⁵, M. Cerv³⁰, A. Cervelli¹⁷, S.A. Cetin^{19c}, A. Chafaq^{135a}, D. Chakraborty¹⁰⁸, I. Chalupkova¹²⁹, P. Chang¹⁶⁵, J.D. Chapman²⁸, D.G. Charlton¹⁸, C.C. Chau¹⁵⁸, C.A. Chavez Barajas¹⁴⁹, S. Cheatham¹⁵², A. Chegwidden⁹⁰, S. Chekanov⁶, S.V. Chekulaev^{159a}, G.A. Chelkov^{65,h}, M.A. Chelstowska⁸⁹, C. Chen⁶⁴, H. Chen²⁵, K. Chen¹⁴⁸, L. Chen^{33d,i}, S. Chen^{33c}, S. Chen¹⁵⁵, X. Chen^{33f}, Y. Chen⁶⁷, H.C. Cheng⁸⁹, Y. Cheng³¹, A. Cheplakov⁶⁵, E. Cheremushkina¹³⁰, R. Cherkaoui El Moursli^{135e}, V. Chernyatin^{25,*}, E. Cheu⁷, L. Chevalier¹³⁶, V. Chiarella⁴⁷, G. Chiarelli^{124a,124b}, G. Chiodini^{73a}, A.S. Chisholm¹⁸, R.T. Chislett⁷⁸, A. Chitan^{26b}, M.V. Chizhov⁶⁵, K. Choi⁶¹, S. Chouridou⁹, B.K.B. Chow¹⁰⁰, V. Christodoulou⁷⁸, D. Chromek-Burckhart³⁰, J. Chudoba¹²⁷, A.J. Chuinard⁸⁷, J.J. Chwastowski³⁹, L. Chytka¹¹⁵, G. Ciapetti^{132a,132b}, A.K. Ciftci^{4a}, D. Cinca⁵³, V. Cindro⁷⁵, I.A. Cioara²¹, A. Ciocio¹⁵, F. Ciotto^{104a,104b}, Z.H. Citron¹⁷², M. Ciubancan^{26b}, A. Clark⁴⁹, B.L. Clark⁵⁷, P.J. Clark⁴⁶, R.N. Clarke¹⁵, C. Clement^{146a,146b}, Y. Coadou⁸⁵, M. Cobal^{164a,164c}, A. Coccaro⁴⁹, J. Cochran⁶⁴, L. Coffey²³, J.G. Cogan¹⁴³, L. Colasurdo¹⁰⁶, B. Cole³⁵, S. Cole¹⁰⁸, A.P. Colijn¹⁰⁷, J. Collot⁵⁵, T. Colombo^{58c}, G. Compostella¹⁰¹, P. Conde Muino^{126a,126b}, E. Coniavitis⁴⁸, S.H. Connell^{145b}, I.A. Connelly⁷⁷, V. Consorti⁴⁸, S. Constantinescu^{26b}, C. Conta^{121a,121b}, G. Conti³⁰, F. Conventi^{104a,j}, M. Cooke¹⁵, B.D. Cooper⁷⁸, A.M. Cooper-Sarkar¹²⁰, T. Cornelissen¹⁷⁵, M. Corradi^{20a}, F. Corriveau^{87,k}, A. Corso-Radu¹⁶³, A. Cortes-Gonzalez¹², G. Cortiana¹⁰¹, G. Costa^{91a}, M.J. Costa¹⁶⁷, D. Costanzo¹³⁹, D. Côté⁸, G. Cottin²⁸, G. Cowan⁷⁷, B.E. Cox⁸⁴, K. Cranmer¹¹⁰, G. Cree²⁹, S. Crépe-Renaudin⁵⁵, F. Crescioli⁸⁰, W.A. Cribbs^{146a,146b}, M. Crispin Ortuzar¹²⁰, M. Cristinziani²¹, V. Croft¹⁰⁶, G. Crosetti^{37a,37b}, T. Cuhadar Donszelmann¹³⁹, J. Cummings¹⁷⁶, M. Curatolo⁴⁷, J. Cúth⁸³, C. Cuthbert¹⁵⁰, H. Cziri¹⁴¹, P. Czodrowski³, S. D'Auria⁵³, M. D'Onofrio⁷⁴, M.J. Da Cunha Sargedas De Sousa^{126a,126b}, C. Da Via⁸⁴, W. Dabrowski^{38a}, A. Dafinca¹²⁰, T. Dai⁸⁹,

O. Dale¹⁴, F. Dallaire⁹⁵, C. Dallapiccola⁸⁶, M. Dam³⁶, J.R. Dandoy³¹, N.P. Dang⁴⁸, A.C. Daniells¹⁸, M. Danninger¹⁶⁸, M. Dano Hoffmann¹³⁶, V. Dao⁴⁸, G. Darbo^{50a}, S. Darmora⁸, J. Dassoulas³, A. Dattagupta⁶¹, W. Davey²¹, C. David¹⁶⁹, T. Davidek¹²⁹, E. Davies^{120,l}, M. Davies¹⁵³, P. Davison⁷⁸, Y. Davygora^{58a}, E. Dawe⁸⁸, I. Dawson¹³⁹, R.K. Daya-Ishmukhametova⁸⁶, K. De⁸, R. de Asmundis^{104a}, A. De Benedetti¹¹³, S. De Castro^{20a,20b}, S. De Cecco⁸⁰, N. De Groot¹⁰⁶, P. de Jong¹⁰⁷, H. De la Torre⁸², F. De Lorenzi⁶⁴, D. De Pedis^{132a}, A. De Salvo^{132a}, U. De Sanctis¹⁴⁹, A. De Santo¹⁴⁹, J.B. De Vivie De Regie¹¹⁷, W.J. Dearnaley⁷², R. Debbe²⁵, C. Debenedetti¹³⁷, D.V. Dedovich⁶⁵, I. Deigaard¹⁰⁷, J. Del Peso⁸², T. Del Prete^{124a,124b}, D. Delgove¹¹⁷, F. Deliot¹³⁶, C.M. Delitzsch⁴⁹, M. Deliyergiyev⁷⁵, A. Dell'Acqua³⁰, L. Dell'Asta²², M. Dell'Orso^{124a,124b}, M. Della Pietra^{104a,j}, D. della Volpe⁴⁹, M. Delmastro⁵, P.A. Delsart⁵⁵, C. Deluca¹⁰⁷, D.A. DeMarco¹⁵⁸, S. Demers¹⁷⁶, M. Demichev⁶⁵, A. Demilly⁸⁰, S.P. Denisov¹³⁰, D. Derendarz³⁹, J.E. Derkaoui^{135d}, F. Derue⁸⁰, P. Dervan⁷⁴, K. Desch²¹, C. Deterre⁴², P.O. Deviveiros³⁰, A. Dewhurst¹³¹, S. Dhaliwal²³, A. Di Ciaccio^{133a,133b}, L. Di Ciaccio⁵, A. Di Domenico^{132a,132b}, C. Di Donato^{104a,104b}, A. Di Girolamo³⁰, B. Di Girolamo³⁰, A. Di Mattia¹⁵², B. Di Micco^{134a,134b}, R. Di Nardo⁴⁷, A. Di Simone⁴⁸, R. Di Sipio¹⁵⁸, D. Di Valentino²⁹, C. Diaconu⁸⁵, M. Diamond¹⁵⁸, F.A. Dias⁴⁶, M.A. Diaz^{32a}, E.B. Diehl⁸⁹, J. Dietrich¹⁶, S. Diglio⁸⁵, A. Dimitrievska¹³, J. Dingfelder²¹, P. Dita^{26b}, S. Dita^{26b}, F. Dittus³⁰, F. Djama⁸⁵, T. Djobava^{51b}, J.I. Djuvsland^{58a}, M.A.B. do Vale^{24c}, D. Dobos³⁰, M. Dobre^{26b}, C. Doglioni⁸¹, T. Dohmae¹⁵⁵, J. Dolejsi¹²⁹, Z. Dolezal¹²⁹, B.A. Dolgoshein^{98,*}, M. Donadelli^{24d}, S. Donati^{124a,124b}, P. Dondero^{121a,121b}, J. Donini³⁴, J. Dopke¹³¹, A. Doria^{104a}, M.T. Dova⁷¹, A.T. Doyle⁵³, E. Drechsler⁵⁴, M. Dris¹⁰, E. Dubreuil³⁴, E. Duchovni¹⁷², G. Duckeck¹⁰⁰, O.A. Ducu^{26b,85}, D. Duda¹⁰⁷, A. Dudarev³⁰, L. Duflot¹¹⁷, L. Duguid⁷⁷, M. Dührssen³⁰, M. Dunford^{58a}, H. Duran Yildiz^{4a}, M. Düren⁵², A. Durglishvili^{51b}, D. Duschinger⁴⁴, M. Dyndal^{38a}, C. Eckardt⁴², K.M. Ecker¹⁰¹, R.C. Edgar⁸⁹, W. Edson², N.C. Edwards⁴⁶, W. Ehrenfeld²¹, T. Eifert³⁰, G. Eigen¹⁴, K. Einsweiler¹⁵, T. Ekelof¹⁶⁶, M. El Kacimi^{135c}, M. Ellert¹⁶⁶, S. Elles⁵, F. Ellinghaus¹⁷⁵, A.A. Elliot¹⁶⁹, N. Ellis³⁰, J. Elmsheuser¹⁰⁰, M. Elsing³⁰, D. Emelianov¹³¹, Y. Enari¹⁵⁵, O.C. Endner⁸³, M. Endo¹¹⁸, J. Erdmann⁴³, A. Ereditato¹⁷, G. Ernis¹⁷⁵, J. Ernst², M. Ernst²⁵, S. Errede¹⁶⁵, E. Ertel⁸³, M. Escalier¹¹⁷, H. Esch⁴³, C. Escobar¹²⁵, B. Esposito⁴⁷, A.I. Etienne¹³⁶, E. Etzion¹⁵³, H. Evans⁶¹, A. Ezhilov¹²³, L. Fabbri^{20a,20b}, G. Facini³¹, R.M. Fakhruddinov¹³⁰, S. Falciano^{132a}, R.J. Falla⁷⁸, J. Faltova¹²⁹, Y. Fang^{33a}, M. Fanti^{91a,91b}, A. Farbin⁸, A. Farilla^{134a}, T. Farooque¹², S. Farrell¹⁵, S.M. Farrington¹⁷⁰, P. Farthouat³⁰, F. Fassi^{135e}, P. Fassnacht³⁰, D. Fassouliotis⁹, M. Fauci Giannelli⁷⁷, A. Favareto^{50a,50b}, L. Fayard¹¹⁷, O.L. Fedin^{123,m}, W. Fedorko¹⁶⁸, S. Feigl³⁰, L. Felgioni⁸⁵, C. Feng^{33d}, E.J. Feng³⁰, H. Feng⁸⁹, A.B. Fenyuk¹³⁰, L. Feremenga⁸, P. Fernandez Martinez¹⁶⁷, S. Fernandez Perez³⁰, J. Ferrando⁵³, A. Ferrari¹⁶⁶, P. Ferrari¹⁰⁷, R. Ferrari^{121a}, D.E. Ferreira de Lima⁵³, A. Ferrer¹⁶⁷, D. Ferrere⁴⁹, C. Ferretti⁸⁹, A. Ferretto Parodi^{50a,50b}, M. Fiascaris³¹, F. Fiedler⁸³, A. Filipčič⁷⁵, M. Filipuzzi⁴², F. Filthaut¹⁰⁶, M. Fincke-Keeler¹⁶⁹, K.D. Finelli¹⁵⁰, M.C.N. Fiolhais^{126a,126c}, L. Fiorini¹⁶⁷, A. Firan⁴⁰, A. Fischer², C. Fischer¹², J. Fischer¹⁷⁵, W.C. Fisher⁹⁰, N. Flaschel⁴², I. Fleck¹⁴¹, P. Fleischmann⁸⁹, G.T. Fletcher¹³⁹, G. Fletcher⁷⁶, R.R.M. Fletcher¹²², T. Flick¹⁷⁵, A. Floderus⁸¹, L.R. Flores Castillo^{60a}, M.J. Flowerdew¹⁰¹, A. Formica¹³⁶, A. Forti⁸⁴, D. Fournier¹¹⁷, H. Fox⁷², S. Fracchia¹², P. Francavilla⁸⁰, M. Franchini^{20a,20b}, D. Francis³⁰, L. Franconi¹¹⁹, M. Franklin⁵⁷, M. Frate¹⁶³, M. Fraternali^{121a,121b}, D. Freeborn⁷⁸, S.T. French²⁸, F. Friedrich⁴⁴, D. Froidevaux³⁰, J.A. Frost¹²⁰, C. Fukunaga¹⁵⁶, E. Fullana Torregrosa⁸³, B.G. Fulsom¹⁴³, T. Fusayasu¹⁰², J. Fuster¹⁶⁷, C. Gabaldon⁵⁵, O. Gabizon¹⁷⁵, A. Gabrielli^{20a,20b}, A. Gabrielli¹⁵, G.P. Gach¹⁸, S. Gadatsch³⁰, S. Gadomski⁴⁹, G. Gagliardi^{50a,50b}, P. Gagnon⁶¹, C. Galea¹⁰⁶, B. Galhardo^{126a,126c}, E.J. Gallas¹²⁰, B.J. Gallop¹³¹, P. Gallus¹²⁸, G. Galster³⁶, K.K. Gan¹¹¹, J. Gao^{33b,85}, Y. Gao⁴⁶, Y.S. Gao^{143,e}, F.M. Garay Walls⁴⁶, F. Garbersson¹⁷⁶, C. García¹⁶⁷, J.E. García Navarro¹⁶⁷, M. Garcia-Sciveres¹⁵, R.W. Gardner³¹, N. Garelli¹⁴³, V. Garonne¹¹⁹, C. Gatti⁴⁷, A. Gaudiello^{50a,50b}, G. Gaudio^{121a}, B. Gaur¹⁴¹, L. Gauthier⁹⁵, P. Gauzzi^{132a,132b}, I.L. Gavrilenko⁹⁶, C. Gay¹⁶⁸, G. Gaycken²¹, E.N. Gazis¹⁰, P. Ge^{33d}, Z. Gecse¹⁶⁸, C.N.P. Gee¹³¹, Ch. Geich-Gimbel²¹,

M.P. Geisler^{58a}, C. Gemme^{50a}, M.H. Genest⁵⁵, S. Gentile^{132a,132b}, M. George⁵⁴, S. George⁷⁷,
D. Gerbaudo¹⁶³, A. Gershon¹⁵³, S. Ghasemi¹⁴¹, H. Ghazlane^{135b}, B. Giacobbe^{20a}, S. Giagu^{132a,132b},
V. Giangiobbe¹², P. Giannetti^{124a,124b}, B. Gibbard²⁵, S.M. Gibson⁷⁷, M. Gignac¹⁶⁸, M. Gilchriese¹⁵,
T.P.S. Gillam²⁸, D. Gillberg³⁰, G. Gilles³⁴, D.M. Gingrich^{3,d}, N. Giokaris⁹, M.P. Giordani^{164a,164c},
F.M. Giorgi^{20a}, F.M. Giorgi¹⁶, P.F. Giraud¹³⁶, P. Giromini⁴⁷, D. Giugni^{91a}, C. Giuliani⁴⁸, M. Giuliani^{58b},
B.K. Gjelsten¹¹⁹, S. Gkaitatzis¹⁵⁴, I. Gkialas¹⁵⁴, E.L. Gkoukousis¹¹⁷, L.K. Gladilin⁹⁹, C. Glasman⁸²,
J. Glatzer³⁰, P.C.F. Glaysher⁴⁶, A. Glazov⁴², M. Goblirsch-Kolb¹⁰¹, J.R. Goddard⁷⁶, J. Godlewski³⁹,
S. Goldfarb⁸⁹, T. Golling⁴⁹, D. Golubkov¹³⁰, A. Gomes^{126a,126b,126d}, R. Gonçalo^{126a},
J. Goncalves Pinto Firmino Da Costa¹³⁶, L. Gonella²¹, S. González de la Hoz¹⁶⁷, G. Gonzalez Parra¹²,
S. Gonzalez-Sevilla⁴⁹, L. Goossens³⁰, P.A. Gorbounov⁹⁷, H.A. Gordon²⁵, I. Gorelov¹⁰⁵, B. Gorini³⁰,
E. Gorini^{73a,73b}, A. Gorišek⁷⁵, E. Gornicki³⁹, A.T. Goshaw⁴⁵, C. Gössling⁴³, M.I. Gostkin⁶⁵,
D. Goujdami^{135c}, A.G. Goussiou¹³⁸, N. Govender^{145b}, E. Gozani¹⁵², H.M.X. Grabas¹³⁷, L. Graber⁵⁴,
I. Grabowska-Bold^{38a}, P.O.J. Gradin¹⁶⁶, P. Grafström^{20a,20b}, K-J. Grahn⁴², J. Gramling⁴⁹,
E. Gramstad¹¹⁹, S. Grancagnolo¹⁶, V. Gratchev¹²³, H.M. Gray³⁰, E. Graziani^{134a}, Z.D. Greenwood^{79,n},
C. Greife²¹, K. Gregersen⁷⁸, I.M. Gregor⁴², P. Grenier¹⁴³, J. Griffiths⁸, A.A. Grillo¹³⁷, K. Grimm⁷²,
S. Grinstein^{12,o}, Ph. Gris³⁴, J.-F. Grivaz¹¹⁷, J.P. Grohs⁴⁴, A. Grohsjean⁴², E. Gross¹⁷²,
J. Grosse-Knetter⁵⁴, G.C. Grossi⁷⁹, Z.J. Grout¹⁴⁹, L. Guan⁸⁹, J. Guenther¹²⁸, F. Guescini⁴⁹, D. Guest¹⁷⁶,
O. Gueta¹⁵³, E. Guido^{50a,50b}, T. Guillemin¹¹⁷, S. Guindon², U. Gul⁵³, C. Gumpert⁴⁴, J. Guo^{33e},
Y. Guo^{33b,p}, S. Gupta¹²⁰, G. Gustavino^{132a,132b}, P. Gutierrez¹¹³, N.G. Gutierrez Ortiz⁷⁸, C. Gutschow⁴⁴,
C. Guyot¹³⁶, C. Gwenlan¹²⁰, C.B. Gwilliam⁷⁴, A. Haas¹¹⁰, C. Haber¹⁵, H.K. Hadavand⁸, N. Haddad^{135e},
P. Haefner²¹, S. Hageböck²¹, Z. Hajduk³⁹, H. Hakobyan¹⁷⁷, M. Haleem⁴², J. Haley¹¹⁴, D. Hall¹²⁰,
G. Halladjian⁹⁰, G.D. Hallewell⁸⁵, K. Hamacher¹⁷⁵, P. Hamal¹¹⁵, K. Hamano¹⁶⁹, A. Hamilton^{145a},
G.N. Hamity¹³⁹, P.G. Hamnett⁴², L. Han^{33b}, K. Hanagaki^{66,q}, K. Hanawa¹⁵⁵, M. Hance¹³⁷, B. Haney¹²²,
P. Hanke^{58a}, R. Hanna¹³⁶, J.B. Hansen³⁶, J.D. Hansen³⁶, M.C. Hansen²¹, P.H. Hansen³⁶, K. Hara¹⁶⁰,
A.S. Hard¹⁷³, T. Harenberg¹⁷⁵, F. Hariri¹¹⁷, S. Harkusha⁹², R.D. Harrington⁴⁶, P.F. Harrison¹⁷⁰,
F. Hartjes¹⁰⁷, M. Hasegawa⁶⁷, Y. Hasegawa¹⁴⁰, A. Hasib¹¹³, S. Hassani¹³⁶, S. Haug¹⁷, R. Hauser⁹⁰,
L. Hauswald⁴⁴, M. Havranek¹²⁷, C.M. Hawkes¹⁸, R.J. Hawkins³⁰, A.D. Hawkins⁸¹, T. Hayashi¹⁶⁰,
D. Hayden⁹⁰, C.P. Hays¹²⁰, J.M. Hays⁷⁶, H.S. Hayward⁷⁴, S.J. Haywood¹³¹, S.J. Head¹⁸, T. Heck⁸³,
V. Hedberg⁸¹, L. Heelan⁸, S. Heim¹²², T. Heim¹⁷⁵, B. Heinemann¹⁵, L. Heinrich¹¹⁰, J. Hejbal¹²⁷,
L. Helary²², S. Hellman^{146a,146b}, D. Hellmich²¹, C. Hensens¹², J. Henderson¹²⁰, R.C.W. Henderson⁷²,
Y. Heng¹⁷³, C. Hengler⁴², S. Henkelmann¹⁶⁸, A. Henrichs¹⁷⁶, A.M. Henriques Correia³⁰,
S. Henrot-Versille¹¹⁷, G.H. Herbert¹⁶, Y. Hernández Jiménez¹⁶⁷, G. Herten⁴⁸, R. Hertenberger¹⁰⁰,
L. Hervas³⁰, G.G. Hesketh⁷⁸, N.P. Hessey¹⁰⁷, J.W. Hetherly⁴⁰, R. Hickling⁷⁶, E. Higón-Rodríguez¹⁶⁷,
E. Hill¹⁶⁹, J.C. Hill²⁸, K.H. Hiller⁴², S.J. Hillier¹⁸, I. Hinchliffe¹⁵, E. Hines¹²², R.R. Hinman¹⁵,
M. Hirose¹⁵⁷, D. Hirschbuehl¹⁷⁵, J. Hobbs¹⁴⁸, N. Hod¹⁰⁷, M.C. Hodgkinson¹³⁹, P. Hodgson¹³⁹,
A. Hoecker³⁰, M.R. Hoferkamp¹⁰⁵, F. Hoenic¹⁰⁰, M. Hohlfeld⁸³, D. Hohn²¹, T.R. Holmes¹⁵,
M. Homann⁴³, T.M. Hong¹²⁵, W.H. Hopkins¹¹⁶, Y. Horii¹⁰³, A.J. Horton¹⁴², J.-Y. Hostachy⁵⁵, S. Hou¹⁵¹,
A. Houmada^{135a}, J. Howard¹²⁰, J. Howarth⁴², M. Hrabovsky¹¹⁵, I. Hristova¹⁶, J. Hrivnac¹¹⁷,
T. Hryn'ova⁵, A. Hrynevich⁹³, C. Hsu^{145c}, P.J. Hsu^{151,r}, S.-C. Hsu¹³⁸, D. Hu³⁵, Q. Hu^{33b}, X. Hu⁸⁹,
Y. Huang⁴², Z. Hubacek¹²⁸, F. Hubaut⁸⁵, F. Huegging²¹, T.B. Huffman¹²⁰, E.W. Hughes³⁵, G. Hughes⁷²,
M. Huhtinen³⁰, T.A. Hülsing⁸³, N. Huseynov^{65,b}, J. Huston⁹⁰, J. Huth⁵⁷, G. Iacobucci⁴⁹, G. Iakovidis²⁵,
I. Ibragimov¹⁴¹, L. Iconomidou-Fayard¹¹⁷, E. Ideal¹⁷⁶, Z. Idrissi^{135e}, P. Iengo³⁰, O. Igonkina¹⁰⁷,
T. Iizawa¹⁷¹, Y. Ikegami⁶⁶, K. Ikematsu¹⁴¹, M. Ikeno⁶⁶, Y. Ilchenko^{31,s}, D. Iliadis¹⁵⁴, N. Ilic¹⁴³,
T. Ince¹⁰¹, G. Introzzi^{121a,121b}, P. Ioannou⁹, M. Iodice^{134a}, K. Iordanidou³⁵, V. Ippolito⁵⁷,
A. Irles Quiles¹⁶⁷, C. Isaksson¹⁶⁶, M. Ishino⁶⁸, M. Ishitsuka¹⁵⁷, R. Ishmukhametov¹¹¹, C. Issever¹²⁰,
S. Istin^{19a}, J.M. Iturbe Ponce⁸⁴, R. Iuppa^{133a,133b}, J. Ivarsson⁸¹, W. Iwanski³⁹, H. Iwasaki⁶⁶, J.M. Izen⁴¹,
V. Izzo^{104a}, S. Jabbar³, B. Jackson¹²², M. Jackson⁷⁴, P. Jackson¹, M.R. Jaekel³⁰, V. Jain², K. Jakobs⁴⁸,

S. Jakobsen³⁰, T. Jakoubek¹²⁷, J. Jakubek¹²⁸, D.O. Jamin¹¹⁴, D.K. Jana⁷⁹, E. Jansen⁷⁸, R. Jansky⁶²,
 J. Janssen²¹, M. Janus⁵⁴, G. Jarlskog⁸¹, N. Javadov^{65,b}, T. Javůrek⁴⁸, L. Jeanty¹⁵, J. Jejelava^{51a,t},
 G.-Y. Jeng¹⁵⁰, D. Jennens⁸⁸, P. Jenni^{48,u}, J. Jentsch⁴³, C. Jeske¹⁷⁰, S. Jézéquel⁵, H. Ji¹⁷³, J. Jia¹⁴⁸,
 Y. Jiang^{33b}, S. Jiggins⁷⁸, J. Jimenez Pena¹⁶⁷, S. Jin^{33a}, A. Jinaru^{26b}, O. Jinnouchi¹⁵⁷, M.D. Joergensen³⁶,
 P. Johansson¹³⁹, K.A. Johns⁷, W.J. Johnson¹³⁸, K. Jon-And^{146a,146b}, G. Jones¹⁷⁰, R.W.L. Jones⁷²,
 T.J. Jones⁷⁴, J. Jongmanns^{58a}, P.M. Jorge^{126a,126b}, K.D. Joshi⁸⁴, J. Jovicevic^{159a}, X. Ju¹⁷³, P. Juscel⁶²,
 A. Juste Rozas^{12,o}, M. Kaci¹⁶⁷, A. Kaczmarek³⁹, M. Kado¹¹⁷, H. Kagan¹¹¹, M. Kagan¹⁴³, S.J. Kahn⁸⁵,
 E. Kajomovitz⁴⁵, C.W. Kalderon¹²⁰, S. Kama⁴⁰, A. Kamenshchikov¹³⁰, N. Kanaya¹⁵⁵, S. Kaneti²⁸,
 V.A. Kantserov⁹⁸, J. Kanzaki⁶⁶, B. Kaplan¹¹⁰, L.S. Kaplan¹⁷³, A. Kapliy³¹, D. Kar^{145c}, K. Karakostas¹⁰,
 A. Karamaoun³, N. Karastathis^{10,107}, M.J. Kareem⁵⁴, E. Karentzos¹⁰, M. Karnevskiy⁸³, S.N. Karpov⁶⁵,
 Z.M. Karpova⁶⁵, K. Karthik¹¹⁰, V. Kartvelishvili⁷², A.N. Karyukhin¹³⁰, K. Kasahara¹⁶⁰, L. Kashif¹⁷³,
 R.D. Kass¹¹¹, A. Kastanas¹⁴, Y. Kataoka¹⁵⁵, C. Kato¹⁵⁵, A. Katre⁴⁹, J. Katzy⁴², K. Kawagoe⁷⁰,
 T. Kawamoto¹⁵⁵, G. Kawamura⁵⁴, S. Kazama¹⁵⁵, V.F. Kazanin^{109,c}, R. Keeler¹⁶⁹, R. Kehoe⁴⁰,
 J.S. Keller⁴², J.J. Kempster⁷⁷, H. Keoshkerian⁸⁴, O. Kepka¹²⁷, B.P. Kerševan⁷⁵, S. Kersten¹⁷⁵,
 R.A. Keyes⁸⁷, F. Khalil-zada¹¹, H. Khandanyan^{146a,146b}, A. Khanov¹¹⁴, A.G. Kharlamov^{109,c},
 T.J. Khoo²⁸, V. Khovanskiy⁹⁷, E. Khramov⁶⁵, J. Khubua^{51b,v}, S. Kido⁶⁷, H.Y. Kim⁸, S.H. Kim¹⁶⁰,
 Y.K. Kim³¹, N. Kimura¹⁵⁴, O.M. Kind¹⁶, B.T. King⁷⁴, M. King¹⁶⁷, S.B. King¹⁶⁸, J. Kirk¹³¹,
 A.E. Kiryunin¹⁰¹, T. Kishimoto⁶⁷, D. Kisiełowska^{38a}, F. Kiss⁴⁸, K. Kiuchi¹⁶⁰, O. Kivernyk¹³⁶,
 E. Kladiva^{144b}, M.H. Klein³⁵, M. Klein⁷⁴, U. Klein⁷⁴, K. Kleinknecht⁸³, P. Klimek^{146a,146b},
 A. Klimentov²⁵, R. Klingenberg⁴³, J.A. Klinger¹³⁹, T. Klioutchnikova³⁰, E.-E. Kluge^{58a}, P. Kluit¹⁰⁷,
 S. Kluth¹⁰¹, J. Knapik³⁹, E. Kneringer⁶², E.B.F.G. Knoops⁸⁵, A. Knue⁵³, A. Kobayashi¹⁵⁵,
 D. Kobayashi¹⁵⁷, T. Kobayashi¹⁵⁵, M. Kobel⁴⁴, M. Kocian¹⁴³, P. Kodys¹²⁹, T. Koffas²⁹, E. Koffeman¹⁰⁷,
 L.A. Kogan¹²⁰, S. Kohlmann¹⁷⁵, Z. Kohout¹²⁸, T. Kohriki⁶⁶, T. Koi¹⁴³, H. Kolanoski¹⁶, M. Kolb^{58b},
 I. Koletsou⁵, A.A. Komar^{96,*}, Y. Komori¹⁵⁵, T. Kondo⁶⁶, N. Kondrashova⁴², K. Köneke⁴⁸,
 A.C. König¹⁰⁶, T. Kono⁶⁶, R. Konoplich^{110,w}, N. Konstantinidis⁷⁸, R. Kopeliansky¹⁵², S. Koperny^{38a},
 L. Köpke⁸³, A.K. Kopp⁴⁸, K. Korcyl³⁹, K. Kordas¹⁵⁴, A. Korn⁷⁸, A.A. Korol^{109,c}, I. Korolkov¹²,
 E.V. Korolkova¹³⁹, O. Kortner¹⁰¹, S. Kortner¹⁰¹, T. Kosek¹²⁹, V.V. Kostyukhin²¹, V.M. Kotov⁶⁵,
 A. Kotwal⁴⁵, A. Kourkoumeli-Charalampidi¹⁵⁴, C. Kourkoumelis⁹, V. Kouskoura²⁵, A. Koutsman^{159a},
 R. Kowalewski¹⁶⁹, T.Z. Kowalski^{38a}, W. Kozanecki¹³⁶, A.S. Kozhin¹³⁰, V.A. Kramarenko⁹⁹,
 G. Kramberger⁷⁵, D. Krasnopevtsev⁹⁸, M.W. Krasny⁸⁰, A. Krasznahorkay³⁰, J.K. Kraus²¹,
 A. Kravchenko²⁵, S. Kreiss¹¹⁰, M. Kretz^{58c}, J. Kretzschmar⁷⁴, K. Kreutzfeldt⁵², P. Krieger¹⁵⁸,
 K. Krizka³¹, K. Kroeninger⁴³, H. Kroha¹⁰¹, J. Kroll¹²², J. Kroseberg²¹, J. Krstic¹³, U. Kruchonak⁶⁵,
 H. Krüger²¹, N. Krumnack⁶⁴, A. Kruse¹⁷³, M.C. Kruse⁴⁵, M. Kruskal²², T. Kubota⁸⁸, H. Kucuk⁷⁸,
 S. Kudah^{4b}, S. Kuehn⁴⁸, A. Kugel^{58c}, F. Kuger¹⁷⁴, A. Kuhl¹³⁷, T. Kuhl⁴², V. Kukhtin⁶⁵, R. Kukla¹³⁶,
 Y. Kulchitsky⁹², S. Kuleshov^{32b}, M. Kuna^{132a,132b}, T. Kunigo⁶⁸, A. Kupco¹²⁷, H. Kurashige⁶⁷,
 Y.A. Kurochkin⁹², V. Kus¹²⁷, E.S. Kuwertz¹⁶⁹, M. Kuze¹⁵⁷, J. Kvita¹¹⁵, T. Kwan¹⁶⁹,
 D. Kyriazopoulos¹³⁹, A. La Rosa¹³⁷, J.L. La Rosa Navarro^{24d}, L. La Rotonda^{37a,37b}, C. Lacasta¹⁶⁷,
 F. Lacava^{132a,132b}, J. Lacey²⁹, H. Lacker¹⁶, D. Lacour⁸⁰, V.R. Lacuesta¹⁶⁷, E. Ladygin⁶⁵, R. Lafaye⁵,
 B. Laforge⁸⁰, T. Lagouri¹⁷⁶, S. Lai⁵⁴, L. Lambourne⁷⁸, S. Lammers⁶¹, C.L. Lampen⁷, W. Lampl⁷,
 E. Lançon¹³⁶, U. Landgraf⁴⁸, M.P.J. Landon⁷⁶, V.S. Lang^{58a}, J.C. Lange¹², A.J. Lankford¹⁶³, F. Lanni²⁵,
 K. Lantsch²¹, A. Lanza^{121a}, S. Laplace⁸⁰, C. Lapoire³⁰, J.F. Laporte¹³⁶, T. Lari^{91a},
 F. Lasagni Manghi^{20a,20b}, M. Lassnig³⁰, P. Laurelli⁴⁷, W. Lavrijsen¹⁵, A.T. Law¹³⁷, P. Laycock⁷⁴,
 T. Lazovich⁵⁷, O. Le Dortz⁸⁰, E. Le Guirriec⁸⁵, E. Le Menedeu¹², M. LeBlanc¹⁶⁹, T. LeCompte⁶,
 F. Ledroit-Guillon⁵⁵, C.A. Lee^{145a}, S.C. Lee¹⁵¹, L. Lee¹, G. Lefebvre⁸⁰, M. Lefebvre¹⁶⁹, F. Legger¹⁰⁰,
 C. Leggett¹⁵, A. Lehan⁷⁴, G. Lehmann Miotto³⁰, X. Lei⁷, W.A. Leight²⁹, A. Leisos^{154,x}, A.G. Leister¹⁷⁶,
 M.A.L. Leite^{24d}, R. Leitner¹²⁹, D. Lellouch¹⁷², B. Lemmer⁵⁴, K.J.C. Leney⁷⁸, T. Lenz²¹, B. Lenzi³⁰,
 R. Leone⁷, S. Leone^{124a,124b}, C. Leonidopoulos⁴⁶, S. Leontsinis¹⁰, C. Leroy⁹⁵, C.G. Lester²⁸,

M. Levchenko¹²³, J. Levêque⁵, D. Levin⁸⁹, L.J. Levinson¹⁷², M. Levy¹⁸, A. Lewis¹²⁰, A.M. Leyko²¹,
M. Leyton⁴¹, B. Li^{33b,y}, H. Li¹⁴⁸, H.L. Li³¹, L. Li⁴⁵, L. Li^{33e}, S. Li⁴⁵, X. Li⁸⁴, Y. Li^{33c,z}, Z. Liang¹³⁷,
H. Liao³⁴, B. Liberti^{133a}, A. Liblong¹⁵⁸, P. Lichard³⁰, K. Lie¹⁶⁵, J. Liebal²¹, W. Liebig¹⁴, C. Limbach²¹,
A. Limosani¹⁵⁰, S.C. Lin^{151,aa}, T.H. Lin⁸³, F. Linde¹⁰⁷, B.E. Lindquist¹⁴⁸, J.T. Linnemann⁹⁰,
E. Lipeles¹²², A. Lipniacka¹⁴, M. Lisovyi^{58b}, T.M. Liss¹⁶⁵, D. Lissauer²⁵, A. Lister¹⁶⁸, A.M. Litke¹³⁷,
B. Liu^{151,ab}, D. Liu¹⁵¹, H. Liu⁸⁹, J. Liu⁸⁵, J.B. Liu^{33b}, K. Liu⁸⁵, L. Liu¹⁶⁵, M. Liu⁴⁵, M. Liu^{33b},
Y. Liu^{33b}, M. Livan^{121a,121b}, A. Lleres⁵⁵, J. Llorente Merino⁸², S.L. Lloyd⁷⁶, F. Lo Sterzo¹⁵¹,
E. Lobodzinska⁴², P. Loch⁷, W.S. Lockman¹³⁷, F.K. Loebinger⁸⁴, A.E. Loevschall-Jensen³⁶,
K.M. Loew²³, A. Loginov¹⁷⁶, T. Lohse¹⁶, K. Lohwasser⁴², M. Lokajicek¹²⁷, B.A. Long²², J.D. Long¹⁶⁵,
R.E. Long⁷², K.A. Looper¹¹¹, L. Lopes^{126a}, D. Lopez Mateos⁵⁷, B. Lopez Paredes¹³⁹, I. Lopez Paz¹²,
J. Lorenz¹⁰⁰, N. Lorenzo Martinez⁶¹, M. Losada¹⁶², P.J. Lösel¹⁰⁰, X. Lou^{33a}, A. Lounis¹¹⁷, J. Love⁶,
P.A. Love⁷², N. Lu⁸⁹, H.J. Lubatti¹³⁸, C. Luci^{132a,132b}, A. Lucotte⁵⁵, C. Luedtke⁴⁸, F. Luehring⁶¹,
W. Lukas⁶², L. Luminari^{132a}, O. Lundberg^{146a,146b}, B. Lund-Jensen¹⁴⁷, D. Lynn²⁵, R. Lysak¹²⁷,
E. Lytken⁸¹, H. Ma²⁵, L.L. Ma^{33d}, G. Maccarrone⁴⁷, A. Macchiolo¹⁰¹, C.M. Macdonald¹³⁹, B. Maček⁷⁵,
J. Machado Miguens^{122,126b}, D. Macina³⁰, D. Madaffari⁸⁵, R. Madar³⁴, H.J. Maddocks⁷², W.F. Mader⁴⁴,
A. Madsen¹⁶⁶, J. Maeda⁶⁷, S. Maeland¹⁴, T. Maeno²⁵, A. Maevskiy⁹⁹, E. Magradze⁵⁴, K. Mahboubi⁴⁸,
J. Mahlstedt¹⁰⁷, C. Maiani¹³⁶, C. Maidantchik^{24a}, A.A. Maier¹⁰¹, T. Maier¹⁰⁰, A. Maio^{126a,126b,126d},
S. Majewski¹¹⁶, Y. Makida⁶⁶, N. Makovec¹¹⁷, B. Malaescu⁸⁰, Pa. Malecki³⁹, V.P. Maleev¹²³, F. Malek⁵⁵,
U. Mallik⁶³, D. Malon⁶, C. Malone¹⁴³, S. Maltezos¹⁰, V.M. Malyshev¹⁰⁹, S. Malyukov³⁰, J. Mamuzic⁴²,
G. Mancini⁴⁷, B. Mandelli³⁰, L. Mandelli^{91a}, I. Mandić⁷⁵, R. Mandrysch⁶³, J. Maneira^{126a,126b},
A. Manfredini¹⁰¹, L. Manhaes de Andrade Filho^{24b}, J. Manjarres Ramos^{159b}, A. Mann¹⁰⁰,
A. Manousakis-Katsikakis⁹, B. Mansoulie¹³⁶, R. Mantifel⁸⁷, M. Mantoani⁵⁴, L. Mapelli³⁰, L. March^{145c},
G. Marchiori⁸⁰, M. Marcisovsky¹²⁷, C.P. Marino¹⁶⁹, M. Marjanovic¹³, D.E. Marley⁸⁹, F. Marroquim^{24a},
S.P. Marsden⁸⁴, Z. Marshall¹⁵, L.F. Marti¹⁷, S. Marti-Garcia¹⁶⁷, B. Martin⁹⁰, T.A. Martin¹⁷⁰,
V.J. Martin⁴⁶, B. Martin dit Latour¹⁴, M. Martinez^{12,o}, S. Martin-Haugh¹³¹, V.S. Martoiu^{26b},
A.C. Martyniuk⁷⁸, M. Marx¹³⁸, F. Marzano^{132a}, A. Marzin³⁰, L. Masetti⁸³, T. Mashimo¹⁵⁵,
R. Mashinistov⁹⁶, J. Masik⁸⁴, A.L. Maslennikov^{109,c}, I. Massa^{20a,20b}, L. Massa^{20a,20b}, P. Mastrandrea⁵,
A. Mastroberardino^{37a,37b}, T. Masubuchi¹⁵⁵, P. Mättig¹⁷⁵, J. Mattmann⁸³, J. Maurer^{26b}, S.J. Maxfield⁷⁴,
D.A. Maximov^{109,c}, R. Mazini¹⁵¹, S.M. Mazza^{91a,91b}, G. Mc Goldrick¹⁵⁸, S.P. Mc Kee⁸⁹, A. McCarn⁸⁹,
R.L. McCarthy¹⁴⁸, T.G. McCarthy²⁹, N.A. McCubbin¹³¹, K.W. McFarlane^{56,*}, J.A. McFayden⁷⁸,
G. Mchedlidze⁵⁴, S.J. McMahon¹³¹, R.A. McPherson^{169,k}, M. Medinnis⁴², S. Meehan^{145a},
S. Mehlhase¹⁰⁰, A. Mehta⁷⁴, K. Meier^{58a}, C. Meineck¹⁰⁰, B. Meirose⁴¹, B.R. Mellado Garcia^{145c},
F. Meloni¹⁷, A. Mengarelli^{20a,20b}, S. Menke¹⁰¹, E. Meoni¹⁶¹, K.M. Mercurio⁵⁷, S. Mergelmeyer²¹,
P. Mermod⁴⁹, L. Merola^{104a,104b}, C. Meroni^{91a}, F.S. Merritt³¹, A. Messina^{132a,132b}, J. Metcalfe²⁵,
A.S. Mete¹⁶³, C. Meyer⁸³, C. Meyer¹²², J-P. Meyer¹³⁶, J. Meyer¹⁰⁷, H. Meyer Zu Theenhausen^{58a},
R.P. Middleton¹³¹, S. Miglioranzi^{164a,164c}, L. Mijović²¹, G. Mikenberg¹⁷², M. Mikestikova¹²⁷,
M. Mikuž⁷⁵, M. Milesi⁸⁸, A. Milic³⁰, D.W. Miller³¹, C. Mills⁴⁶, A. Milov¹⁷², D.A. Milstead^{146a,146b},
A.A. Minaenko¹³⁰, Y. Minami¹⁵⁵, I.A. Minashvili⁶⁵, A.I. Mincer¹¹⁰, B. Mindur^{38a}, M. Mineev⁶⁵,
Y. Ming¹⁷³, L.M. Mir¹², K.P. Mistry¹²², T. Mitani¹⁷¹, J. Mitrevski¹⁰⁰, V.A. Mitsou¹⁶⁷, A. Miucci⁴⁹,
P.S. Miyagawa¹³⁹, J.U. Mjörnmark⁸¹, T. Moa^{146a,146b}, K. Mochizuki⁸⁵, S. Mohapatra³⁵, W. Mohr⁴⁸,
S. Molander^{146a,146b}, R. Moles-Valls²¹, R. Monden⁶⁸, K. Mönig⁴², C. Monini⁵⁵, J. Monk³⁶,
E. Monnier⁸⁵, A. Montalbano¹⁴⁸, J. Montejo Berlingen¹², F. Monticelli⁷¹, S. Monzani^{132a,132b},
R.W. Moore³, N. Morange¹¹⁷, D. Moreno¹⁶², M. Moreno Llácer⁵⁴, P. Morettini^{50a}, D. Mori¹⁴²,
T. Mori¹⁵⁵, M. Morii⁵⁷, M. Morinaga¹⁵⁵, V. Morisbak¹¹⁹, S. Moritz⁸³, A.K. Morley¹⁵⁰, G. Mornacchi³⁰,
J.D. Morris⁷⁶, S.S. Mortensen³⁶, A. Morton⁵³, L. Morvaj¹⁰³, M. Mosidze^{51b}, J. Moss¹⁴³,
K. Motohashi¹⁵⁷, R. Mount¹⁴³, E. Mountricha²⁵, S.V. Mouraviev^{96,*}, E.J.W. Moyse⁸⁶, S. Muanza⁸⁵,
R.D. Mudd¹⁸, F. Mueller¹⁰¹, J. Mueller¹²⁵, R.S.P. Mueller¹⁰⁰, T. Mueller²⁸, D. Muenstermann⁴⁹,

P. Mullen⁵³, G.A. Mullier¹⁷, J.A. Murillo Quijada¹⁸, W.J. Murray^{170,131}, H. Musheghyan⁵⁴, E. Musto¹⁵²,
 A.G. Myagkov^{130.ac}, M. Myska¹²⁸, B.P. Nachman¹⁴³, O. Nackenhorst⁵⁴, J. Nadal⁵⁴, K. Nagai¹²⁰,
 R. Nagai¹⁵⁷, Y. Nagai⁸⁵, K. Nagano⁶⁶, A. Nagarkar¹¹¹, Y. Nagasaka⁵⁹, K. Nagata¹⁶⁰, M. Nagel¹⁰¹,
 E. Nagy⁸⁵, A.M. Nairz³⁰, Y. Nakahama³⁰, K. Nakamura⁶⁶, T. Nakamura¹⁵⁵, I. Nakano¹¹²,
 H. Namasivayam⁴¹, R.F. Naranjo Garcia⁴², R. Narayan³¹, D.I. Narrias Villar^{58a}, T. Naumann⁴²,
 G. Navarro¹⁶², R. Nayyar⁷, H.A. Neal⁸⁹, P.Yu. Nechaeva⁹⁶, T.J. Neep⁸⁴, P.D. Nef¹⁴³, A. Negri^{121a,121b},
 M. Negrini^{20a}, S. Nektarijevic¹⁰⁶, C. Nellist¹¹⁷, A. Nelson¹⁶³, S. Nemecek¹²⁷, P. Nemethy¹¹⁰,
 A.A. Nepomuceno^{24a}, M. Nessi^{30.ad}, M.S. Neubauer¹⁶⁵, M. Neumann¹⁷⁵, R.M. Neves¹¹⁰, P. Nevski²⁵,
 P.R. Newman¹⁸, D.H. Nguyen⁶, R.B. Nickerson¹²⁰, R. Nicolaidou¹³⁶, B. Nicquevert³⁰, J. Nielsen¹³⁷,
 N. Nikiforou³⁵, A. Nikiforov¹⁶, V. Nikolaenko^{130.ac}, I. Nikolic-Audit⁸⁰, K. Nikolopoulos¹⁸,
 J.K. Nilsen¹¹⁹, P. Nilsson²⁵, Y. Ninomiya¹⁵⁵, A. Nisati^{132a}, R. Nisius¹⁰¹, T. Nobe¹⁵⁵, M. Nomachi¹¹⁸,
 I. Nomidis²⁹, T. Nooney⁷⁶, S. Norberg¹¹³, M. Nordberg³⁰, O. Novgorodova⁴⁴, S. Nowak¹⁰¹,
 M. Nozaki⁶⁶, L. Nozka¹¹⁵, K. Ntekas¹⁰, G. Nunes Hanninger⁸⁸, T. Nunnemann¹⁰⁰, E. Nurse⁷⁸, F. Nuti⁸⁸,
 B.J. O'Brien⁴⁶, F. O'grady⁷, D.C. O'Neil¹⁴², V. O'Shea⁵³, F.G. Oakham^{29.d}, H. Oberlack¹⁰¹,
 T. Obermann²¹, J. Ocariz⁸⁰, A. Ochi⁶⁷, I. Ochoa³⁵, J.P. Ochoa-Ricoux^{32a}, S. Oda⁷⁰, S. Odaka⁶⁶,
 H. Ogren⁶¹, A. Oh⁸⁴, S.H. Oh⁴⁵, C.C. Ohm¹⁵, H. Ohman¹⁶⁶, H. Oide³⁰, W. Okamura¹¹⁸, H. Okawa¹⁶⁰,
 Y. Okumura³¹, T. Okuyama⁶⁶, A. Olariu^{26b}, S.A. Olivares Pino⁴⁶, D. Oliveira Damazio²⁵,
 A. Olszewski³⁹, J. Olszowska³⁹, A. Onofre^{126a,126e}, K. Onogi¹⁰³, P.U.E. Onyisi^{31.s}, C.J. Oram^{159a},
 M.J. Oreglia³¹, Y. Oren¹⁵³, D. Orestano^{134a,134b}, N. Orlando¹⁵⁴, C. Oropeza Barrera⁵³, R.S. Orr¹⁵⁸,
 B. Osculati^{50a,50b}, R. Ospanov⁸⁴, G. Otero y Garzon²⁷, H. Otono⁷⁰, M. Ouchrif^{135d}, F. Ould-Saada¹¹⁹,
 A. Ouraou¹³⁶, K.P. Oussoren¹⁰⁷, Q. Ouyang^{33a}, A. Ovcharova¹⁵, M. Owen⁵³, R.E. Owen¹⁸,
 V.E. Ozcan^{19a}, N. Ozturk⁸, K. Pachal¹⁴², A. Pacheco Pages¹², C. Padilla Aranda¹², M. Pagáčová⁴⁸,
 S. Pagan Griso¹⁵, E. Paganis¹³⁹, F. Paige²⁵, P. Pais⁸⁶, K. Pajchel¹¹⁹, G. Palacino^{159b}, S. Palestini³⁰,
 M. Palka^{38b}, D. Pallin³⁴, A. Palma^{126a,126b}, Y.B. Pan¹⁷³, E. Panagiotopoulou¹⁰, C.E. Pandini⁸⁰,
 J.G. Panduro Vazquez⁷⁷, P. Pani^{146a,146b}, S. Panitkin²⁵, D. Pantea^{26b}, L. Paolozzi⁴⁹,
 Th.D. Papadopoulou¹⁰, K. Papageorgiou¹⁵⁴, A. Paramonov⁶, D. Paredes Hernandez¹⁵⁴, M.A. Parker²⁸,
 K.A. Parker¹³⁹, F. Parodi^{50a,50b}, J.A. Parsons³⁵, U. Parzefall⁴⁸, E. Pasqualucci^{132a}, S. Passaggio^{50a},
 F. Pastore^{134a,134b,*}, Fr. Pastore⁷⁷, G. Pásztor²⁹, S. Patariaia¹⁷⁵, N.D. Patel¹⁵⁰, J.R. Pater⁸⁴, T. Pauly³⁰,
 J. Pearce¹⁶⁹, B. Pearson¹¹³, L.E. Pedersen³⁶, M. Pedersen¹¹⁹, S. Pedraza Lopez¹⁶⁷, R. Pedro^{126a,126b},
 S.V. Peleganchuk^{109.c}, D. Pelikan¹⁶⁶, O. Penc¹²⁷, C. Peng^{33a}, H. Peng^{33b}, B. Penning³¹, J. Penwell⁶¹,
 D.V. Perepelitsa²⁵, E. Perez Codina^{159a}, M.T. Pérez García-Estañ¹⁶⁷, L. Perini^{91a,91b}, H. Pernegger³⁰,
 S. Perrella^{104a,104b}, R. Peschke⁴², V.D. Peshekhonov⁶⁵, K. Peters³⁰, R.F.Y. Peters⁸⁴, B.A. Petersen³⁰,
 T.C. Petersen³⁶, E. Petit⁴², A. Petridis¹, C. Petridou¹⁵⁴, P. Petroff¹¹⁷, E. Petrolo^{132a}, F. Petrucci^{134a,134b},
 N.E. Pettersson¹⁵⁷, R. Pezoa^{32b}, P.W. Phillips¹³¹, G. Piacquadio¹⁴³, E. Pianori¹⁷⁰, A. Picazio⁴⁹,
 E. Piccaro⁷⁶, M. Piccinini^{20a,20b}, M.A. Pickering¹²⁰, R. Piegaia²⁷, D.T. Pignotti¹¹¹, J.E. Pilcher³¹,
 A.D. Pilkington⁸⁴, A.W.J. Pin⁸⁴, J. Pina^{126a,126b,126d}, M. Pinamonti^{164a,164c,ae}, J.L. Pinfeld³, A. Pingel³⁶,
 S. Pires⁸⁰, H. Pirumov⁴², M. Pitt¹⁷², C. Pizio^{91a,91b}, L. Plazak^{144a}, M.-A. Pleier²⁵, V. Pleskot¹²⁹,
 E. Plotnikova⁶⁵, P. Plucinski^{146a,146b}, D. Pluth⁶⁴, R. Poettgen^{146a,146b}, L. Poggioli¹¹⁷, D. Pohl²¹,
 G. Polesello^{121a}, A. Poley⁴², A. Policicchio^{37a,37b}, R. Polifka¹⁵⁸, A. Polini^{20a}, C.S. Pollard⁵³,
 V. Polychronakos²⁵, K. Pommès³⁰, L. Pontecorvo^{132a}, B.G. Pope⁹⁰, G.A. Popeneciu^{26c}, D.S. Popovic¹³,
 A. Poppleton³⁰, S. Pospisil¹²⁸, K. Potamianos¹⁵, I.N. Potrap⁶⁵, C.J. Potter¹⁴⁹, C.T. Potter¹¹⁶,
 G. Poulard³⁰, J. Poveda³⁰, V. Pozdnyakov⁶⁵, P. Pralavorio⁸⁵, A. Pranko¹⁵, S. Prasad³⁰, S. Prell⁶⁴,
 D. Price⁸⁴, L.E. Price⁶, M. Primavera^{73a}, S. Prince⁸⁷, M. Proissl⁴⁶, K. Prokofiev^{60c}, F. Prokoshin^{32b},
 E. Protopapadaki¹³⁶, S. Protopopescu²⁵, J. Proudfoot⁶, M. Przybycien^{38a}, E. Ptacek¹¹⁶,
 D. Puddu^{134a,134b}, E. Pueschel⁸⁶, D. Puldon¹⁴⁸, M. Purohit^{25.af}, P. Puzo¹¹⁷, J. Qian⁸⁹, G. Qin⁵³, Y. Qin⁸⁴,
 A. Quadt⁵⁴, D.R. Quarrie¹⁵, W.B. Quayle^{164a,164b}, M. Queitsch-Maitland⁸⁴, D. Quilty⁵³, S. Raddum¹¹⁹,
 V. Radeka²⁵, V. Radescu⁴², S.K. Radhakrishnan¹⁴⁸, P. Radloff¹¹⁶, P. Rados⁸⁸, F. Ragusa^{91a,91b},

G. Rahal¹⁷⁸, S. Rajagopalan²⁵, M. Rammensee³⁰, C. Rangel-Smith¹⁶⁶, F. Rauscher¹⁰⁰, S. Rave⁸³, T. Ravenscroft⁵³, M. Raymond³⁰, A.L. Read¹¹⁹, N.P. Readioff⁷⁴, D.M. Rebuzzi^{121a,121b}, A. Redelbach¹⁷⁴, G. Redlinger²⁵, R. Reece¹³⁷, K. Reeves⁴¹, L. Rehnisch¹⁶, J. Reichert¹²², H. Reisin²⁷, C. Rembser³⁰, H. Ren^{33a}, A. Renaud¹¹⁷, M. Rescigno^{132a}, S. Resconi^{91a}, O.L. Rezanova^{109,c}, P. Reznicek¹²⁹, R. Rezvani⁹⁵, R. Richter¹⁰¹, S. Richter⁷⁸, E. Richter-Was^{38b}, O. Ricken²¹, M. Ridel⁸⁰, P. Rieck¹⁶, C.J. Riegel¹⁷⁵, J. Rieger⁵⁴, O. Rifki¹¹³, M. Rijssenbeek¹⁴⁸, A. Rimoldi^{121a,121b}, L. Rinaldi^{20a}, B. Ristić⁴⁹, E. Ritsch³⁰, I. Riu¹², F. Rizatdinova¹¹⁴, E. Rizvi⁷⁶, S.H. Robertson^{87,k}, A. Robichaud-Veronneau⁸⁷, D. Robinson²⁸, J.E.M. Robinson⁴², A. Robson⁵³, C. Roda^{124a,124b}, S. Roe³⁰, O. Røhne¹¹⁹, S. Rolli¹⁶¹, A. Romaniouk⁹⁸, M. Romano^{20a,20b}, S.M. Romano Saez³⁴, E. Romero Adam¹⁶⁷, N. Rompotis¹³⁸, M. Ronzani⁴⁸, L. Roos⁸⁰, E. Ros¹⁶⁷, S. Rosati^{132a}, K. Rosbach⁴⁸, P. Rose¹³⁷, P.L. Rosendahl¹⁴, O. Rosenthal¹⁴¹, V. Rossetti^{146a,146b}, E. Rossi^{104a,104b}, L.P. Rossi^{50a}, J.H.N. Rosten²⁸, R. Rosten¹³⁸, M. Rotaru^{26b}, I. Roth¹⁷², J. Rothberg¹³⁸, D. Rousseau¹¹⁷, C.R. Royon¹³⁶, A. Rozanov⁸⁵, Y. Rozen¹⁵², X. Ruan^{145c}, F. Rubbo¹⁴³, I. Rubinskiy⁴², V.I. Rud⁹⁹, C. Rudolph⁴⁴, M.S. Rudolph¹⁵⁸, F. Rühr⁴⁸, A. Ruiz-Martinez³⁰, Z. Rurikova⁴⁸, N.A. Rusakovich⁶⁵, A. Ruschke¹⁰⁰, H.L. Russell¹³⁸, J.P. Rutherford⁷, N. Ruthmann³⁰, Y.F. Ryabov¹²³, M. Rybar¹⁶⁵, G. Rybkin¹¹⁷, N.C. Ryder¹²⁰, A.F. Saavedra¹⁵⁰, G. Sabato¹⁰⁷, S. Sacerdoti²⁷, A. Saddique³, H.F.W. Sadrozinski¹³⁷, R. Sadykov⁶⁵, F. Safai Tehrani^{132a}, P. Saha¹⁰⁸, M. Sahinsoy^{58a}, M. Saimpert¹³⁶, T. Saito¹⁵⁵, H. Sakamoto¹⁵⁵, Y. Sakurai¹⁷¹, G. Salamanna^{134a,134b}, A. Salamon^{133a}, J.E. Salazar Loyola^{32b}, M. Saleem¹¹³, D. Salek¹⁰⁷, P.H. Sales De Bruin¹³⁸, D. Salihagic¹⁰¹, A. Salnikov¹⁴³, J. Salt¹⁶⁷, D. Salvatore^{37a,37b}, F. Salvatore¹⁴⁹, A. Salvucci^{60a}, A. Salzburger³⁰, D. Sammel⁴⁸, D. Sampsonidis¹⁵⁴, A. Sanchez^{104a,104b}, J. Sánchez¹⁶⁷, V. Sanchez Martinez¹⁶⁷, H. Sandaker¹¹⁹, R.L. Sandbach⁷⁶, H.G. Sander⁸³, M.P. Sanders¹⁰⁰, M. Sandhoff¹⁷⁵, C. Sandoval¹⁶², R. Sandstroem¹⁰¹, D.P.C. Sankey¹³¹, M. Sannino^{50a,50b}, A. Sansoni⁴⁷, C. Santoni³⁴, R. Santonico^{133a,133b}, H. Santos^{126a}, I. Santoyo Castillo¹⁴⁹, K. Sapp¹²⁵, A. Sapronov⁶⁵, J.G. Saraiva^{126a,126d}, B. Sarrazin²¹, O. Sasaki⁶⁶, Y. Sasaki¹⁵⁵, K. Sato¹⁶⁰, G. Sauvage^{5,*}, E. Sauvan⁵, G. Savage⁷⁷, P. Savard^{158,d}, C. Sawyer¹³¹, L. Sawyer^{79,n}, J. Saxon³¹, C. Sbarra^{20a}, A. Sbrizzi^{20a,20b}, T. Scanlon⁷⁸, D.A. Scannicchio¹⁶³, M. Scarcella¹⁵⁰, V. Scarfone^{37a,37b}, J. Schaarschmidt¹⁷², P. Schacht¹⁰¹, D. Schaefer³⁰, R. Schaefer⁴², J. Schaeffer⁸³, S. Schaepe²¹, S. Schaetzel^{58b}, U. Schäfer⁸³, A.C. Schaffer¹¹⁷, D. Schaile¹⁰⁰, R.D. Schamberger¹⁴⁸, V. Scharf^{58a}, V.A. Schegelsky¹²³, D. Scheirich¹²⁹, M. Schernau¹⁶³, C. Schiavi^{50a,50b}, C. Schillo⁴⁸, M. Schioppa^{37a,37b}, S. Schlenker³⁰, K. Schmieden³⁰, C. Schmitt⁸³, S. Schmitt^{58b}, S. Schmitt⁴², B. Schneider^{159a}, Y.J. Schnellbach⁷⁴, U. Schnoor⁴⁴, L. Schoeffel¹³⁶, A. Schoening^{58b}, B.D. Schoenrock⁹⁰, E. Schopf²¹, A.L.S. Schorlemmer⁵⁴, M. Schott⁸³, D. Schouten^{159a}, J. Schovancova⁸, S. Schramm⁴⁹, M. Schreyer¹⁷⁴, N. Schuh⁸³, M.J. Schultens²¹, H.-C. Schultz-Coulon^{58a}, H. Schulz¹⁶, M. Schumacher⁴⁸, B.A. Schumm¹³⁷, Ph. Schune¹³⁶, C. Schwanenberger⁸⁴, A. Schwartzman¹⁴³, T.A. Schwarz⁸⁹, Ph. Schwegler¹⁰¹, H. Schweiger⁸⁴, Ph. Schwemling¹³⁶, R. Schwienhorst⁹⁰, J. Schwindling¹³⁶, T. Schwindt²¹, F.G. Sciacca¹⁷, E. Scifo¹¹⁷, G. Sciolla²³, F. Scuri^{124a,124b}, F. Scutti²¹, J. Searcy⁸⁹, G. Sedov⁴², E. Sedykh¹²³, P. Seema²¹, S.C. Seidel¹⁰⁵, A. Seiden¹³⁷, F. Seifert¹²⁸, J.M. Seixas^{24a}, G. Sekhniaidze^{104a}, K. Sekhon⁸⁹, S.J. Sekula⁴⁰, D.M. Seliverstov^{123,*}, N. Semprini-Cesari^{20a,20b}, C. Serfon³⁰, L. Serin¹¹⁷, L. Serkin^{164a,164b}, T. Serre⁸⁵, M. Sessa^{134a,134b}, R. Seuster^{159a}, H. Severini¹¹³, T. Sfiligoj⁷⁵, F. Sforza³⁰, A. Sfyrla³⁰, E. Shabalina⁵⁴, M. Shamim¹¹⁶, L.Y. Shan^{33a}, R. Shang¹⁶⁵, J.T. Shank²², M. Shapiro¹⁵, P.B. Shatalov⁹⁷, K. Shaw^{164a,164b}, S.M. Shaw⁸⁴, A. Shcherbakova^{146a,146b}, C.Y. Shehu¹⁴⁹, P. Sherwood⁷⁸, L. Shi^{151,ag}, S. Shimizu⁶⁷, C.O. Shimmin¹⁶³, M. Shimojima¹⁰², M. Shiyakova⁶⁵, A. Shmeleva⁹⁶, D. Shoaleh Saadi⁹⁵, M.J. Shochet³¹, S. Shojaii^{91a,91b}, S. Shrestha¹¹¹, E. Shulga⁹⁸, M.A. Shupe⁷, S. Shushkevich⁴², P. Sicho¹²⁷, P.E. Sidebo¹⁴⁷, O. Sidiropoulou¹⁷⁴, D. Sidorov¹¹⁴, A. Sidoti^{20a,20b}, F. Siegert⁴⁴, Dj. Sijacki¹³, J. Silva^{126a,126d}, Y. Silver¹⁵³, S.B. Silverstein^{146a}, V. Simak¹²⁸, O. Simard⁵, Lj. Simic¹³, S. Simion¹¹⁷, E. Simioni⁸³, B. Simmons⁷⁸, D. Simon³⁴, P. Sinervo¹⁵⁸, N.B. Sinev¹¹⁶,

M. Sioli^{20a,20b}, G. Siragusa¹⁷⁴, A.N. Sisakyan^{65,*}, S.Yu. Sivoklov⁹⁹, J. Sjölin^{146a,146b}, T.B. Sjursen¹⁴,
M.B. Skinner⁷², H.P. Skottowe⁵⁷, P. Skubic¹¹³, M. Slater¹⁸, T. Slavicek¹²⁸, M. Slawinska¹⁰⁷,
K. Sliwa¹⁶¹, V. Smakhtin¹⁷², B.H. Smart⁴⁶, L. Smestad¹⁴, S.Yu. Smirnov⁹⁸, Y. Smirnov⁹⁸,
L.N. Smirnova^{99,ah}, O. Smirnova⁸¹, M.N.K. Smith³⁵, R.W. Smith³⁵, M. Smizanska⁷², K. Smolek¹²⁸,
A.A. Snesev⁹⁶, G. Snidero⁷⁶, S. Snyder²⁵, R. Sobie^{169,k}, F. Socher⁴⁴, A. Soffer¹⁵³, D.A. Soh^{151,ag},
G. Sokhranyi⁷⁵, C.A. Solans³⁰, M. Solar¹²⁸, J. Solc¹²⁸, E.Yu. Soldatov⁹⁸, U. Soldevila¹⁶⁷,
A.A. Solodkov¹³⁰, A. Soloshenko⁶⁵, O.V. Solovyanov¹³⁰, V. Solovyev¹²³, P. Sommer⁴⁸, H.Y. Song^{33b,y},
N. Soni¹, A. Sood¹⁵, A. Sopcak¹²⁸, B. Sopko¹²⁸, V. Sopko¹²⁸, V. Sorin¹², D. Sosa^{58b}, M. Sosebee⁸,
C.L. Sotiropoulou^{124a,124b}, R. Soualah^{164a,164c}, A.M. Soukharev^{109,c}, D. South⁴², B.C. Sowden⁷⁷,
S. Spagnolo^{73a,73b}, M. Spalla^{124a,124b}, M. Spangenberg¹⁷⁰, F. Spanò⁷⁷, W.R. Spearman⁵⁷, D. Sperlich¹⁶,
F. Spettel¹⁰¹, R. Spighi^{20a}, G. Spigo³⁰, L.A. Spiller⁸⁸, M. Spousta¹²⁹, R.D. St. Denis^{53,*}, A. Stabile^{91a},
S. Staerz⁴⁴, J. Stahlman¹²², R. Stamen^{58a}, S. Stamm¹⁶, E. Stanecka³⁹, C. Stanescu^{134a},
M. Stanescu-Bellu⁴², M.M. Stanitzki⁴², S. Stapes¹¹⁹, E.A. Starchenko¹³⁰, J. Stark⁵⁵, P. Staroba¹²⁷,
P. Starovoitov^{58a}, R. Staszewski³⁹, P. Steinberg²⁵, B. Stelzer¹⁴², H.J. Stelzer³⁰, O. Stelzer-Chilton^{159a},
H. Stenzel⁵², G.A. Stewart⁵³, J.A. Stillings²¹, M.C. Stockton⁸⁷, M. Stoebe⁸⁷, G. Stoica^{26b}, P. Stolte⁵⁴,
S. Stonjek¹⁰¹, A.R. Stradling⁸, A. Straessner⁴⁴, M.E. Stramaglia¹⁷, J. Strandberg¹⁴⁷,
S. Strandberg^{146a,146b}, A. Strandlie¹¹⁹, E. Strauss¹⁴³, M. Strauss¹¹³, P. Strizenec^{144b}, R. Ströhmer¹⁷⁴,
D.M. Strom¹¹⁶, R. Stroynowski⁴⁰, A. Strubig¹⁰⁶, S.A. Stucci¹⁷, B. Stugu¹⁴, N.A. Styles⁴², D. Su¹⁴³,
J. Su¹²⁵, R. Subramaniam⁷⁹, A. Succurro¹², Y. Sugaya¹¹⁸, M. Suk¹²⁸, V.V. Sulin⁹⁶, S. Sultansoy^{4c},
T. Sumida⁶⁸, S. Sun⁵⁷, X. Sun^{33a}, J.E. Sundermann⁴⁸, K. Suruliz¹⁴⁹, G. Susinno^{37a,37b}, M.R. Sutton¹⁴⁹,
S. Suzuki⁶⁶, M. Svatos¹²⁷, M. Swiatlowski¹⁴³, I. Sykora^{144a}, T. Sykora¹²⁹, D. Ta⁴⁸, C. Taccini^{134a,134b},
K. Tackmann⁴², J. Taenzer¹⁵⁸, A. Taffard¹⁶³, R. Tafirout^{159a}, N. Taiblum¹⁵³, H. Takai²⁵, R. Takashima⁶⁹,
H. Takeda⁶⁷, T. Takeshita¹⁴⁰, Y. Takubo⁶⁶, M. Talby⁸⁵, A.A. Talyshev^{109,c}, J.Y.C. Tam¹⁷⁴, K.G. Tan⁸⁸,
J. Tanaka¹⁵⁵, R. Tanaka¹¹⁷, S. Tanaka⁶⁶, B.B. Tannenwald¹¹¹, N. Tannoury²¹, S. Tapprogge⁸³,
S. Tarem¹⁵², F. Tarrade²⁹, G.F. Tartarelli^{91a}, P. Tas¹²⁹, M. Tasevsky¹²⁷, T. Tashiro⁶⁸, E. Tassi^{37a,37b},
A. Tavares Delgado^{126a,126b}, Y. Tayalati^{135d}, F.E. Taylor⁹⁴, G.N. Taylor⁸⁸, P.T.E. Taylor⁸⁸, W. Taylor^{159b},
F.A. Teischinger³⁰, M. Teixeira Dias Castanheira⁷⁶, P. Teixeira-Dias⁷⁷, K.K. Temming⁴⁸, D. Temple¹⁴²,
H. Ten Kate³⁰, P.K. Teng¹⁵¹, J.J. Teoh¹¹⁸, F. Tepel¹⁷⁵, S. Terada⁶⁶, K. Terashi¹⁵⁵, J. Terron⁸², S. Terzo¹⁰¹,
M. Testa⁴⁷, R.J. Teuscher^{158,k}, T. Theveneaux-Pelzer³⁴, J.P. Thomas¹⁸, J. Thomas-Wilsker⁷⁷,
E.N. Thompson³⁵, P.D. Thompson¹⁸, R.J. Thompson⁸⁴, A.S. Thompson⁵³, L.A. Thomsen¹⁷⁶,
E. Thomson¹²², M. Thomson²⁸, R.P. Thun^{89,*}, M.J. Tibbetts¹⁵, R.E. Ticse Torres⁸⁵,
V.O. Tikhomirov^{96,ai}, Yu.A. Tikhonov^{109,c}, S. Timoshenko⁹⁸, E. Tiouchichine⁸⁵, P. Tipton¹⁷⁶,
S. Tisserant⁸⁵, K. Todome¹⁵⁷, T. Todorov^{5,*}, S. Todorova-Nova¹²⁹, J. Tojo⁷⁰, S. Tokár^{144a},
K. Tokushuku⁶⁶, K. Tollefson⁹⁰, E. Tolley⁵⁷, L. Tomlinson⁸⁴, M. Tomoto¹⁰³, L. Tompkins^{143,aj},
K. Toms¹⁰⁵, E. Torrence¹¹⁶, H. Torres¹⁴², E. Torró Pastor¹³⁸, J. Toth^{85,ak}, F. Touchard⁸⁵, D.R. Tovey¹³⁹,
T. Trefzger¹⁷⁴, L. Tremblet³⁰, A. Tricoli³⁰, I.M. Trigger^{159a}, S. Trincaz-Duvoid⁸⁰, M.F. Tripiana¹²,
W. Trischuk¹⁵⁸, B. Trocme⁵⁵, C. Troncon^{91a}, M. Trotter-McDonald¹⁵, M. Trovatelli¹⁶⁹,
L. Truong^{164a,164c}, M. Trzebinski³⁹, A. Trzupek³⁹, C. Tsarouchas³⁰, J.C-L. Tseng¹²⁰, P.V. Tsiareshka⁹²,
D. Tsionou¹⁵⁴, G. Tsipolitis¹⁰, N. Tsirintanis⁹, S. Tsiskaridze¹², V. Tsiskaridze⁴⁸, E.G. Tskhadadze^{51a},
I.I. Tsukerman⁹⁷, V. Tsulaia¹⁵, S. Tsuno⁶⁶, D. Tsybychev¹⁴⁸, A. Tudorache^{26b}, V. Tudorache^{26b},
A.N. Tuna⁵⁷, S.A. Tupputi^{20a,20b}, S. Turchikhin^{99,ah}, D. Turecek¹²⁸, R. Turra^{91a,91b}, A.J. Turvey⁴⁰,
P.M. Tuts³⁵, A. Tykhonov⁴⁹, M. Tylmad^{146a,146b}, M. Tyndel¹³¹, I. Ueda¹⁵⁵, R. Ueno²⁹,
M. Ughetto^{146a,146b}, M. Ugland¹⁴, F. Ukegawa¹⁶⁰, G. Unal³⁰, A. Undrus²⁵, G. Unel¹⁶³, F.C. Ungaro⁴⁸,
Y. Unno⁶⁶, C. Unverdorben¹⁰⁰, J. Urban^{144b}, P. Urquijo⁸⁸, P. Urrejola⁸³, G. Usai⁸, A. Usanova⁶²,
L. Vacavant⁸⁵, V. Vacek¹²⁸, B. Vachon⁸⁷, C. Valderanis⁸³, N. Valencic¹⁰⁷, S. Valentini^{20a,20b},
A. Valero¹⁶⁷, L. Valery¹², S. Valkar¹²⁹, S. Vallecorsa⁴⁹, J.A. Valls Ferrer¹⁶⁷, W. Van Den Wollenberg¹⁰⁷,
P.C. Van Der Deijl¹⁰⁷, R. van der Geer¹⁰⁷, H. van der Graaf¹⁰⁷, N. van Eldik¹⁵², P. van Gemmeren⁶,

J. Van Nieuwkoop¹⁴², I. van Vulpen¹⁰⁷, M.C. van Woerden³⁰, M. Vanadia^{132a,132b}, W. Vandelli³⁰, R. Vanguri¹²², A. Vaniachine⁶, F. Vannucci⁸⁰, G. Vardanyan¹⁷⁷, R. Vari^{132a}, E.W. Varnes⁷, T. Varol⁴⁰, D. Varouchas⁸⁰, A. Vartapetian⁸, K.E. Varvell¹⁵⁰, F. Vazeille³⁴, T. Vazquez Schroeder⁸⁷, J. Veatch⁷, L.M. Veloce¹⁵⁸, F. Veloso^{126a,126c}, T. Velz²¹, S. Veneziano^{132a}, A. Ventura^{73a,73b}, D. Ventura⁸⁶, M. Venturi¹⁶⁹, N. Venturi¹⁵⁸, A. Venturini²³, V. Vercesi^{121a}, M. Verducci^{132a,132b}, W. Verkerke¹⁰⁷, J.C. Vermeulen¹⁰⁷, A. Vest⁴⁴, M.C. Vetterli^{142,d}, O. Viazlo⁸¹, I. Vichou¹⁶⁵, T. Vickey¹³⁹, O.E. Vickey Boeriu¹³⁹, G.H.A. Viehhauser¹²⁰, S. Viel¹⁵, R. Vigne⁶², M. Villa^{20a,20b}, M. Villaplana Perez^{91a,91b}, E. Vilucchi⁴⁷, M.G. Vincter²⁹, V.B. Vinogradov⁶⁵, I. Vivarelli¹⁴⁹, F. Vives Vaque³, S. Vlachos¹⁰, D. Vladoiu¹⁰⁰, M. Vlasak¹²⁸, M. Vogel^{32a}, P. Vokac¹²⁸, G. Volpi^{124a,124b}, M. Volpi⁸⁸, H. von der Schmitt¹⁰¹, H. von Radziewski⁴⁸, E. von Toerne²¹, V. Vorobel¹²⁹, K. Vorobev⁹⁸, M. Vos¹⁶⁷, R. Voss³⁰, J.H. Vossebeld⁷⁴, N. Vranjes¹³, M. Vranjes Milosavljevic¹³, V. Vrba¹²⁷, M. Vreeswijk¹⁰⁷, R. Vuillermet³⁰, I. Vukotic³¹, Z. Vykydal¹²⁸, P. Wagner²¹, W. Wagner¹⁷⁵, H. Wahlberg⁷¹, S. Wahrmund⁴⁴, J. Wakabayashi¹⁰³, J. Walder⁷², R. Walker¹⁰⁰, W. Walkowiak¹⁴¹, C. Wang¹⁵¹, F. Wang¹⁷³, H. Wang¹⁵, H. Wang⁴⁰, J. Wang⁴², J. Wang¹⁵⁰, K. Wang⁸⁷, R. Wang⁶, S.M. Wang¹⁵¹, T. Wang²¹, T. Wang³⁵, X. Wang¹⁷⁶, C. Wanotayaroj¹¹⁶, A. Warburton⁸⁷, C.P. Ward²⁸, D.R. Wardrope⁷⁸, A. Washbrook⁴⁶, C. Wasicki⁴², P.M. Watkins¹⁸, A.T. Watson¹⁸, I.J. Watson¹⁵⁰, M.F. Watson¹⁸, G. Watts¹³⁸, S. Watts⁸⁴, B.M. Waugh⁷⁸, S. Webb⁸⁴, M.S. Weber¹⁷, S.W. Weber¹⁷⁴, J.S. Webster³¹, A.R. Weidberg¹²⁰, B. Weinert⁶¹, J. Weingarten⁵⁴, C. Weiser⁴⁸, H. Weits¹⁰⁷, P.S. Wells³⁰, T. Wenaus²⁵, T. Wengler³⁰, S. Wenig³⁰, N. Wermes²¹, M. Werner⁴⁸, P. Werner³⁰, M. Wessels^{58a}, J. Wetter¹⁶¹, K. Whalen¹¹⁶, A.M. Wharton⁷², A. White⁸, M.J. White¹, R. White^{32b}, S. White^{124a,124b}, D. Whiteson¹⁶³, F.J. Wickens¹³¹, W. Wiedenmann¹⁷³, M. Wielers¹³¹, P. Wienemann²¹, C. Wiglesworth³⁶, L.A.M. Wiik-Fuchs²¹, A. Wildauer¹⁰¹, H.G. Wilkens³⁰, H.H. Williams¹²², S. Williams¹⁰⁷, C. Willis⁹⁰, S. Willocq⁸⁶, A. Wilson⁸⁹, J.A. Wilson¹⁸, I. Wingerter-Seez⁵, F. Winklmeier¹¹⁶, B.T. Winter²¹, M. Wittgen¹⁴³, J. Wittkowski¹⁰⁰, S.J. Wollstadt⁸³, M.W. Wolter³⁹, H. Wolters^{126a,126c}, B.K. Wosiek³⁹, J. Wotschack³⁰, M.J. Woudstra⁸⁴, K.W. Wozniak³⁹, M. Wu⁵⁵, M. Wu³¹, S.L. Wu¹⁷³, X. Wu⁴⁹, Y. Wu⁸⁹, T.R. Wyatt⁸⁴, B.M. Wynne⁴⁶, S. Xella³⁶, D. Xu^{33a}, L. Xu²⁵, B. Yabsley¹⁵⁰, S. Yacoub^{145a}, R. Yakabe⁶⁷, M. Yamada⁶⁶, D. Yamaguchi¹⁵⁷, Y. Yamaguchi¹¹⁸, A. Yamamoto⁶⁶, S. Yamamoto¹⁵⁵, T. Yamanaka¹⁵⁵, K. Yamauchi¹⁰³, Y. Yamazaki⁶⁷, Z. Yan²², H. Yang^{33e}, H. Yang¹⁷³, Y. Yang¹⁵¹, W-M. Yao¹⁵, Y. Yasu⁶⁶, E. Yatsenko⁵, K.H. Yau Wong²¹, J. Ye⁴⁰, S. Ye²⁵, I. Yeletsikh⁶⁵, A.L. Yen⁵⁷, E. Yildirim⁴², K. Yorita¹⁷¹, R. Yoshida⁶, K. Yoshihara¹²², C. Young¹⁴³, C.J.S. Young³⁰, S. Youssef²², D.R. Yu¹⁵, J. Yu⁸, J.M. Yu⁸⁹, J. Yu¹¹⁴, L. Yuan⁶⁷, S.P.Y. Yuen²¹, A. Yurkewicz¹⁰⁸, I. Yusuff^{28,al}, B. Zabinski³⁹, R. Zaidan⁶³, A.M. Zaitsev^{130,ac}, J. Zalieckas¹⁴, A. Zaman¹⁴⁸, S. Zambito⁵⁷, L. Zanello^{132a,132b}, D. Zanzi⁸⁸, C. Zeitnitz¹⁷⁵, M. Zeman¹²⁸, A. Zemla^{38a}, Q. Zeng¹⁴³, K. Zengel²³, O. Zenin¹³⁰, T. Ženiš^{144a}, D. Zerwas¹¹⁷, D. Zhang⁸⁹, F. Zhang¹⁷³, G. Zhang^{33b}, H. Zhang^{33c}, J. Zhang⁶, L. Zhang⁴⁸, R. Zhang^{33b,i}, X. Zhang^{33d}, Z. Zhang¹¹⁷, X. Zhao⁴⁰, Y. Zhao^{33d,117}, Z. Zhao^{33b}, A. Zhemchugov⁶⁵, J. Zhong¹²⁰, B. Zhou⁸⁹, C. Zhou⁴⁵, L. Zhou³⁵, L. Zhou⁴⁰, M. Zhou¹⁴⁸, N. Zhou^{33f}, C.G. Zhu^{33d}, H. Zhu^{33a}, J. Zhu⁸⁹, Y. Zhu^{33b}, X. Zhuang^{33a}, K. Zhukov⁹⁶, A. Zibell¹⁷⁴, D. Zieminska⁶¹, N.I. Zimine⁶⁵, C. Zimmermann⁸³, S. Zimmermann⁴⁸, Z. Zinonos⁵⁴, M. Zinser⁸³, M. Ziolkowski¹⁴¹, L. Živković¹³, G. Zobernig¹⁷³, A. Zoccoli^{20a,20b}, M. zur Nedden¹⁶, G. Zurzolo^{104a,104b}, L. Zwalinski³⁰.

¹ Department of Physics, University of Adelaide, Adelaide, Australia

² Physics Department, SUNY Albany, Albany NY, United States of America

³ Department of Physics, University of Alberta, Edmonton AB, Canada

⁴ (a) Department of Physics, Ankara University, Ankara; (b) Istanbul Aydin University, Istanbul; (c)

Division of Physics, TOBB University of Economics and Technology, Ankara, Turkey

⁵ LAPP, CNRS/IN2P3 and Université Savoie Mont Blanc, Annecy-le-Vieux, France

- ⁶ High Energy Physics Division, Argonne National Laboratory, Argonne IL, United States of America
- ⁷ Department of Physics, University of Arizona, Tucson AZ, United States of America
- ⁸ Department of Physics, The University of Texas at Arlington, Arlington TX, United States of America
- ⁹ Physics Department, University of Athens, Athens, Greece
- ¹⁰ Physics Department, National Technical University of Athens, Zografou, Greece
- ¹¹ Institute of Physics, Azerbaijan Academy of Sciences, Baku, Azerbaijan
- ¹² Institut de Física d'Altes Energies and Departament de Física de la Universitat Autònoma de Barcelona, Barcelona, Spain
- ¹³ Institute of Physics, University of Belgrade, Belgrade, Serbia
- ¹⁴ Department for Physics and Technology, University of Bergen, Bergen, Norway
- ¹⁵ Physics Division, Lawrence Berkeley National Laboratory and University of California, Berkeley CA, United States of America
- ¹⁶ Department of Physics, Humboldt University, Berlin, Germany
- ¹⁷ Albert Einstein Center for Fundamental Physics and Laboratory for High Energy Physics, University of Bern, Bern, Switzerland
- ¹⁸ School of Physics and Astronomy, University of Birmingham, Birmingham, United Kingdom
- ¹⁹ ^(a) Department of Physics, Bogazici University, Istanbul; ^(b) Department of Physics Engineering, Gaziantep University, Gaziantep; ^(c) Department of Physics, Dogus University, Istanbul, Turkey
- ²⁰ ^(a) INFN Sezione di Bologna; ^(b) Dipartimento di Fisica e Astronomia, Università di Bologna, Bologna, Italy
- ²¹ Physikalisches Institut, University of Bonn, Bonn, Germany
- ²² Department of Physics, Boston University, Boston MA, United States of America
- ²³ Department of Physics, Brandeis University, Waltham MA, United States of America
- ²⁴ ^(a) Universidade Federal do Rio De Janeiro COPPE/EE/IF, Rio de Janeiro; ^(b) Electrical Circuits Department, Federal University of Juiz de Fora (UFJF), Juiz de Fora; ^(c) Federal University of Sao Joao del Rei (UFSJ), Sao Joao del Rei; ^(d) Instituto de Fisica, Universidade de Sao Paulo, Sao Paulo, Brazil
- ²⁵ Physics Department, Brookhaven National Laboratory, Upton NY, United States of America
- ²⁶ ^(a) Transilvania University of Brasov, Brasov, Romania; ^(b) National Institute of Physics and Nuclear Engineering, Bucharest; ^(c) National Institute for Research and Development of Isotopic and Molecular Technologies, Physics Department, Cluj Napoca; ^(d) University Politehnica Bucharest, Bucharest; ^(e) West University in Timisoara, Timisoara, Romania
- ²⁷ Departamento de Física, Universidad de Buenos Aires, Buenos Aires, Argentina
- ²⁸ Cavendish Laboratory, University of Cambridge, Cambridge, United Kingdom
- ²⁹ Department of Physics, Carleton University, Ottawa ON, Canada
- ³⁰ CERN, Geneva, Switzerland
- ³¹ Enrico Fermi Institute, University of Chicago, Chicago IL, United States of America
- ³² ^(a) Departamento de Física, Pontificia Universidad Católica de Chile, Santiago; ^(b) Departamento de Física, Universidad Técnica Federico Santa María, Valparaíso, Chile
- ³³ ^(a) Institute of High Energy Physics, Chinese Academy of Sciences, Beijing; ^(b) Department of Modern Physics, University of Science and Technology of China, Anhui; ^(c) Department of Physics, Nanjing University, Jiangsu; ^(d) School of Physics, Shandong University, Shandong; ^(e) Department of Physics and Astronomy, Shanghai Key Laboratory for Particle Physics and Cosmology, Shanghai Jiao Tong University, Shanghai; ^(f) Physics Department, Tsinghua University, Beijing 100084, China
- ³⁴ Laboratoire de Physique Corpusculaire, Clermont Université and Université Blaise Pascal and CNRS/IN2P3, Clermont-Ferrand, France
- ³⁵ Nevis Laboratory, Columbia University, Irvington NY, United States of America
- ³⁶ Niels Bohr Institute, University of Copenhagen, Kobenhavn, Denmark

- 37 ^(a) INFN Gruppo Collegato di Cosenza, Laboratori Nazionali di Frascati; ^(b) Dipartimento di Fisica, Università della Calabria, Rende, Italy
- 38 ^(a) AGH University of Science and Technology, Faculty of Physics and Applied Computer Science, Krakow; ^(b) Marian Smoluchowski Institute of Physics, Jagiellonian University, Krakow, Poland
- 39 Institute of Nuclear Physics Polish Academy of Sciences, Krakow, Poland
- 40 Physics Department, Southern Methodist University, Dallas TX, United States of America
- 41 Physics Department, University of Texas at Dallas, Richardson TX, United States of America
- 42 DESY, Hamburg and Zeuthen, Germany
- 43 Institut für Experimentelle Physik IV, Technische Universität Dortmund, Dortmund, Germany
- 44 Institut für Kern- und Teilchenphysik, Technische Universität Dresden, Dresden, Germany
- 45 Department of Physics, Duke University, Durham NC, United States of America
- 46 SUPA - School of Physics and Astronomy, University of Edinburgh, Edinburgh, United Kingdom
- 47 INFN Laboratori Nazionali di Frascati, Frascati, Italy
- 48 Fakultät für Mathematik und Physik, Albert-Ludwigs-Universität, Freiburg, Germany
- 49 Section de Physique, Université de Genève, Geneva, Switzerland
- 50 ^(a) INFN Sezione di Genova; ^(b) Dipartimento di Fisica, Università di Genova, Genova, Italy
- 51 ^(a) E. Andronikashvili Institute of Physics, Iv. Javakhishvili Tbilisi State University, Tbilisi; ^(b) High Energy Physics Institute, Tbilisi State University, Tbilisi, Georgia
- 52 II Physikalisches Institut, Justus-Liebig-Universität Giessen, Giessen, Germany
- 53 SUPA - School of Physics and Astronomy, University of Glasgow, Glasgow, United Kingdom
- 54 II Physikalisches Institut, Georg-August-Universität, Göttingen, Germany
- 55 Laboratoire de Physique Subatomique et de Cosmologie, Université Grenoble-Alpes, CNRS/IN2P3, Grenoble, France
- 56 Department of Physics, Hampton University, Hampton VA, United States of America
- 57 Laboratory for Particle Physics and Cosmology, Harvard University, Cambridge MA, United States of America
- 58 ^(a) Kirchhoff-Institut für Physik, Ruprecht-Karls-Universität Heidelberg, Heidelberg; ^(b) Physikalisches Institut, Ruprecht-Karls-Universität Heidelberg, Heidelberg; ^(c) ZITI Institut für technische Informatik, Ruprecht-Karls-Universität Heidelberg, Mannheim, Germany
- 59 Faculty of Applied Information Science, Hiroshima Institute of Technology, Hiroshima, Japan
- 60 ^(a) Department of Physics, The Chinese University of Hong Kong, Shatin, N.T., Hong Kong; ^(b) Department of Physics, The University of Hong Kong, Hong Kong; ^(c) Department of Physics, The Hong Kong University of Science and Technology, Clear Water Bay, Kowloon, Hong Kong, China
- 61 Department of Physics, Indiana University, Bloomington IN, United States of America
- 62 Institut für Astro- und Teilchenphysik, Leopold-Franzens-Universität, Innsbruck, Austria
- 63 University of Iowa, Iowa City IA, United States of America
- 64 Department of Physics and Astronomy, Iowa State University, Ames IA, United States of America
- 65 Joint Institute for Nuclear Research, JINR Dubna, Dubna, Russia
- 66 KEK, High Energy Accelerator Research Organization, Tsukuba, Japan
- 67 Graduate School of Science, Kobe University, Kobe, Japan
- 68 Faculty of Science, Kyoto University, Kyoto, Japan
- 69 Kyoto University of Education, Kyoto, Japan
- 70 Department of Physics, Kyushu University, Fukuoka, Japan
- 71 Instituto de Física La Plata, Universidad Nacional de La Plata and CONICET, La Plata, Argentina
- 72 Physics Department, Lancaster University, Lancaster, United Kingdom
- 73 ^(a) INFN Sezione di Lecce; ^(b) Dipartimento di Matematica e Fisica, Università del Salento, Lecce, Italy

- ⁷⁴ Oliver Lodge Laboratory, University of Liverpool, Liverpool, United Kingdom
- ⁷⁵ Department of Physics, Jožef Stefan Institute and University of Ljubljana, Ljubljana, Slovenia
- ⁷⁶ School of Physics and Astronomy, Queen Mary University of London, London, United Kingdom
- ⁷⁷ Department of Physics, Royal Holloway University of London, Surrey, United Kingdom
- ⁷⁸ Department of Physics and Astronomy, University College London, London, United Kingdom
- ⁷⁹ Louisiana Tech University, Ruston LA, United States of America
- ⁸⁰ Laboratoire de Physique Nucléaire et de Hautes Energies, UPMC and Université Paris-Diderot and CNRS/IN2P3, Paris, France
- ⁸¹ Fysiska institutionen, Lunds universitet, Lund, Sweden
- ⁸² Departamento de Física Teórica C-15, Universidad Autónoma de Madrid, Madrid, Spain
- ⁸³ Institut für Physik, Universität Mainz, Mainz, Germany
- ⁸⁴ School of Physics and Astronomy, University of Manchester, Manchester, United Kingdom
- ⁸⁵ CPPM, Aix-Marseille Université and CNRS/IN2P3, Marseille, France
- ⁸⁶ Department of Physics, University of Massachusetts, Amherst MA, United States of America
- ⁸⁷ Department of Physics, McGill University, Montreal QC, Canada
- ⁸⁸ School of Physics, University of Melbourne, Victoria, Australia
- ⁸⁹ Department of Physics, The University of Michigan, Ann Arbor MI, United States of America
- ⁹⁰ Department of Physics and Astronomy, Michigan State University, East Lansing MI, United States of America
- ⁹¹ ^(a) INFN Sezione di Milano; ^(b) Dipartimento di Fisica, Università di Milano, Milano, Italy
- ⁹² B.I. Stepanov Institute of Physics, National Academy of Sciences of Belarus, Minsk, Republic of Belarus
- ⁹³ National Scientific and Educational Centre for Particle and High Energy Physics, Minsk, Republic of Belarus
- ⁹⁴ Department of Physics, Massachusetts Institute of Technology, Cambridge MA, United States of America
- ⁹⁵ Group of Particle Physics, University of Montreal, Montreal QC, Canada
- ⁹⁶ P.N. Lebedev Institute of Physics, Academy of Sciences, Moscow, Russia
- ⁹⁷ Institute for Theoretical and Experimental Physics (ITEP), Moscow, Russia
- ⁹⁸ National Research Nuclear University MEPhI, Moscow, Russia
- ⁹⁹ D.V. Skobeltsyn Institute of Nuclear Physics, M.V. Lomonosov Moscow State University, Moscow, Russia
- ¹⁰⁰ Fakultät für Physik, Ludwig-Maximilians-Universität München, München, Germany
- ¹⁰¹ Max-Planck-Institut für Physik (Werner-Heisenberg-Institut), München, Germany
- ¹⁰² Nagasaki Institute of Applied Science, Nagasaki, Japan
- ¹⁰³ Graduate School of Science and Kobayashi-Maskawa Institute, Nagoya University, Nagoya, Japan
- ¹⁰⁴ ^(a) INFN Sezione di Napoli; ^(b) Dipartimento di Fisica, Università di Napoli, Napoli, Italy
- ¹⁰⁵ Department of Physics and Astronomy, University of New Mexico, Albuquerque NM, United States of America
- ¹⁰⁶ Institute for Mathematics, Astrophysics and Particle Physics, Radboud University Nijmegen/Nikhef, Nijmegen, Netherlands
- ¹⁰⁷ Nikhef National Institute for Subatomic Physics and University of Amsterdam, Amsterdam, Netherlands
- ¹⁰⁸ Department of Physics, Northern Illinois University, DeKalb IL, United States of America
- ¹⁰⁹ Budker Institute of Nuclear Physics, SB RAS, Novosibirsk, Russia
- ¹¹⁰ Department of Physics, New York University, New York NY, United States of America
- ¹¹¹ Ohio State University, Columbus OH, United States of America

- ¹¹² Faculty of Science, Okayama University, Okayama, Japan
- ¹¹³ Homer L. Dodge Department of Physics and Astronomy, University of Oklahoma, Norman OK, United States of America
- ¹¹⁴ Department of Physics, Oklahoma State University, Stillwater OK, United States of America
- ¹¹⁵ Palacký University, RCPTM, Olomouc, Czech Republic
- ¹¹⁶ Center for High Energy Physics, University of Oregon, Eugene OR, United States of America
- ¹¹⁷ LAL, Université Paris-Sud and CNRS/IN2P3, Orsay, France
- ¹¹⁸ Graduate School of Science, Osaka University, Osaka, Japan
- ¹¹⁹ Department of Physics, University of Oslo, Oslo, Norway
- ¹²⁰ Department of Physics, Oxford University, Oxford, United Kingdom
- ¹²¹ ^(a) INFN Sezione di Pavia; ^(b) Dipartimento di Fisica, Università di Pavia, Pavia, Italy
- ¹²² Department of Physics, University of Pennsylvania, Philadelphia PA, United States of America
- ¹²³ National Research Centre "Kurchatov Institute" B.P.Konstantinov Petersburg Nuclear Physics Institute, St. Petersburg, Russia
- ¹²⁴ ^(a) INFN Sezione di Pisa; ^(b) Dipartimento di Fisica E. Fermi, Università di Pisa, Pisa, Italy
- ¹²⁵ Department of Physics and Astronomy, University of Pittsburgh, Pittsburgh PA, United States of America
- ¹²⁶ ^(a) Laboratório de Instrumentação e Física Experimental de Partículas - LIP, Lisboa; ^(b) Faculdade de Ciências, Universidade de Lisboa, Lisboa; ^(c) Department of Physics, University of Coimbra, Coimbra; ^(d) Centro de Física Nuclear da Universidade de Lisboa, Lisboa; ^(e) Departamento de Física, Universidade do Minho, Braga; ^(f) Departamento de Física Teórica y del Cosmos and CAFPE, Universidad de Granada, Granada (Spain); ^(g) Dep Física and CEFITEC of Faculdade de Ciências e Tecnologia, Universidade Nova de Lisboa, Caparica, Portugal
- ¹²⁷ Institute of Physics, Academy of Sciences of the Czech Republic, Praha, Czech Republic
- ¹²⁸ Czech Technical University in Prague, Praha, Czech Republic
- ¹²⁹ Faculty of Mathematics and Physics, Charles University in Prague, Praha, Czech Republic
- ¹³⁰ State Research Center Institute for High Energy Physics, Protvino, Russia
- ¹³¹ Particle Physics Department, Rutherford Appleton Laboratory, Didcot, United Kingdom
- ¹³² ^(a) INFN Sezione di Roma; ^(b) Dipartimento di Fisica, Sapienza Università di Roma, Roma, Italy
- ¹³³ ^(a) INFN Sezione di Roma Tor Vergata; ^(b) Dipartimento di Fisica, Università di Roma Tor Vergata, Roma, Italy
- ¹³⁴ ^(a) INFN Sezione di Roma Tre; ^(b) Dipartimento di Matematica e Fisica, Università Roma Tre, Roma, Italy
- ¹³⁵ ^(a) Faculté des Sciences Ain Chock, Réseau Universitaire de Physique des Hautes Energies - Université Hassan II, Casablanca; ^(b) Centre National de l'Energie des Sciences Techniques Nucleaires, Rabat; ^(c) Faculté des Sciences Semlalia, Université Cadi Ayyad, LPHEA-Marrakech; ^(d) Faculté des Sciences, Université Mohamed Premier and LPTPM, Oujda; ^(e) Faculté des sciences, Université Mohammed V, Rabat, Morocco
- ¹³⁶ DSM/IRFU (Institut de Recherches sur les Lois Fondamentales de l'Univers), CEA Saclay (Commissariat à l'Energie Atomique et aux Energies Alternatives), Gif-sur-Yvette, France
- ¹³⁷ Santa Cruz Institute for Particle Physics, University of California Santa Cruz, Santa Cruz CA, United States of America
- ¹³⁸ Department of Physics, University of Washington, Seattle WA, United States of America
- ¹³⁹ Department of Physics and Astronomy, University of Sheffield, Sheffield, United Kingdom
- ¹⁴⁰ Department of Physics, Shinshu University, Nagano, Japan
- ¹⁴¹ Fachbereich Physik, Universität Siegen, Siegen, Germany
- ¹⁴² Department of Physics, Simon Fraser University, Burnaby BC, Canada

- ¹⁴³ SLAC National Accelerator Laboratory, Stanford CA, United States of America
- ¹⁴⁴ ^(a) Faculty of Mathematics, Physics & Informatics, Comenius University, Bratislava; ^(b) Department of Subnuclear Physics, Institute of Experimental Physics of the Slovak Academy of Sciences, Kosice, Slovak Republic
- ¹⁴⁵ ^(a) Department of Physics, University of Cape Town, Cape Town; ^(b) Department of Physics, University of Johannesburg, Johannesburg; ^(c) School of Physics, University of the Witwatersrand, Johannesburg, South Africa
- ¹⁴⁶ ^(a) Department of Physics, Stockholm University; ^(b) The Oskar Klein Centre, Stockholm, Sweden
- ¹⁴⁷ Physics Department, Royal Institute of Technology, Stockholm, Sweden
- ¹⁴⁸ Departments of Physics & Astronomy and Chemistry, Stony Brook University, Stony Brook NY, United States of America
- ¹⁴⁹ Department of Physics and Astronomy, University of Sussex, Brighton, United Kingdom
- ¹⁵⁰ School of Physics, University of Sydney, Sydney, Australia
- ¹⁵¹ Institute of Physics, Academia Sinica, Taipei, Taiwan
- ¹⁵² Department of Physics, Technion: Israel Institute of Technology, Haifa, Israel
- ¹⁵³ Raymond and Beverly Sackler School of Physics and Astronomy, Tel Aviv University, Tel Aviv, Israel
- ¹⁵⁴ Department of Physics, Aristotle University of Thessaloniki, Thessaloniki, Greece
- ¹⁵⁵ International Center for Elementary Particle Physics and Department of Physics, The University of Tokyo, Tokyo, Japan
- ¹⁵⁶ Graduate School of Science and Technology, Tokyo Metropolitan University, Tokyo, Japan
- ¹⁵⁷ Department of Physics, Tokyo Institute of Technology, Tokyo, Japan
- ¹⁵⁸ Department of Physics, University of Toronto, Toronto ON, Canada
- ¹⁵⁹ ^(a) TRIUMF, Vancouver BC; ^(b) Department of Physics and Astronomy, York University, Toronto ON, Canada
- ¹⁶⁰ Faculty of Pure and Applied Sciences, University of Tsukuba, Tsukuba, Japan
- ¹⁶¹ Department of Physics and Astronomy, Tufts University, Medford MA, United States of America
- ¹⁶² Centro de Investigaciones, Universidad Antonio Narino, Bogota, Colombia
- ¹⁶³ Department of Physics and Astronomy, University of California Irvine, Irvine CA, United States of America
- ¹⁶⁴ ^(a) INFN Gruppo Collegato di Udine, Sezione di Trieste, Udine; ^(b) ICTP, Trieste; ^(c) Dipartimento di Chimica, Fisica e Ambiente, Università di Udine, Udine, Italy
- ¹⁶⁵ Department of Physics, University of Illinois, Urbana IL, United States of America
- ¹⁶⁶ Department of Physics and Astronomy, University of Uppsala, Uppsala, Sweden
- ¹⁶⁷ Instituto de Física Corpuscular (IFIC) and Departamento de Física Atómica, Molecular y Nuclear and Departamento de Ingeniería Electrónica and Instituto de Microelectrónica de Barcelona (IMB-CNM), University of Valencia and CSIC, Valencia, Spain
- ¹⁶⁸ Department of Physics, University of British Columbia, Vancouver BC, Canada
- ¹⁶⁹ Department of Physics and Astronomy, University of Victoria, Victoria BC, Canada
- ¹⁷⁰ Department of Physics, University of Warwick, Coventry, United Kingdom
- ¹⁷¹ Waseda University, Tokyo, Japan
- ¹⁷² Department of Particle Physics, The Weizmann Institute of Science, Rehovot, Israel
- ¹⁷³ Department of Physics, University of Wisconsin, Madison WI, United States of America
- ¹⁷⁴ Fakultät für Physik und Astronomie, Julius-Maximilians-Universität, Würzburg, Germany
- ¹⁷⁵ Fachbereich C Physik, Bergische Universität Wuppertal, Wuppertal, Germany
- ¹⁷⁶ Department of Physics, Yale University, New Haven CT, United States of America
- ¹⁷⁷ Yerevan Physics Institute, Yerevan, Armenia

¹⁷⁸ Centre de Calcul de l'Institut National de Physique Nucléaire et de Physique des Particules (IN2P3), Villeurbanne, France

^a Also at Department of Physics, King's College London, London, United Kingdom

^b Also at Institute of Physics, Azerbaijan Academy of Sciences, Baku, Azerbaijan

^c Also at Novosibirsk State University, Novosibirsk, Russia

^d Also at TRIUMF, Vancouver BC, Canada

^e Also at Department of Physics, California State University, Fresno CA, United States of America

^f Also at Department of Physics, University of Fribourg, Fribourg, Switzerland

^g Also at Departamento de Física e Astronomia, Faculdade de Ciências, Universidade do Porto, Portugal

^h Also at Tomsk State University, Tomsk, Russia

ⁱ Also at CPPM, Aix-Marseille Université and CNRS/IN2P3, Marseille, France

^j Also at Università di Napoli Parthenope, Napoli, Italy

^k Also at Institute of Particle Physics (IPP), Canada

^l Also at Particle Physics Department, Rutherford Appleton Laboratory, Didcot, United Kingdom

^m Also at Department of Physics, St. Petersburg State Polytechnical University, St. Petersburg, Russia

ⁿ Also at Louisiana Tech University, Ruston LA, United States of America

^o Also at Institutio Catalana de Recerca i Estudis Avancats, ICREA, Barcelona, Spain

^p Also at Department of Physics, The University of Michigan, Ann Arbor MI, United States of America

^q Also at Graduate School of Science, Osaka University, Osaka, Japan

^r Also at Department of Physics, National Tsing Hua University, Taiwan

^s Also at Department of Physics, The University of Texas at Austin, Austin TX, United States of America

^t Also at Institute of Theoretical Physics, Iliia State University, Tbilisi, Georgia

^u Also at CERN, Geneva, Switzerland

^v Also at Georgian Technical University (GTU), Tbilisi, Georgia

^w Also at Manhattan College, New York NY, United States of America

^x Also at Hellenic Open University, Patras, Greece

^y Also at Institute of Physics, Academia Sinica, Taipei, Taiwan

^z Also at LAL, Université Paris-Sud and CNRS/IN2P3, Orsay, France

^{aa} Also at Academia Sinica Grid Computing, Institute of Physics, Academia Sinica, Taipei, Taiwan

^{ab} Also at School of Physics, Shandong University, Shandong, China

^{ac} Also at Moscow Institute of Physics and Technology State University, Dolgoprudny, Russia

^{ad} Also at Section de Physique, Université de Genève, Geneva, Switzerland

^{ae} Also at International School for Advanced Studies (SISSA), Trieste, Italy

^{af} Also at Department of Physics and Astronomy, University of South Carolina, Columbia SC, United States of America

^{ag} Also at School of Physics and Engineering, Sun Yat-sen University, Guangzhou, China

^{ah} Also at Faculty of Physics, M.V.Lomonosov Moscow State University, Moscow, Russia

^{ai} Also at National Research Nuclear University MEPhI, Moscow, Russia

^{aj} Also at Department of Physics, Stanford University, Stanford CA, United States of America

^{ak} Also at Institute for Particle and Nuclear Physics, Wigner Research Centre for Physics, Budapest, Hungary

^{al} Also at University of Malaya, Department of Physics, Kuala Lumpur, Malaysia

* Deceased